DECLARATION

I hereby declare that this submission is my own work and that, to the best of my knowledge and belief, it contains no material previously published or written by another person nor material which to a substantial extent has been accepted for the award of any other degree or diploma of the university or other institute of higher learning, except where due acknowledgment has been made in the text.

Camerino, March 2019

Angela Piersanti

International School of Advanced Studies

Doctoral Course in Life and Health Sciences

Curriculum: Molecular Biology and Cellular Biotechnology

PhD thesis

Genes and Genomes in Ciliates:

- **Gene expression analysis in *Tetrahymena thermophila* under stress conditions**
- **Approach to the characterization of the germline (micronuclear) genome in *Euplotes crassus***

Candidate:

Angela Piersanti

Series and year of attendance:

096523 XXXI cycle

Supervisors:

Prof. Cristina Miceli

Prof. Sandra Pucciarelli

March 2019

Acknowledgements

This study was carried out in the molecular and cellular biology laboratory (head of the laboratory Prof. Cristina Miceli) at the University of Camerino (Italy). The toxicology study was performed in the Laboratory of Environmental Toxicology (head of the laboratory Prof. Anne Kahru) of the National Institute of Chemical Physics and Biophysics, Tallinn, (Estonia). The pilot RNA sequencing study was performed in the Protozoan Functional Genomics laboratory (head of the laboratory Prof. Wei Miao) at the Institute of Hydrobiology, Chinese Academy of Sciences in Wuhan (China). Most of the transformation experiments were performed in the Epigenetic Mechanisms of Complex Genome Editing in Eukaryotes Laboratory (head of the laboratory Prof. Mariusz Nowacki), Institute of Cell Biology, University of Bern (Switzerland). The work was supported by the International School of Advanced Studies of the University of Camerino, the European Cooperation in Science and Technology (COST) action BM1102 “Ciliates as model systems to study genome evolution, mechanisms of non-Mendelian inheritance, and their roles in environmental adaptation”, and last but not least by the Marine Microbiology Initiative (MMI, funded by Gordon and Betty Moore foundation) in the frame of a project in collaboration with the University of Bern and the University of Connecticut (USA).

First and foremost, I am grateful to my supervisors Prof. Cristina Miceli and Prof. Sandra Pucciarelli, not only for giving me the opportunity to be a member of the research group, but also for the intellectual guidance, encouragement and valuable suggestions. I would like to thank especially Rachele Cesaroni, Dr. Matteo Mozzicafreddo, Dr. Patrizia Ballarini, Piero Saltalamacchia, Dr. Daniela Sparvoli, Dr. Kesava Priyan, Maria Sindhura John, Dr. Nagothu Joseph Amruthraj, Qin Di, Alessio Mancini and Francesca Papi, from our laboratory. I also want to thank other members of the International School of Advanced Studies at University of Camerino and of the School of Bioscience and Veterinary Medicine for their help and support during these years: Prof. Roberto Ciccocioppo, Dr. Cristina Soave, Prof. Anna Maria Eleuteri, Dr. Massimiliano Cuccioloni, Prof. Luca A. Vitali, Dr. Dezemona Petrelli, Roberto Rosati, Prof Guido Favia, Prof. Irene Ricci, Dr. Alessia Cappelli, Dr. Claudia Damiani, Dr. Matteo Valzano, Dr. Dario Pediconi and Dr. Maura Montani.

I would like to express my gratitude to Dr. Katre Juganson for her great help during my stay in Tallinn.

I wish to thank Prof. Wei Miao, Jing Zhang, Wei Wei, Kangping Zhao and Dr. Miao Tien for the warm and supportive atmosphere in Wuhan.

I am thankful to Prof. Mariusz Nowacki that gave me the opportunity to join his laboratory and to work with Prof. Estienne C. Swart, Rachele Cesaroni, Dr. Iwona Rzeszutek and Dr. Xyrus Maurer-Alcalá. I also want to thank all the members of his laboratory for creating a friendly and stimulating context. I also gratefully acknowledge Prof. Lawrence. A. Klobutcher (University of Connecticut Health Center) for his precious advice and support in the frame of the MMI project.

Finally, I am very thankful to my family and all my friends for the support and understanding.

Table of contents

List of figures

List of tables

List of abbreviations

S.I. (Système International d'Unités) abbreviations for units and standard notations for chemical elements, formulae and chemical abbreviations are used in this work. Other abbreviations are listed below.

Ω	Ohm
µFD	Microfarad
Ag	Silver
AgNPs	Silver nanoparticles
AuNPs	Golden nanoparticles
bp	Base pairs
BP	Biological process
BSA	Bovine serum albumin
CAS	Chinese Academy of Sciences
Cbs	Chromosome breakage sequence
CC	Cellular component
cDNA	Complementary DNA
CDS	Coding sequence
CHEF	Contour-clamped homogenous electric field
COST	European Cooperation in Science and Technology
CPM	Count per million
CTH	Cathepsin
Cy3	Cyanine
DEA	Differential Expression Analysis
DEGs	Differential Expressed Genes
DNA	Deoxyribonucleic acid
DNase I	Deoxyribonuclease I
dNTP	Deoxynucleotide
E-Cbs	*Euplotes* chromosome breakage sequence
E. crassus	*Euplotes crassus*
e.g.	*Exempli gratia* (for example)
EC_{50}	Median effective concentration of the toxicant that induces a designated effect in 50% of the test organisms after a specified

	exposure time
EDTA	Ethylenediamine-tetraacetic acid disodium salt
EtBr	Ethidium bromide
EtOH	Ethanol
FC	Fold change
FW	Forward primer
G418	Geneticin
gDNA	genomic DNA
GFP	Green fluorescent protein
GO	Gene Ontology
GPX	Glutathione PeroXidase
GSEA	Gene Set Enrichment Analysis
h	Hours
HEM	Hemoglobin
HEPES	4-(2-hydroxyethyl)-1-piperazineethanesulfonic acid
hsp70	Heat Shock Protein 70
IESs	Internally eliminated sequences
IHB	Institute of Hydrobiology
inches Hg	Inch of mercury
kbp	Kilobase pairs
KEGG	Kyoto Encyclopedia of Genes and Genomes
LB-medium	Luria-Bertani-medium
MAC	Macronucleus
MDSs	Macronuclear-destined sequences
MDS plot	multi-dimensional scaling plot
MF	Molecular function
mic	Micronucleus
min	Minute
MMETSP	Marine Microbial Eukaryote Transcriptome Sequencing Project
MMI	Marine Microbiology Initiative
mRNA	messenger RNA
MTT	Metallothioneine
neo	neomycin-resistance (neo) gene
NICPB	National Institute of Chemical Physics and Biophysics
NPs	Nanoparticles

PacBio	Pacific biosciences SMRT sequencing
PCR	Polymerase chain reaction
pdi	Polydispersity index
PEG	Polyethylene glycol
PFGE	Pulsed Field Gel Electrophoresis
PND	Programmed nuclear death
psi	Pound-force per square inch
PRF	Programmed ribosomal frameshift
qPCR	Quantitative polymerase chain reaction
rDNA	Ribosomal DNA
RNA	Ribonucleic acid
RNAi	RNA interference
RNA-Seq	RNA Sequencing
ROS	Reactive oxygen species
rpm	Rounds per minute
rRNA	Ribosomal RNA
RV	Reverse primer
SDS	Sodium dodecyl sulphate
sec	Seconds
SPP	Supplemented proteose peptone
T. thermophila	*Tetrahymena thermophila*
Tec	Transposonlike *E. crassus*
TEM	Transmission electron microscopy
TetraFGD	Tetrahymena Functional Genomic Database
TGD	Tetrahymena Genome Database
UTR	Untranslated region
UV	Ultraviolet
V	Volt
V0	Vegetative cell
V1	Cell undergoing binary fission

Preface

I carried out my PhD work at the University of Camerino in the molecular and cellular biology laboratory under the supervision of prof. Cristina Miceli and prof. Sandra Pucciarelli. The research activities of the laboratory are mainly focused on the study of molecular and cellular adaptations and responsive mechanisms of eukaryotic microorganisms to environmental changes and stressed conditions. The research approach includes the study of genome organization and control of gene expression. Ciliated protozoa, such as the freshwater *Tetrahymena thermophila* (Order Hymenostomatida) and marine *Euplotes* species (Order Hypotrichida), are used as model organisms.

General objectives of my thesis were to demonstrate the applicability of transcriptional profiling, for elucidating the mechanisms of toxic action of engineered nanomaterials in the ciliate *Tetrahymena thermophila*, endorsing it as a valid model organism for the freshwater environmental pollution studies and to pave the way to the use of marine *Euplotes* species as additional valid models for studies on the marine environment.

Despite their genetic diversity, all ciliates are characterized by two common features: the possession of complexes of cilia, used for swimming or crawling and for phagocytic food capture, and the presence of nuclear dimorphism. Each ciliate contains a germ line diploid micronucleus (mic), inactive in vegetative cells, but transcriptionally active in mating cells and responsible for the genetic continuity during sexual reproduction, and a larger polyploid somatic macronucleus (MAC), the site of transcriptional activity in the vegetative growing cell. Different ciliate species can contain different numbers of micronuclei: *Tetrahymena* and *Euplotes* species have one mic, which divides mitotically during vegetative growth. *Tetrahymena* species have a single ovoid MAC. *Euplotes* species contain a single, highly elongated MAC (Prescott 1994) (Figure 1).

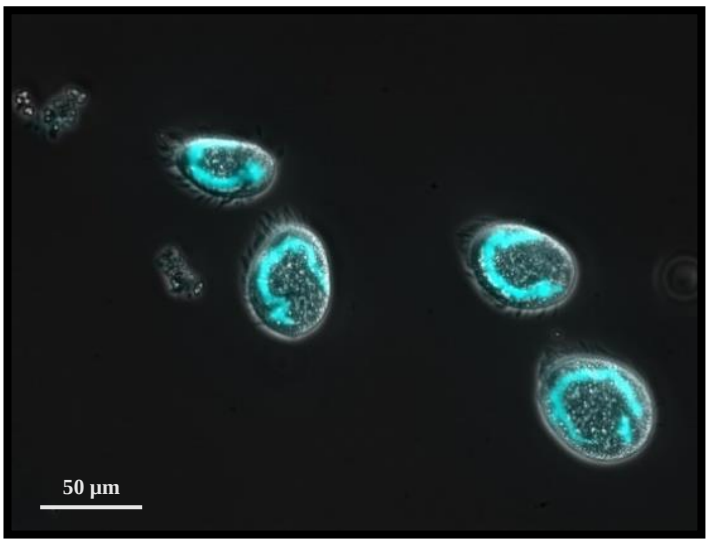

Figure 1. Fluorescence microscopy image of *Euplotes crassus*. MAC appear blue after staining with a nuclear dye DAPI.

When two starved cells of different mating type undergo conjugation, they exchange haploid mic and develop a new MAC from the mic. The developing MAC is called the Anlagen. During its differentiation several programmed DNA rearrangements occur (M.-C. Yao and Chao 2005): 1) the deletion of segments of the mic genome known as internally eliminated sequences (IESs); 2) the site-specific fragmentation of the chromosomes (Fan and Yao 2000); 3) the addition of a telomere to each new end (Yu and Blackburn 1991) generating the MAC chromosomes (Eisen et al. 2006) , and 4) their amplification (M. C. Yao, Yao, and Monks 1990). In *Tetrahymena* approximately 6,000 IESs are removed, resulting in the MAC genome being 10% to 20% smaller than that of the mic (M. C. Yao et al. 1984). Hypotrichs undergo the same three global genomic changes of elimination, fragmentation, and amplification during MAC development, but the phenomena are more extreme and entail the elimination of 96% of the mic genomic DNA complexity in *Oxytricha* species and 98% in *Stylonychia lemnae* (Prescott 1994), generating very small chromosomes called nanochromosomes that in most cases contain a single genetic unit. Conjugation results in complete genome replacement in each exconjugant and genetic identity of both exconjugants in some species (Orias, Cervantes, and Hamilton 2011).

T. thermophila has normal dimensions of about 50 µm in length and 20 µm in width. It swims in temperate freshwater environments like streams, lakes and ponds, and it tolerates a wide range of temperatures, from 12°C up to about 41°C (Frankel 1999).

T. thermophila cell is covered by multi-layer cortex that is semi-rigid and arranged into 18-21 longitudinal rows (ciliary rows) of cortical units containing basal bodies mostly accompanied by the cilia. Nutrients are taken up via pinocytosis and phagocytosis, the latter is the main feeding mechanism of *Tetrahymena*. Food vacuoles are formed in an oral apparatus made up of four compound ciliary elements (hence Tetra-hymena) embedded within fibrillar structures located near the anterior end of the cell. Near the posterior end of the cell is located cytoproct where undigested food particles are excreted from the cell. An osmoregulatory organelle, the contractile vacuole, accumulates and releases collected fluid through contractile vacuole (CV) pores (Figure 2) (Wloga and Frankel 2012; Nusblat, Bright, and Turkewitz 2012; Frankel J. 2007).

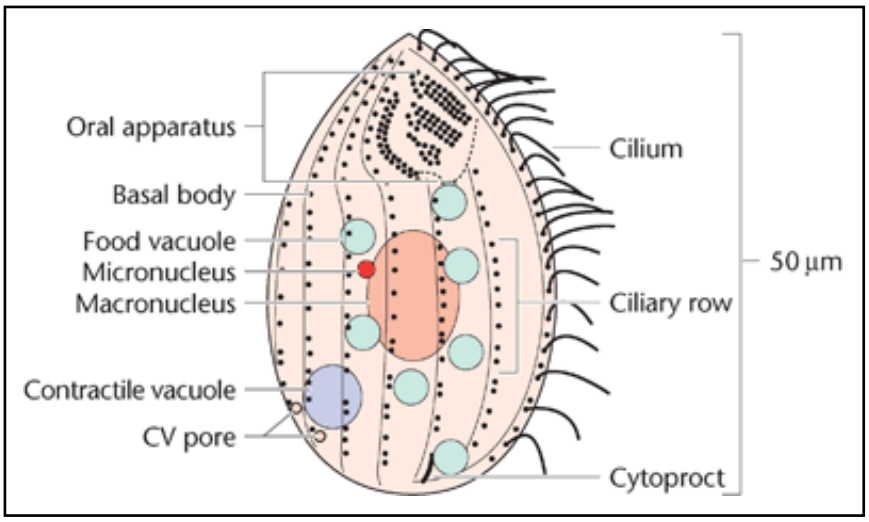

Figure 2. A schematic diagram of the organisation of *T. thermophila*. The anterior end of the cell is oriented upwards, and the ventral (oral) surface of the cell faces the viewer. 7 of the 18–21 ciliary rows are seen, with basal bodies shown as dots next to longitudinally oriented microtubule bands. Cilia are drawn emerging from the basal bodies of only one of the ciliary rows and omitted from the other rows. (Frankel J. 2007)

Having a doubling time of less than 3 h, *T. thermophila* is considered one of the fastest growing eukaryotes. It can readily grow to a high density on a wide range of media. Its life cycle (Figure 3) allows the use of conventional tools of genetic analysis, and molecular genetic tools suitable for gene function analysis. In addition, although it is unicellular, it possesses most of the conserved cell structures and molecular processes found in multicellular eukaryotes. Fundamental discoveries of molecular biology were made in this ciliate protozoan and it has been the first member of the phylum Ciliophora to have its complete somatic (MAC) genome sequenced (Eisen et al. 2006). The amplified MAC genome consists of about 104 Mb, that contain more than 27,000 protein coding genes. The *Tetrahymena* Functional Genomics Database (TetraFGD) is

available (Xiong et al. 2013) and it facilitates the study of the molecular bases of environmental responses, since data obtained in different environmental conditions can be easily compared.

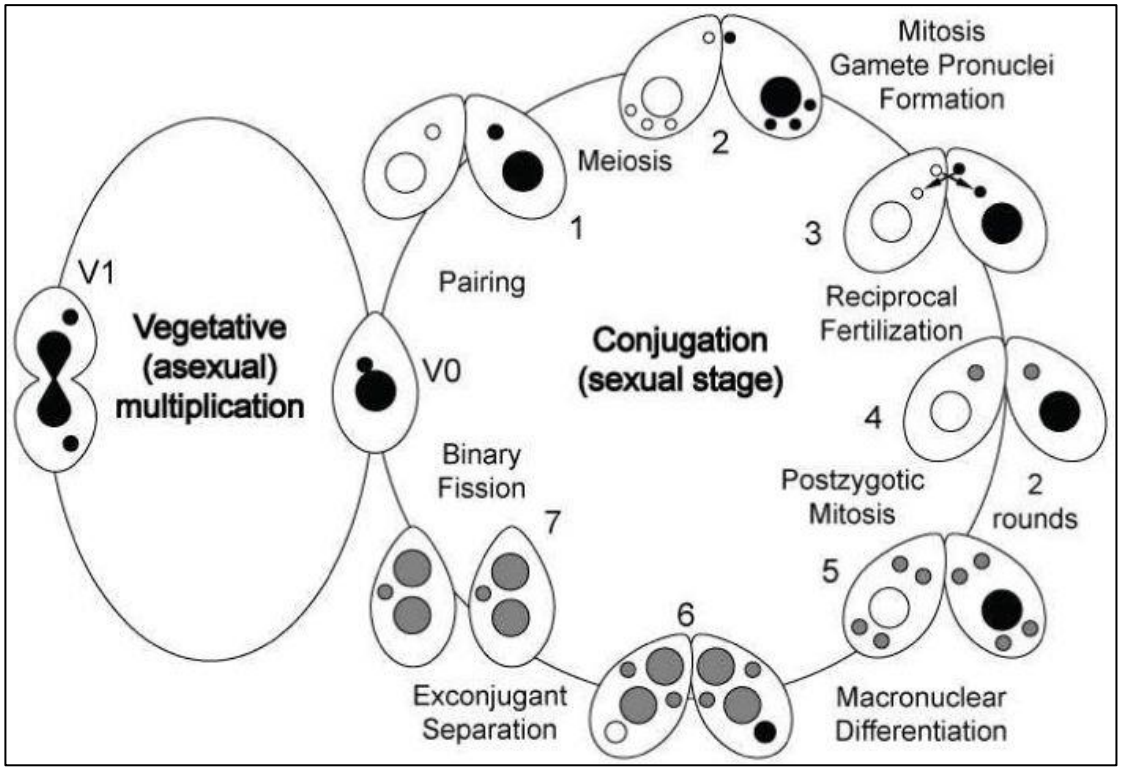

Figure 3. The *Tetrahymena* life cycle.
In the vegetative (asexual) multiplication. V0: vegetative cell. V1: cell undergoing binary fission. mic and MAC divide mitotically and amitotically, respectively. In conjugation, sexual (non-reproductive) stage of the life cycle, events occur in synchrony in each conjugant. 1. Starved cells of different mating type form pairs. 2. Meiosis generates four haploid products, three of which are resorbed by programmed nuclear death (PND). 3. The functional meiotic product undergoes mitosis, generating the haploid migratory (anterior) and stationary (posterior) gamete pronuclei. Migratory pronuclei are reciprocally exchanged. 4. Incoming migratory and resident stationary pronuclei fuse, generating the diploid fertilization nucleus. 5. The fertilization nucleus undergoes two rounds of mitosis, generating four diploid anlagen, which will differentiate into new polyploid MACs (anterior two) and new diploid mics (posterior two). 6. New MACs and mics take up a central position and characteristic arrangement. The parental MAC migrates posteriorly and is resorbed by PND. 7. Exconjugant cells separate. One new mic is resorbed by PND. Not shown: at the first post-conjugation cell division (after stage 7), a new MAC and a mitotic daughter of the surviving new mic are distributed to each daughter cell, thus restoring the vegetative one mic, one MAC nuclear organization (stage V0). From Orias et al. 2011.

The research work of my thesis is divided in three parts: two extensive Chapters and one Additional Project section as an appendix. In Chapter 1, I reported a study on the potential toxic effect of silver nanoparticles (AgNPs) accumulation in the environment, using *T. thermophila* as a model organism. This was started by a trilateral collaboration project including Estonia and China in the frame of the European

Cooperation in Science and Technology (COST) action BM1102 entitled “Ciliates as model systems to study genome evolution, mechanisms of non-Mendelian inheritance, and their roles in environmental adaptation” and coordinated by our laboratory.

Since the nano-industry has grown incredibly fast in the last few years (Ivask et al. 2014) and AgNPs are the most widely commercialized NPs that are used as antimicrobials in various consumer products (Bondarenko, Juganson, et al. 2013), concentrations of Ag ions are increasing in soil and water (Aueviriyavit, Phummiratch, and Maniratanachote 2014). The collateral dispersion of AgNPs in the environment may pose a threat to non-target organisms (Ivask et al. 2014). Therefore, to understand their toxicity mechanisms is essential for the design of more efficient nano-antimicrobials and for the design of biologically and environmentally benign nanomaterials.

In a previous study, only a few genes known to be involved in detoxification by oxidative stress were analysed by qPCR, after exposure of *T. thermophila* to AgNPs compared with the effect of a soluble silver salt, $AgNO_3$, to evaluate the contribution of the dissolved silver to the overall toxic effect of AgNPs (Juganson et al. 2017). This study showed that Ag-ions play a major role in the toxicity of AgNPs in *T. thermophila*. However, although oxidative stress related genes were overexpressed in AgNP-exposed *Tetrahymena*, the intracellular ROS level was not elevated, possibly due to *Tetrahymena's* very efficient antioxidant defense mechanisms that certainly involves other not yet investigated genes. The study also highlighted the relevance of the AgNPs toxicity for environmentally abundant organisms and still left open the question of which other genes are involved in the *Tetrahymena* response to AgNPs. Does the organization in AgNPs produce a different effect on the total gene expression regulation with respect to the effect induced by the silver ions released by the salt $AgNO_3$?

Therefore, to answer to these open questions and to obtain a global vision of the changes occurring in *T. thermophila* gene expression, we decided to perform an RNA sequencing analysis to compare the cell’s exposure to $AgNO_3$ and to AgNPs. For this purpose, I went to the The National Institute of Chemical Physics and Biophysics (NICPB) of Tallinn (Estonia) to repeat the toxicity test and to learn how to handle AgNPs. Then I joined the Protozoan Functional Genomics laboratory at the Institute of Hydrobiology (IHB), Chinese Academy of Sciences (CAS) in Wuhan (China). In this laboratory coordinated by Dr. Wei Miao, a deep RNA-sequencing study of *T. thermophila* during the three major stages of the life cycle (growth, starvation and conjugation) was performed and a *Tetrahymena* functional database (TetraFGD) was developed (Xiong et al. 2013). There, as a pilot experiment, I exposed *T. thermophila* to

two sub-lethal concentrations of silver compounds and collected the cells after 2 and 24 h to perform RNA isolation and RNA-sequencing. Differential gene expression was analyzed. The experimental sequences were compared with the controls to evaluate quantitatively the inhibition or increase of gene expression due to NPs or Ag ions. Then, I performed gene set enrichment analyses.
According to these results we decided to investigate further the 24 h exposure condition, which was considered more consistent for the biological model, also considering *T. thermophila* doubling time.
Later, at the University of Camerino, I performed a biological replica of the 24 h exposure experiment to obtain statistically significant data. I also validated my data with qPCR and all this work is reported in detail in Chapter 1 of my thesis.

The results presented in Chapter 1 confirmed that *T. thermophila* is a valid freshwater model organism to study stress response mechanisms. No similar models are provided so far from the marine environment. In order to propose a seawater counterpart, my attention was focused on *Euplotes* marine species. These species still require analysis of the genomes to have a reference for the environmental response studies.
Some steps in this direction have already been done in our laboratory in collaborations, through a first assembly of MAC genomes of *Euplotes crassus* and *E. focardii* that revealed important aspects of the translation machinery that frequently uses frameshifting (Lobanov et al. 2017). This analysis was followed by a more deeply annotation of the *Euplotes* MAC to which I am currently contributing (data not yet published). However, *Euplotes* mic sequences are still unknown as well as the details on the DNA rearrangements to produce the MAC genome by transpositions and DNA elimination. This gap is significant for our research because the mechanisms of the stress response are most probably influenced by the DNA rearrangements and transpositions. To address this gap in research, **I developed a technique to isolate *E. crassus* micronuclear chromosomes, as reported in Chapter 2 of this thesis**. This work was supported by The Marine Microbiology Initiative (MMI, funded by Gordon and Betty Moore foundation) and developed in collaboration with the University of Bern and the University of Connecticut.

Finally, in order to generate real valid genetic models with *Euplotes* species, comparable with the *Tetrahymena* model, it would be necessary to establish genetic manipulation techniques for functional studies and further applications. **In the**

Additional Project section of this thesis are listed different experimental approaches for *Euplotes* transfection. This study was also supported by MMI which aims to accelerate development of genetic tools to enable development of experimental model systems in marine microbial ecology.
The MMI also co-funded my PhD scholarship.

The three parts of my thesis are written to be used for three independent publications. I apologize for repetitions mainly present in the three introductions.

Chapter 1

1.0 Differential gene expression analysis in the freshwater ciliate *Tetrahymena thermophila* under stress by silver nanoparticles

1.1 Introduction and aims

Nanotechnology has become a major scientific challenge in the last few years, and researchers are continuing to discover unique properties and applications of nanomaterials. There are different purposes for the use of nanoparticles (NPs) in improving human health, environmental quality, computer science technology and general devices. They have already found their commercial applications in various products (Salata 2004). Nevertheless, the same properties which make NPs so attractive for their use in new products have also led to concerns that NPs may raise the risk for humans and the environment (Dubey et al. 2015). If compared to their respective bulk materials, NPs possess different physical and chemical properties, such as lower melting points, specific optical properties, mechanical strengths, specific magnetizations and higher specific surface areas. These properties proved to be attractive in various industrial applications (Horikoshi and Serpone 2013). Another property of NPs is a high surface-to-volume ratio, that means that a higher portion of the atoms, constituting the material, are located at the surface of the particle itself. These atoms are in a different bonding state compared to those located inside, more unbound and active, resulting in easy bonding with contacting materials and influencing the particle properties like reactivity, adsorption rate, solubility and bioavailability. There is increasing evidence that the unique desired physicochemical properties of NPs, which make nanomaterials more efficient in industrial applications, render these materials also more harmful to living organisms (Bondarenko, Juganson, et al. 2013). At least it is known that the major phenomena driving NPs toxicity are: dissolution, organism-dependent cellular uptake, induction of oxidative stress and consequent cellular damages (Ivask et al. 2014).

NPs are abundant in nature, as they are produced in many natural processes, including photochemical reactions, volcanic eruptions, forest fires, simple erosion, and by plants, animals and microbes (Buzea, Pacheco, and Robbie 2010). They can also be produced as a by-product of many human industrial and domestic activities, such as cooking, material fabrication and transport using internal combustion and jet engines. Different methods are successfully used to obtain AgNPs, including physical (Brobbey et al. 2017; He, Ren, and Chen 2017), chemical (Han et al. 2017; Khatoon et al. 2017), physicochemical (Verma et al. 2017) and biological synthesis approaches (Dutta et al.

2017; Singh et al. 2017). Recent results show that the properties of AgNPs largely vary based on the diversified synthesis processes (Akter et al. 2018).

Among the metal NPs, AgNPs have the highest degree of commercialization due to their known antimicrobial properties (Gopinath et al. 2010; Sotiriou and Pratsinis 2011; Youngs et al. 2012; Guo et al. 2014; Dubey et al. 2015). AgNPs are important in many industries, such as pharmaceuticals, cosmetics, textiles, surface coatings, electronic components, and food packaging (Nadagouda, Speth, and Varma 2011; Benn et al. 2010).

The use of silver as a bactericide and fungicide has been known for more than 20 centuries. In the 19th century its use in medicine was widespread, but it declined with the advent of antibiotics (Hobman and Crossman 2015). However, problems arising from the emergence of antibiotic resistant strains have led to renewed interest in silver as an antibiotic agent. Recent studies have confirmed that silver particles have effects against a wide spectrum of Gram-negative and Gram-positive bacteria and some also exhibit anti-fungal and antiviral activity (Rai, Yadav, and Gade 2009). Currently, nanosilver is perhaps the most preferred antimicrobial nanomaterial and AgNPs coatings have been used to inhibit the unwanted growth of bacterial biofilms in medical catheters, prostheses, heart valves, etc. (Ivask et al. 2014). Direct contact between a bacterial cell and AgNPs' surface enhances the toxicity of nanosilver. More specifically, cell-NP contact increases the cellular uptake of particle-associated Ag ions, generating toxicity (Bondarenko, Juganson, et al. 2013).

Even if AgNPs possess tremendous advantages that recommend them for novel biomedical applications, their toxicity recently became an intensive subject of study (Burdușel et al. 2018). AgNPs could be released into the environment during the production, transport, erosion, washing, and disposal of AgNPs products (Nowack and Mueller 2008). There are two major classes of products which expedite the release of AgNPs into the environment: the cosmetics and healing lubricants, which via dermal exposure are eventually released into water bodies while bathing, and the nanomaterials incorporated into textile fabrics, which upon washing are released into the water stream (Wiesner et al. 2009). The broad industrial applications have high potential to increase environmental exposure, and it may have negative impacts on the ecosystems and pose a threat to ‘‘non-target’’ organisms, such as natural microbes and aquatic biota (Fabrega et al. 2011; Anjum et al. 2013). AgNPs are of especially high concern, because

according to the recent scientific literature, aquatic species are extremely sensitive to AgNPs (Kahru and Dubourguier 2010; Bondarenko, Juganson, et al. 2013).

The intrinsic biocide activity of AgNPs is influenced by different physicochemical features, including morphology, size, dissolution states, surface charge, and surface coating (Durán et al. 2016; Koduru et al. 2018). Cell type, exposure time, and amount of AgNPs also play an important role in cytotoxicity. The shape of the AgNPs might influence the cellular uptake mechanism (diffusion, phagocytosis and endocytosis), which in turn modulates the cytotoxicity (AshaRani et al. 2009). The concentration range of NPs that can induce toxicity depends on the particle size, type of medium, temperature, and time of exposure (Kittler et al. 2010). More aggregated particles showed fewer effects on the cellular level (Lankoff et al. 2012). The NPs surface coating defines much of their bioactivity. Therefore, it is one of the main factors influencing the final toxicological outcome (Ashkarran et al. 2012; Lesniak et al. 2013). For better understanding of NPs toxicity, it is important to explore their physicochemical properties in the media where the biological toxicity tests are performed. As dissolution is one of the main contributors to the toxicity of AgNPs (Holl 2009; Casals, Gonzalez, and Puntes 2012), it is important to distinguish the effect of Ag ions and AgNPs (Johnston et al. 2010; Bouwmeester et al. 2011). Several studies have shown that AgNP-induced toxicity is triggered by microbial membrane damage, caused by the attachment of AgNPs on the cell surface, and subsequent structural and functional alterations (such as gap formation and membrane destabilization); and microbial sub-cellular structure damage, caused by the release of free Ag ions and subsequent reactive oxygen species (ROS) generation or essential macromolecule (proteins, enzymes, and nucleotides) inactivation (Foldbjerg et al. 2009; Durán et al. 2016; Akter et al. 2018).

Studies of the toxicity mechanisms are crucial for understanding the impact of NPs on the living organisms and to explore the functional and long terms applications of AgNPs. These studies are crucial for the design of more efficient nano-antimicrobials, and evenly for the design of nanomaterials that are biologically and/or environmentally benign throughout their life-cycle. The toxicity effects induced by AgNPs have been evaluated using numerous in vitro and in vivo models, but still there are contradictions in interpretations due to disparity in methodology tested (Dubey et al. 2015). Only a few specific genes have been found to be influenced specifically by NPs till now, and it

would be helpful to check the entire gene expression profile. Previous studies, that analyze the gene expression profile of unicellular eukaryotes exposed to AgNPs, lack a control for the evaluation of the Ag ions effect (Simon et al. 2013; Pan, Zhang, and Lin 2018).

In the current study we used the freshwater ciliate *Tetrahymena thermophila* to elucidate the environmental effects of AgNPs using next-generation sequencing technologies (Marioni et al. 2008). *T. thermophila* is an ecologically relevant model organism for nanotoxicology (Mortimer, Kahru, and Slaveykova 2014; Mortimer et al. 2014; Mortimer et al. 2016). It has the advantages of a short life cycle, cosmopolitan distribution, simplicity, high degree of reproducibility, and quick responses to environmental disturbances. In addition, although it is unicellular, it possesses most of the conserved cell structures and molecular processes found in multicellular eukaryotes. With this approach, we expected to obtain a global and reliable vision of the changes occurring in gene expression after exposure to Collargol (well characterized protein-stabilized AgNPs). We also compared the results with the effect of the soluble silver salt $AgNO_3$ to evaluate the contribution of the dissolved silver to the overall toxic effect of AgNPs. We tested two sub-lethal concentrations to evaluate the impact of these substances in viable cells after 24 h of exposure. The experimental RNA sequencing results were compared with the control to evaluate quantitatively the inhibition or increase of gene expression due to NPs or silver ions. Then, gene set enrichment analysis was performed and by complementing the differential expression analysis information with the *Tetrahymena* functional genomic database TetraFGD (Miao Laboratory 2017), we contributed to a better understanding of the mechanism of AgNPs toxicity.

1.2 Experimental procedures

1.2.1 Chemicals

Casein-coated colloidal silver NPs, called Collargol (batch N 297, from Laboratories Argenol S. L.) dispersed in MilliQ water at 1 g/L and $AgNO_3$ as a 0,1 M solution (Sigma-Aldrich) were kindly supplied by Dr. K. Juganson (NICPB, Tallinn, Estonia). Stock suspensions and solutions of silver compounds were stored at 4°C in the dark.

The dilutions of NPs and $AgNO_3$ were prepared in MilliQ water. Physicochemical characterization of this type of AgNP have been reported previously (Blinova et al. 2013; Bondarenko, Ivask, et al. 2013) and are summarized in Table 1 (Juganson et al. 2017).

Table 1. Physicochemical parameters of AgNPs (Collargol) (Modified by Juganson et al. 2017).

Parameter		Reference
Primary size (diameter)	14.6 ± 4.7 nm	(Bondarenko, Ivask, et al. 2013)
Coating	casein (30% of total mass)	(Bondarenko, Ivask, et al. 2013)
Shape according to TEM	Spherical	(Blinova et al. 2013)
Hydrodynamic diameter in MilliQ water	44 nm (pdi = 0.2)	(Bondarenko, Ivask, et al. 2013)
Zeta potential in MilliQ water	-42.7 mV	(Blinova et al. 2013)
Solubility in MilliQ water	6.9% at 5 mg/L in 24 h	(Käosaar et al. 2016)

TEM = transmission electron microscopy;
pdi = polydispersity index;
MilliQ water = ultrapure water.

1.2.2 *T. thermophila* strain CU428 culture

T. thermophila strain CU428, whose macronuclear genome is sequenced, was kindly supplied by Professor W. Miao (IHB, CAS, Wuhan, China).

100 µl of cells were transferred to 5 ml of SPP medium (2% protease peptone, 0,1% yeast extract, 0.2% glucose and 0.003% Fe-EDTA) supplemented with the antibiotics streptomycin sulphate and penicillin G, at 250 µg/ml (CARLO ERBA Reagents), and the fungicide amphotericin B at 1.25 µg/ml (CARLO ERBA Reagents). The cells were incubated at 30°C under shaking in a glass flask to grow o/n. Cell density was determined by counting the cells in a haemocytometer (Neubauer). To allow the counting, *T. thermophila* cells were fixed in 5% formalin (Mortimer, Kasemets, and Kahru 2010). When cells were in their logarithmic growth phase, with a doubling time of less than 3 h and a density of about 3 ~ 4×10^5 cells/ml, they were harvested by centrifugation at 1300 rpm for 5 min, at room temperature, and washed twice with MilliQ water.

1.2.3 Toxicity test

100 µL of *T. thermophila* culture, with a density of 10^6 cells/ ml, was added to 100 µL of test solutions (Collargol and $AgNO_3$ at different concentrations in MilliQ water) in triplicate. After 24 h exposure in 96-well plates at 25°C in the dark, the toxicity of Collargol and $AgNO_3$ was evaluated by measuring the cellular ATP content using the luciferin-luciferase assay (Sigma-Aldrich). The toxicity test has been performed In the Laboratory of Environmental Toxicology of the National Institute of Chemical Physics and Biophysics of Tallinn (Estonia) (Juganson et al. 2017; Jemec et al. 2016; Mortimer, Kasemets, and Kahru 2010).

1.2.4 Exposure of *T. thermophila* to silver compounds

T. thermophila CU428 strain was exposed to two sub-lethal concentrations of Collargol at 10 mg Ag/L and 20 mg Ag/L. $AgNO_3$ was used as a control for dissolved Ag ions, expected to be present in AgNP dispersions, respectively at 0.76 mg Ag/L and 1.5 mg Ag/L of $AgNO_3$, as previously determined by Juganson et.al. 2017.

In the current study, the exposures were conducted in MilliQ water to avoid interactions of media components with AgNPs and dissolved Ag ions. *T. thermophila*, is known to survive in water for at least a week (Koppelhus, Hellung-Larsen, and Leick 1994), and the starved cells undergo physiological, biochemical and molecular changes (Cassidy-Hanley 2012). However, these were not crucial factors in interpreting the results because the exposures to AgNPs and control chemicals occurred in the same conditions. Thus, any difference in gene expression or physiology of protozoa were assumed to be induced by the chemical exposures (Juganson et al. 2017).

The experiment has been performed in triplicate, in 6-well plates, non-tissue culture treated, with each well filled with 5 ml of *T. thermophila* culture, with a density of 5.5×10^5 cells/ml. 0.5 ml of the toxicants were added to the cells and 0.5 ml of MilliQ water to the controls; the final cell density was 5×10^5 cell/ml. The plates were incubated at 25°C in the dark. Visible light was avoided since it promotes the biosynthesis of AgNPs from Ag ions by *T. thermophila* (Juganson et al. 2013). The cells have been visualized with light microscope to monitor any changes.

1.2.5 RNA isolation

After 24 h exposure, 5.5 ml of *T. thermophila* culture, with a density of 5×10^5 cells/ml, were collected by centrifuging for 15 min at 3000 rpm. The cell pellet was dissolved in TRI Reagent (Sigma-Aldrich) and RNA was isolated according to the manufacturer's protocol. Agarose gel electrophoresis (1%), Nanodrop™ 1000 UV-Vis Spectrophotometer (Thermo Fisher Scientific) and Agilent 2100 Bioanalyzer (Agilent Technologies) were used to check the integrity, concentration and quality of RNA.

1.2.6 RNA sequencing and bioinformatic analysis

RNA-Seq data were obtained for 16 RNA samples of *T. thermophila* (4 samples without toxicants as controls, 3 samples stressed with Collargol 10 mg Ag/L, 3 samples stressed with Collargol 20 mg Ag/L, 3 samples stressed with $AgNO_3$ 0.76 mg Ag/L and 3 samples stressed with $AgNO_3$ 1.52 mg Ag/L) using an Illumina NextSeq 500 deep sequencing system (producing paired-end reads with an Illumina 1.9 encoding and 75 bp of read length). Library preparation was conducted with the Illumina TruSeq Stranded mRNA Library Preparation Kit and the reads quality, obtained from the sequencing, was checked using the FastQC software (Andrews S. 2010). Transcriptome assembly was performed using the Trinity package included in the "RNA-Seq De novo Assembly" section of Blast2GO (Grabherr et al. 2011), and a range from 84.7% to 85% of paired-end reads were mapped to the *T. thermophila* transcriptome obtained from the *Tetrahymena* Genome Database (TGD) (Stover et al. 2006).

Then the experimental samples were compared with the control to evaluate quantitatively the inhibition or increase of gene expression due to NPs or silver ions. The Differential Expression Analysis (DEA) was carried out using the edgeR package (TMM as normalization method and GLM likelihood ratio test as statistical test), included in the "Pairwise Differential Expression Analysis" section of Blast2GO (Robinson, McCarthy, and Smyth 2009) to calculate normalized fold change and counts-per-million (CPM) ensuring that expression levels for different genes and transcripts can be compared across runs. Stringent default criteria were set: genes showing $|\log2 (\text{fold change})| > 1$ and FDR < 0.05 in all the 3 replica are defined as Differential Expressed Genes (DEGs).

To assign gene function to contigs, the Gene Set Enrichment Analysis (GSEA) in Blast2GO (Götz et al. 2008) was performed.

1.2.7 Gene expression validation

Real-time PCR was used to confirm the effects of Collargol and $AgNO_3$ on the expression levels of selected genes listed in Table 2. Genes among the DGE list were selected considering their physiological expression profile in TetraFGD (Miao Laboratory 2017) and their associated biological role. Primers (Thermo Fisher Scientific) were designed using the Primer-BLAST application included in the NCBI website. The specificity of each primer set and annealing temperature to optimize PCR conditions and the fluorescence signal specificity of PCR amplification were confirmed through assessment of the product melting curves and the efficiency was between 94.7% and 102.4% with $r^2 = 0.99$.

800 ng of each RNA sample were retrotranscribed to cDNA using an iScript gDNA Clear cDNA Synthesis Kit (Bio-Rad) with iScript DNase to digest genomic DNA contamination. 0.3 µL (12.5 ng) of cDNA from each sample was used in qPCR using SsoAdvanced Universal SYBR Green Supermix and the CFX Connect Real-Time PCR Detection System (Bio-Rad). All reactions were performed in triplicate in a final volume of 20 µl. Thermal cycling conditions were as follows: 3 min denaturation at 98°C followed by 40 cycles for 15 sec denaturation at 98°C, 30 sec annealing and elongation at 60. 17S rRNA and Hsp705 genes were references for normalization, and the relative amount of mRNA was calculated using the $2^{-\Delta\Delta Ct}$ method (Livak and Schmittgen 2001).

Table 2. List of primers used in this study.

Gene name	Primer	Sequence
Ribosomal protein (GenBank: M10932.1)	17S*	FW: 5' GAATTGACGGAACAGCACACC 3' RV: 5' TCACTCCACCAACTAAGAACGGC 3'
HSP70a paralog SSA5 (TTHERM_00558440)	hsp705*	FW: 5' TCTCAAAGCCAGTCAAGAATGC 3' RV: 5' GCCATAAGCAATAGCAGCAGC 3'
Metallothionein (TTHERM_00660230)	MTT5*	FW: 5' GTCGGTTCAGGAGAAGGATGC 3' RV: 5' CCTCCAGGGCAGCATTCTTTAG 3'
Metallothionein (TTHERM_00241640)	MTT1*	FW: 5' GCGGATGTTGCTGCGTAAGTAA 3' RV: 5' GGGATCAAAGCAGCAGGGTTTA 3'
Metallothionein (TTHERM_00433530)	MTT4	FW: 5' GTTACTGAAAGCTGTGGCTGC 3' RV: 5' ATGCGGTTCTACTTCTAACTGTAAATGC 3'
Hemoglobin 1 (TTHERM_00535150)	HEM1	FW: 5' CTTACTATGCTTTTAGGAGGACCCAA 3' RV: 5' CATTGAGAATCTTGCCGCCAC 3'
CaTHepsin 12 (TTHERM_00561510)	CTH12	FW: 5' GAATGCCAGATAAATTGTCAGACGTG 3' RV: 5' CTCATAATAACGCTACTATTGGTCTAACTC 3'
HSP70a paralog SSA4 (TTHERM_01080440)	hsp703*	FW: 5' TCTAAAAGCTAAGTCCACGAAGTT 3' RV: 5' AACCAGTTAGAATTGCAGCCTATA 3'
26S proteasome subunit P45 fam. Prot. (TTHERM_00551090)	RPT6	FW: 5' GGACGCCGAAGAAAACTTAGGT 3' RV: 5' ACAAGGAAGCCTTAAAGAAGACTATTGG 3'
26S proteasome non-ATPase reg. subunit 6 (TTHERM_00191240)	RPN7	FW: 5' GGACGCCGAAGAAAACTTAGGT 3' RV: 5' ACAAGGAAGCCTTAAAGAAGACTATTGG 3'

*17S, hsp705, MTT5, MTT1 and hsp703 primers have been previously used in (Juganson et al. 2017).

1.2.8 Data analysis

For the toxicity test, the concentration-effect curves by the log-normal model were constructed and the EC_{50} values (the effective concentration that induces a response in 50% of the population) with 95% confidence intervals were calculated based on nominal concentrations using REGTOX software for Microsoft Excel™ (Vindimian 2001). All data were expressed as the average of three independent experiments ± standard deviation (SD).

For qPCR experiments the statistical analyses were performed with CFX Maestro™ Software for Bio-Rad CFX Real-Time PCR Systems. One-way ANOVA analyses were used to assess significant differences ($p < 0.01$).

1.3 Results and discussion

1.3.1 Toxicity test

We first verified that the toxicity of AgNPs increased in a concentration-dependent manner. Based on this result, we selected two sub-lethal concentrations of Collargol, at 10 mg Ag/L and 20 mg Ag/L. In order to see the effects of AgNPs in viable cells and evaluate their impact in the gene expression, only sub-lethal concentrations were used for the RNA-sequencing analysis after 24 h exposure. We decided to investigate the 24 h exposure condition since it was considered more consistent for the biological model considering its doubling time.

$AgNO_3$ was used as an ionic silver control, at concentrations equal to the dissolved silver concentration in the dispersion of AgNPs. Specifically, 0.76 mg Ag/L and 1.52 mg Ag/L of $AgNO_3$ were used (Figure 4).

T. thermophila is known to show a higher tolerance to Ag compounds (EC_{50} values in Table 3) than other freshwater invertebrates (Juganson et al. 2013; Juganson et al. 2017). Such results are remarkable considering that the toxicity assays were performed in MilliQ water, where the effects of the medium components on the Ag ions complexation and speciation were eliminated. These features are presumably a result of the adaption to high environmental concentrations of pollutants as protozoa are also present in the wastewater purification process (Esteban, Tellez, and Bautista 1991). Indeed, the EC_{50} after 24 h of exposure to the toxicants is higher than the EC_{50} after 2 h. Changes in the cells were visible in AgNPs exposed samples, where food vacuoles appeared dark after 2 h and 24 h exposure (Figure 5), due to internalised AgNPs After 24 h extracellular agglomerates of expelled food vacuole contents were also present (not shown in the picture).

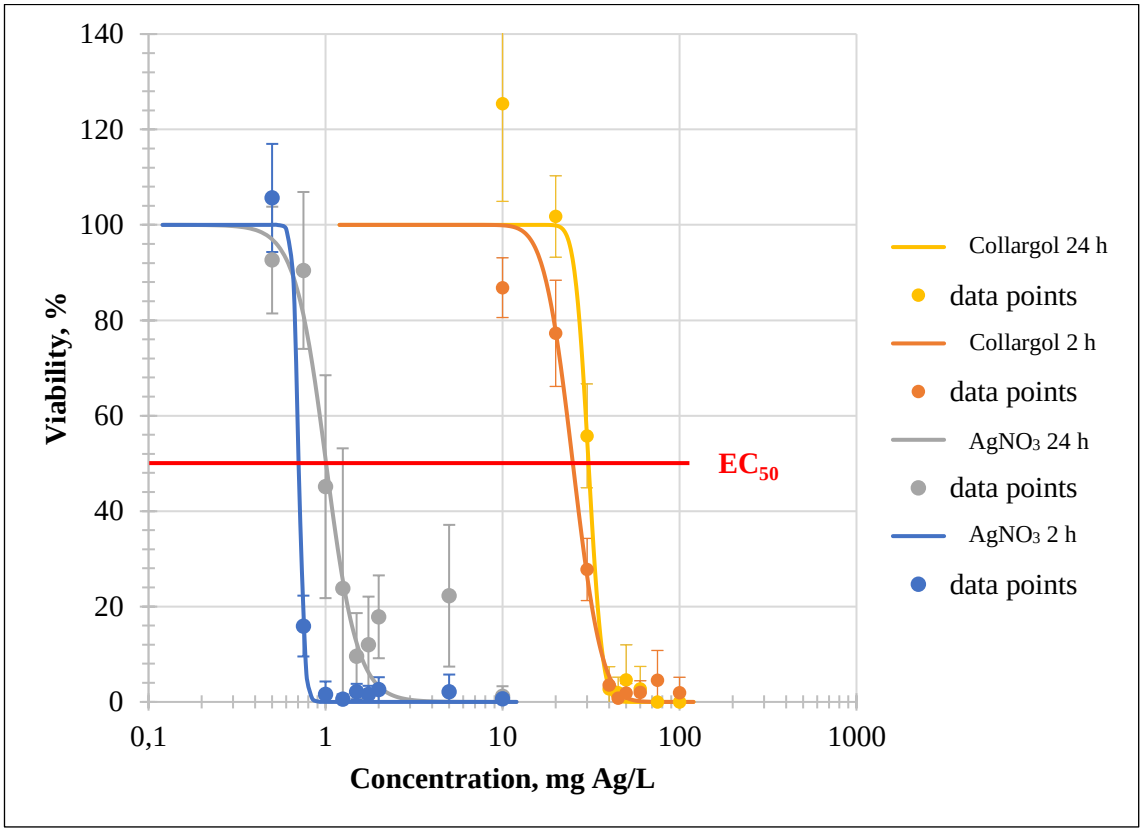

Figure 4. Viability of *T. thermophila* strain CU428 upon exposure to Ag compounds for 2 and 24 h**:** a concentration-effect analysis. Data points are the average values of at least 3 replicates and error bars indicate standard deviations. ATP concentration was used as a viability endpoint. Concentration-effect curves were generated using REGTOX software for Microsoft Excel™.

Table 3. EC_{50} values (95% confidence intervals).

	Collargol (mg Ag/L)		$AgNO_3$ (mg Ag/L)	
2 h	28.1	(25.2-32.4)	0.96	(0.87-0.98)
24 h	38.2	(33.1-45.8)	1.05	(1.02-1.17)

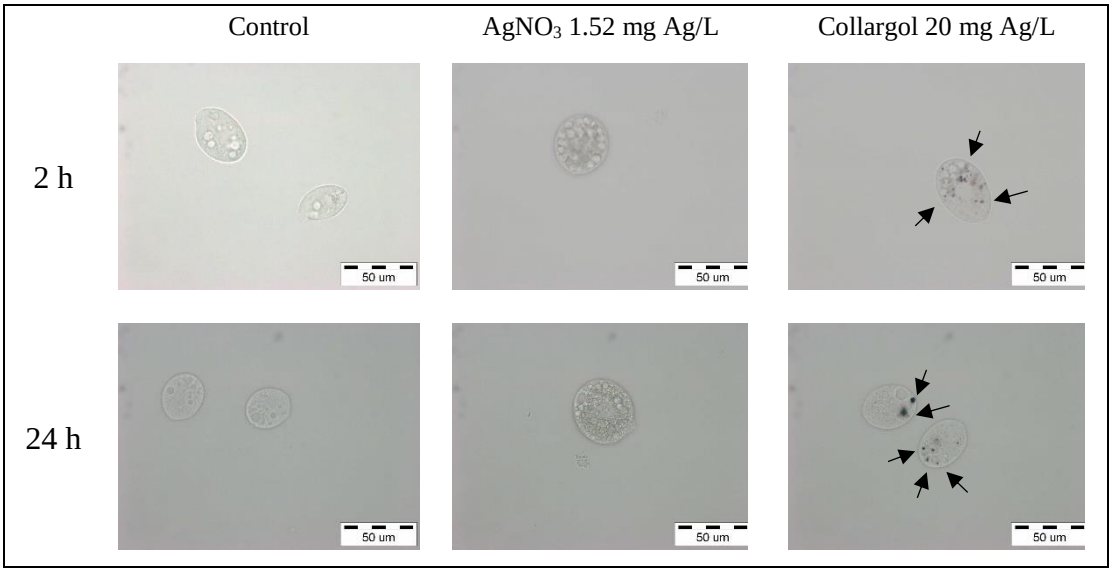

Figure 5. Images of live *T. thermophila* cells after 2 h and 24 h incubation in MilliQ water (Control) and exposure to sub-lethal concentration of 20 mg Ag/L of AgNPs or 1.52 mg Ag/L of $AgNO_3$ in MilliQ water. Arrows indicate food vacuoles filled with AgNPs (Collargol 20 mg Ag/L).

1.3.2 Differentially expressed genes (DEGs)

To explore the overall differences between the expression profiles of the different samples we clustered them in two dimensions using multi-dimensional scaling (MDS) plots. This is both an analysis step and a quality control step. The distance between each group of samples can be interpreted as the leading log-fold change between the samples for the genes that best distinguish that group of samples. (Chen, Lun, and Smyth 2016). The MDS plot shows that replicates from the same treatment cluster together, while samples from different treatments are well separated. In other words, differences between different treatments are larger than those within the same treatment, meaning that there are likely to be statistically significant differences between different treatments. It also verified the reproducibility and reliability of the RNA-Seq data. (Figure 6).

The expression profiles of the control samples are in agreement with the data available on TetraFGD (Miao Laboratory 2017) after 24 h of starvation. The number of DEGs at different concentration is shown in Figure 7. Both Ag compounds resulted in either inhibition and increase of gene expression. AgNPs clearly affected a higher number of genes. As summarised in Figure 7, there are 43 DEGs (37 up and 6 down-regulated) are in the sample exposed to Collargol 10 mg Ag/L and 271 DEGs (201 up and 70 down-

regulated) in the sample exposed to Collargol 20 mg Ag/L. 5 up-regulated genes in *T. thermophila* exposed to $AgNO_3$ 0.76 mg Ag/L and 54 DEGs (52 up and 2 down-regulaed) in the sample exposed to $AgNO_3$ 1.52 mg Ag/L.

32 DEGs changed their expression only in the incubation with $AgNO_3$, 24 genes are affected by both Ag compounds, 257 differentially affected genes are specifically affected by Collargol and most of them (223 genes) are triggered only at the highest Collargol concentration (Figure 8).

In many cases there is a linear tendency (of up or down regulation) that is concentration dependent. To obtain a global visualization of the results, we generated heatmaps for all DEGs under each stress condition (Figure 9 and Table 4).

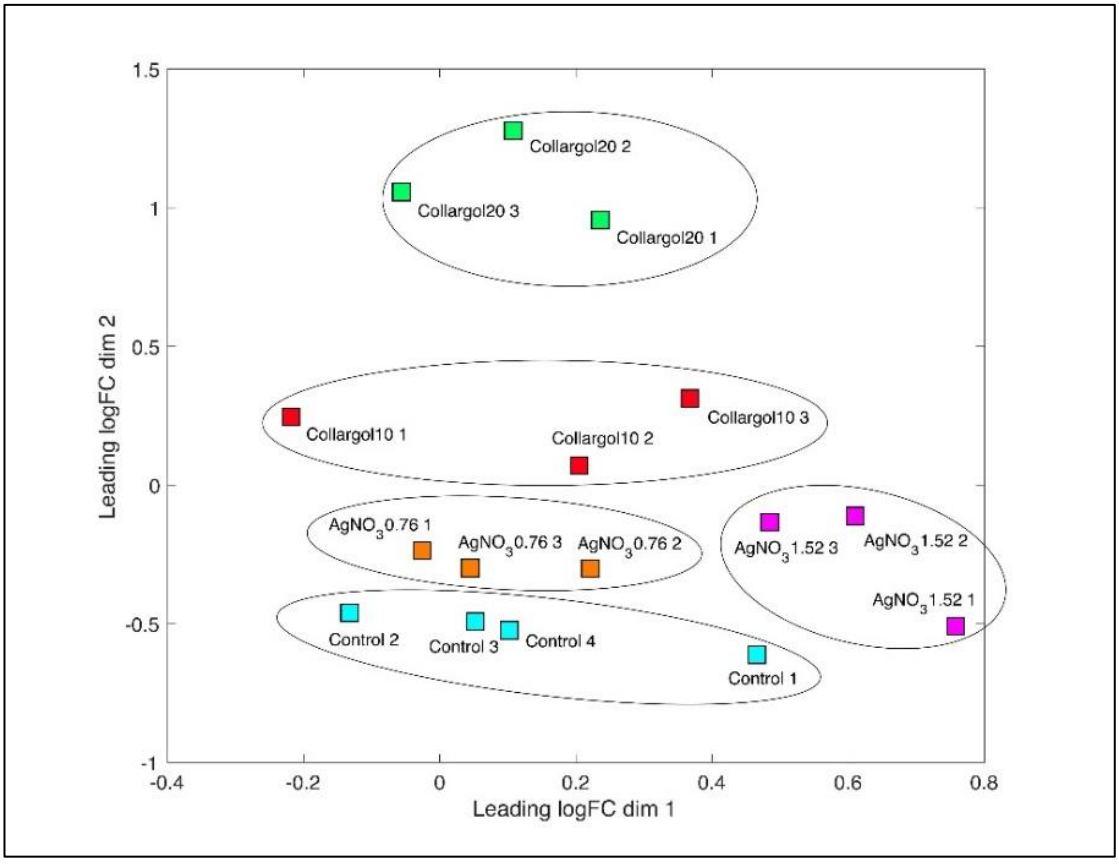

Figure 6. The MDS plot explores the overall differences between the expression profiles of the different samples. It shows similarity between samples in which distances correspond to leading log-fold-changes (Leading logFC) between each pair of RNA samples. The leading log-fold-change is the average (root-mean-square) of the largest absolute log-fold-changes between each pair of samples. Each colour indicates a different treatment and each square represents one treatment replica. The numbers in the data labels stand for the concentration of each compound.

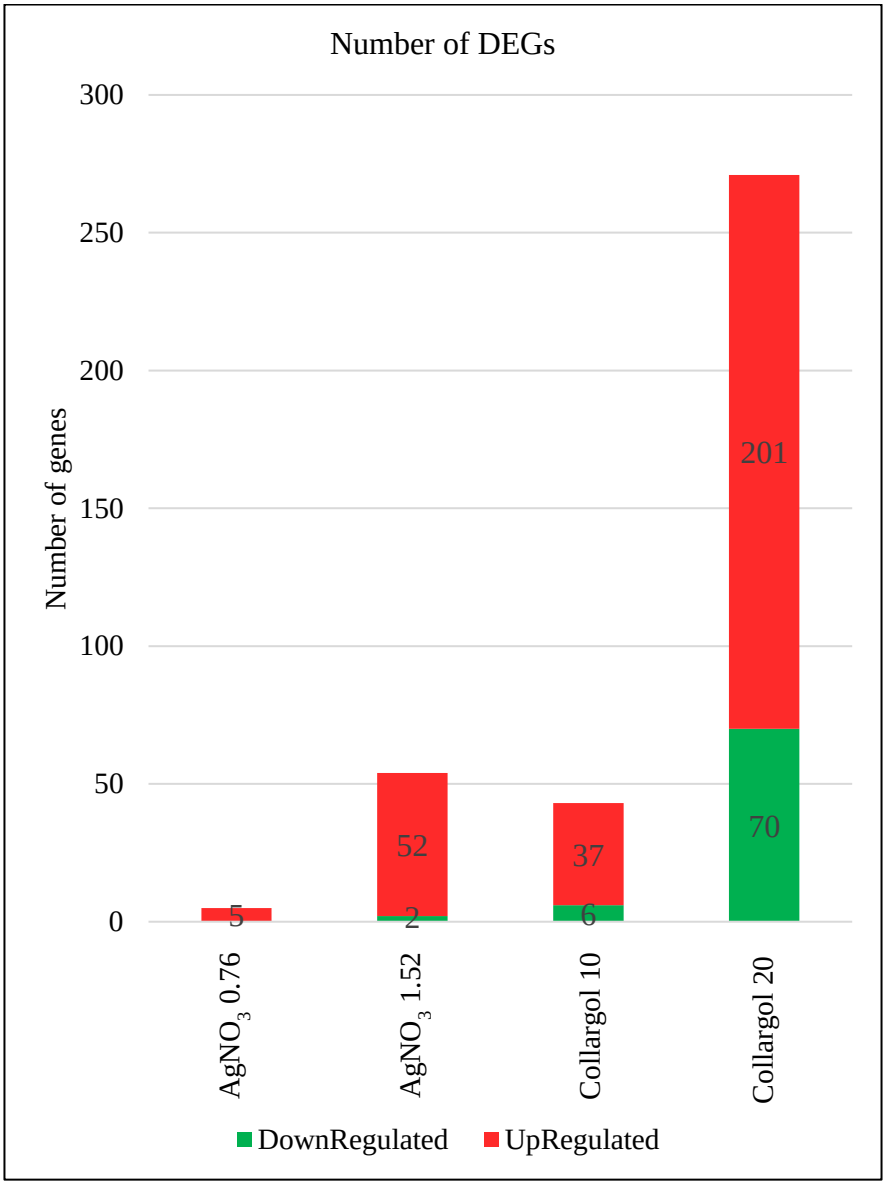

Figure 7. Histogram showing the number of DEGs in each compared group.

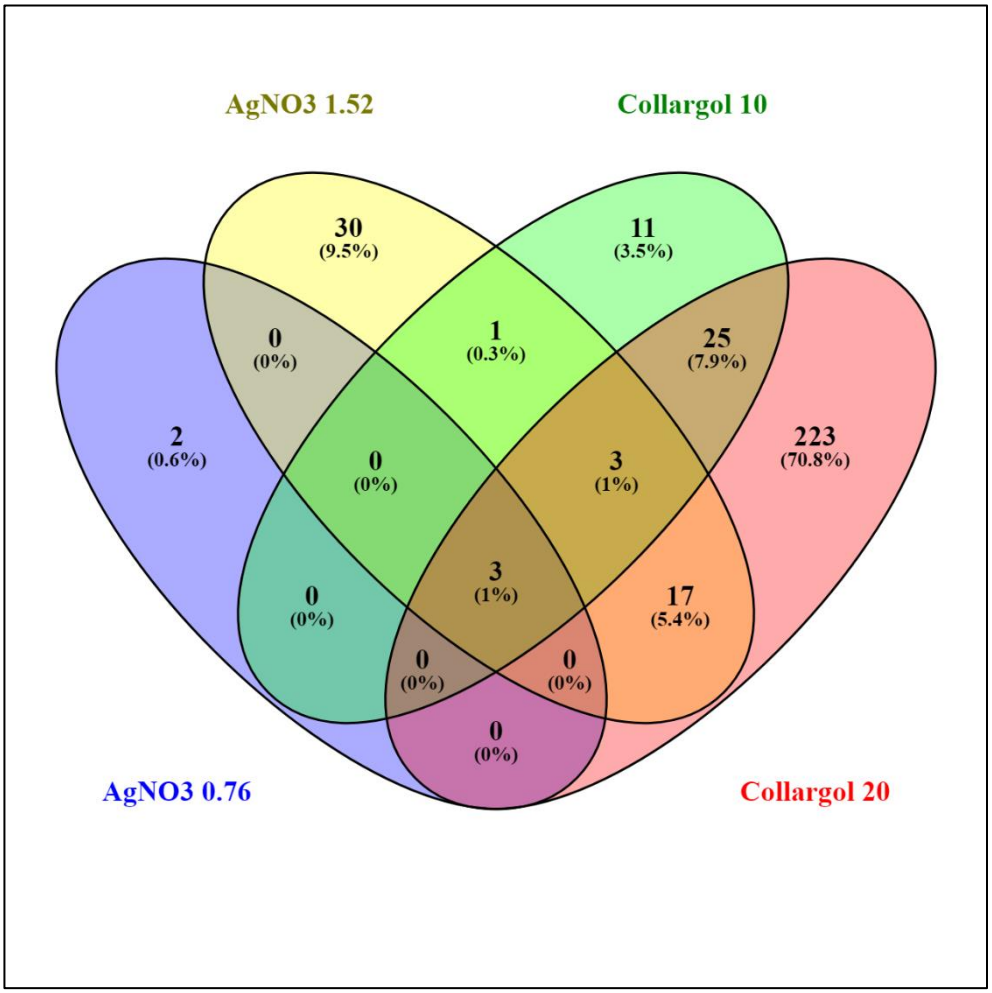

Figure 8. Venn diagram showing DEGs among the four treatments.(Oliveros 2015).

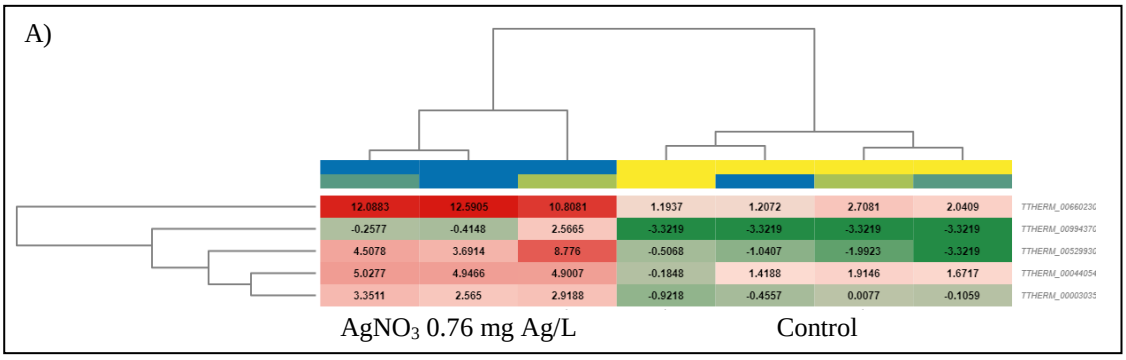

B)

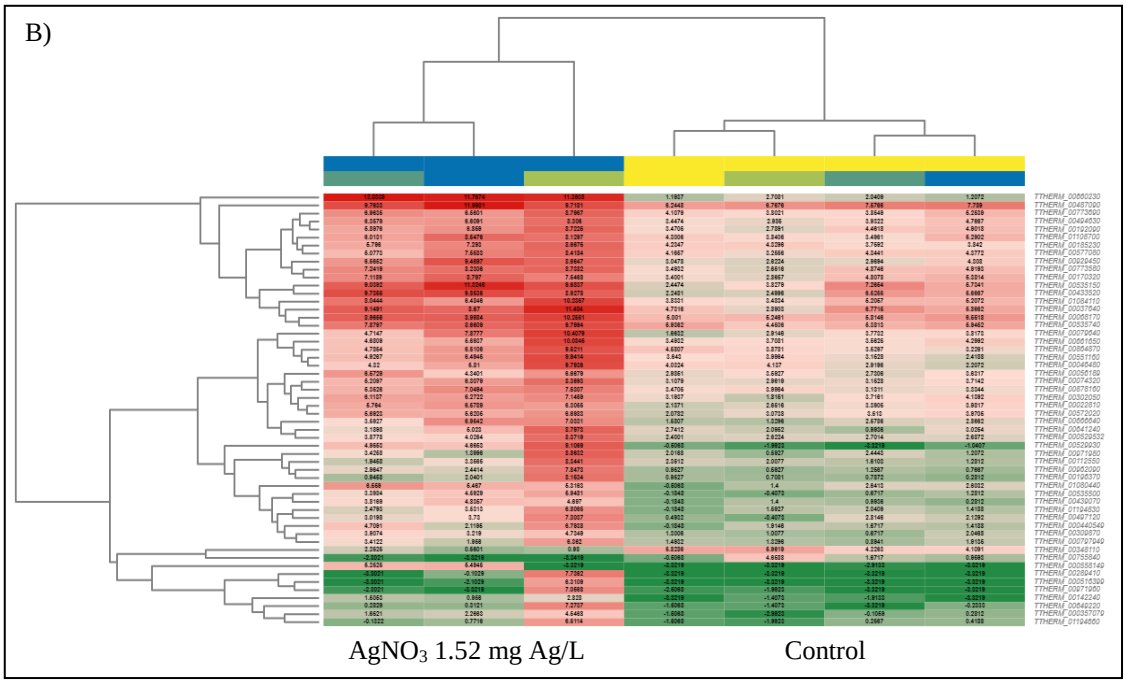

$AgNO_3$ 1.52 mg Ag/L Control

C)

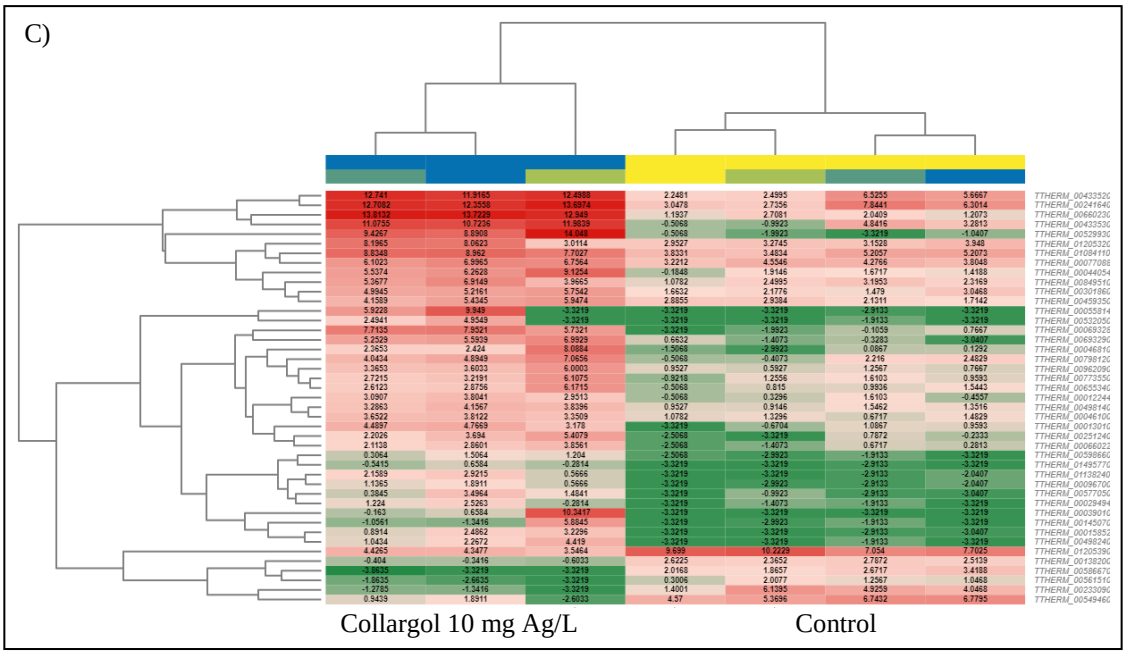

Collargol 10 mg Ag/L Control

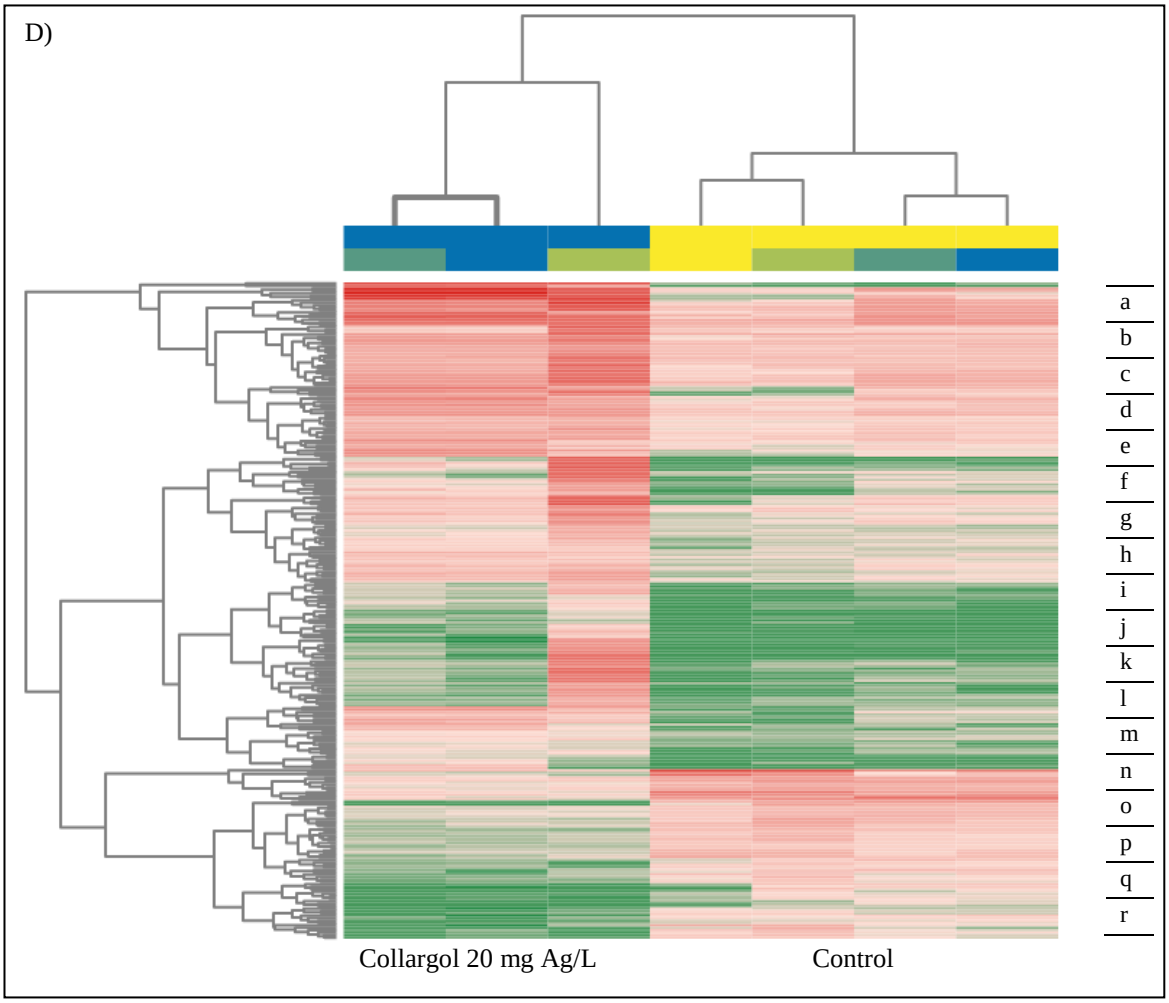

Figure 9. Heatmaps of all DEGs between different treatment groups. CPM values are used to generate the heatmaps. The numerical values are represented by a range of colours, from red (more expressed) to green (less expressed). The dendrograms added to the left and top side are produced by a hierarchical clustering method that takes as input the Euclidean distance computed between genes (left) and samples (top). A) $AgNO_3$ 0.76 mg Ag/L. B) $AgNO_3$ 1.52 mg Ag/L. C) Collargol 10 mg Ag/L. D) Collargol 20 mg Ag/L. The genes list is not displayed in Figure 9.D) because it is not readable; involved genes are listed in Table 4.

Table 4. List of 271 DEGs in Collargol 20 mg Ag/L shown in Figure 9.D.

a) 1 - 15	1	TTHERM_00529930
	2	TTHERM_00039010
	3	TTHERM_00433520
	4	TTHERM_00660230
	5	TTHERM_00640030
	6	TTHERM_00142420
	7	TTHERM_01222600
	8	TTHERM_00569200
	9	TTHERM_00251190
	10	TTHERM_00535150
	11	TTHERM_00058260
	12	TTHERM_00160810
	13	TTHERM_00804710
	14	TTHERM_00954210
	15	TTHERM_00462900
b) 16 - 30	16	TTHERM_00249710
	17	TTHERM_00572020
	18	TTHERM_00079730
	19	TTHERM_00529870
	20	TTHERM_00239090
	21	TTHERM_00191240
	22	TTHERM_00661650
	23	TTHERM_00420410
	24	TTHERM_01049360
	25	TTHERM_00102730
	26	TTHERM_00655970
	27	TTHERM_000723629
	28	TTHERM_00503800
	29	TTHERM_00890130
	30	TTHERM_00318570
c) 31 - 45	31	TTHERM_00497060
	32	TTHERM_00145060
	33	TTHERM_00227040
	34	TTHERM_00717640
	35	TTHERM_01205320
	36	TTHERM_00943020
	37	TTHERM_00446110
	38	TTHERM_00313800
	39	TTHERM_000529532
	40	TTHERM_00666640
	41	TTHERM_00138010
	42	TTHERM_00239310
	43	TTHERM_00526449
	44	TTHERM_00125160
	45	TTHERM_00572000

d) 46 - 60	46	TTHERM_00301860
	47	TTHERM_000043960
	48	TTHERM_000440549
	49	TTHERM_00365350
	50	TTHERM_00798120
	51	TTHERM_00211510
	52	TTHERM_00498240
	53	TTHERM_00069540
	54	TTHERM_00405450
	55	TTHERM_00234140
	56	TTHERM_000947489
	57	TTHERM_00798150
	58	TTHERM_00187230
	59	TTHERM_000566889
	60	TTHERM_01080440
e) 61 - 75	61	TTHERM_00160800
	62	TTHERM_00046090
	63	TTHERM_00961860
	64	TTHERM_00439070
	65	TTHERM_00030430
	66	TTHERM_000452041
	67	TTHERM_000735269
	68	TTHERM_00568050
	69	TTHERM_00475050
	70	TTHERM_00688790
	71	TTHERM_00773550
	72	TTHERM_00004850
	73	TTHERM_00151150
	74	TTHERM_00051700
	75	TTHERM_00962090
f) 75 - 90	76	TTHERM_00426250
	77	TTHERM_000723219
	78	TTHERM_00498140
	79	TTHERM_00526310
	80	TTHERM_01141610
	81	TTHERM_00535500
	82	TTHERM_00152000
	83	TTHERM_00971980
	84	TTHERM_00760550
	85	TTHERM_00575380
	86	TTHERM_00187260
	87	TTHERM_00460610
	88	TTHERM_00203060
	89	TTHERM_000158529
	90	TTHERM_01149330

g) 91 - 105	91	TTHERM_00142240
	92	TTHERM_000062688
	93	TTHERM_000242186
	94	TTHERM_000748977
	95	TTHERM_000066709
	96	TTHERM_00035350
	97	TTHERM_00927210
	98	TTHERM_000593091
	99	TTHERM_002653522
	100	TTHERM_00700930
	101	TTHERM_00798140
	102	TTHERM_000476968
	103	TTHERM_000661568
	104	TTHERM_00647470
	105	TTHERM_00895760
h) 106 - 120	106	TTHERM_00405500
	107	TTHERM_00476930
	108	TTHERM_00516420
	109	TTHERM_00649220
	110	TTHERM_00046110
	111	TTHERM_00895770
	112	TTHERM_00575390
	113	TTHERM_00971970
	114	TTHERM_00660280
	115	TTHERM_00476950
	116	TTHERM_00187210
	117	TTHERM_00654020
	118	TTHERM_00351140
	119	TTHERM_01227870
	120	TTHERM_00046810
i) 121 - 135	121	TTHERM_000693289
	122	TTHERM_00158000
	123	TTHERM_000660229
	124	TTHERM_00251240
	125	TTHERM_00693290
	126	TTHERM_000145038
	127	TTHERM_00146110
	128	TTHERM_00148970
	129	TTHERM_01736560
	130	TTHERM_00301870
	131	TTHERM_00837980
	132	TTHERM_00124060
	133	TTHERM_01105030
	134	TTHERM_00703880
	135	TTHERM_01495770

j) 136 - 150	136	TTHERM_00365360
	137	TTHERM_01138240
	138	TTHERM_000558149
	139	TTHERM_00191050
	140	TTHERM_000191059
	141	TTHERM_00532610
	142	TTHERM_00670280
	143	TTHERM_01456070
	144	TTHERM_00471760
	145	TTHERM_00191020
	146	TTHERM_00161860
	147	TTHERM_00390120
	148	TTHERM_00549460
	149	TTHERM_00233090
	150	TTHERM_00977590
k) 151-165	151	TTHERM_00825310
	152	TTHERM_00492540
	153	TTHERM_01193540
	154	TTHERM_00137880
	155	TTHERM_00384990
	156	TTHERM_00483520
	157	TTHERM_000346609
	158	TTHERM_00947340
	159	TTHERM_001205271
	160	TTHERM_01074540
	161	TTHERM_00937710
	162	TTHERM_01075750
	163	TTHERM_00734050
	164	TTHERM_00316060
	165	TTHERM_00942880
l) 166 - 180	166	TTHERM_00655340
	167	TTHERM_00433530
	168	TTHERM_00145070
	169	TTHERM_00241650
	170	TTHERM_00241640
	171	TTHERM_000357079
	172	TTHERM_00241620
	173	TTHERM_00695600
	174	TTHERM_00895750
	175	TTHERM_00508970
	176	TTHERM_00691090
	177	TTHERM_00143560
	178	TTHERM_000193311
	179	TTHERM_00998920
	180	TTHERM_00449110

m) 181 - 195	181	TTHERM_00549410
	182	TTHERM_00856670
	183	TTHERM_00518469
	184	TTHERM_01044650
	185	TTHERM_01085680
	186	TTHERM_00191060
	187	TTHERM_00144970
	188	TTHERM_00189610
	189	TTHERM_00654080
	190	TTHERM_00274510
	191	TTHERM_00185270
	192	TTHERM_00283760
	193	TTHERM_00929450
	194	TTHERM_00405400
	195	TTHERM_00878160
n) 196 - 210	196	TTHERM_00037640
	197	TTHERM_01150350
	198	TTHERM_00572010
	199	TTHERM_00927240
	200	TTHERM_01325790
	201	TTHERM_00476940
	202	TTHERM_00034920
	203	TTHERM_000032894
	204	TTHERM_00191140
	205	TTHERM_01194830
	206	TTHERM_00448660
	207	TTHERM_00780980
	208	TTHERM_00142430
	209	TTHERM_00803680
	210	TTHERM_00942980
o) 211 - 225	211	TTHERM_00624230
	212	TTHERM_00695650
	213	TTHERM_000401918
	214	TTHERM_001035531
	215	TTHERM_00861580
	216	TTHERM_00263660
	217	TTHERM_01346830
	218	TTHERM_00002770
	219	TTHERM_00577080
	220	TTHERM_00577050
	221	TTHERM_00133680
	222	TTHERM_00196220
	223	TTHERM_00829370
	224	TTHERM_00047580
	225	TTHERM_000327209

p) 226 - 240	226	TTHERM_00245120
	227	TTHERM_01135130
	228	TTHERM_01220430
	229	TTHERM_00013430
	230	TTHERM_00047530
	231	TTHERM_00105169
	232	TTHERM_00023959
	233	TTHERM_00129490
	234	TTHERM_00503780
	235	TTHERM_00616330
	236	TTHERM_00463290
	237	TTHERM_00509030
	238	TTHERM_00895640
	239	TTHERM_00655480
	240	TTHERM_00476810
q) 241 - 255	241	TTHERM_00551090
	242	TTHERM_00895630
	243	TTHERM_000784569
	244	TTHERM_001553979
	245	TTHERM_000487129
	246	TTHERM_00096700
	247	TTHERM_00721250
	248	TTHERM_00049120
	249	TTHERM_00274520
	250	TTHERM_00923150
	251	TTHERM_00157960
	252	TTHERM_000382269
	253	TTHERM_00599920
	254	TTHERM_00378450
	255	TTHERM_00300400
r) 256 - 271	256	TTHERM_00198520
	257	TTHERM_00861570
	258	TTHERM_00561510
	259	TTHERM_00773180
	260	TTHERM_00292110
	261	TTHERM_000580366
	262	TTHERM_000637329
	263	TTHERM_000455599
	264	TTHERM_00586670
	265	TTHERM_00204150
	266	TTHERM_00313580
	267	TTHERM_01060860
	268	TTHERM_00609380
	269	TTHERM_00559950
	270	TTHERM_00467450
	271	TTHERM_00816260

1.3.3 Gene Set Enrichment Analysis (GSEA)

The GSEA of these DEGs indicated their involvement in various pathways. Most of the DEGs reported here, are induced by exposure to AgNPs. These genes are involved in various biological processes (BP) and molecular functions (MF), *e.g.*: transport, ion transport, response to stress and to stimulus, protein phosphorylation, oxidation-reduction process, response to oxidative stress and glutathione peroxidase activity (Figure 10).

Both AnNPs and $AgNO_3$ treatments trigger the DEGs involved in ion binding mechanisms and the proteolysis pathway (Figure 11). The enrichment of proteolysis pathway genes is a signal of protein damage that is possibly caused by the oxidative damage produced by Ag compounds (Pan, Zhang, and Lin 2018).

$AgNO_3$ treatment is specifically associated with the upregulation of genes encoding vesicle-mediated transport membrane proteins (Figure 12) which can be explained by the fact that the ciliate *T. thermophila* is able to internalize metal ions by phagocytosis. This means that the cell is exposed not only through its cell surface but also via internal membranes (Juganson et al. 2017; Mortimer, Kasemets, and Kahru 2010; Kahru et al. 2008).

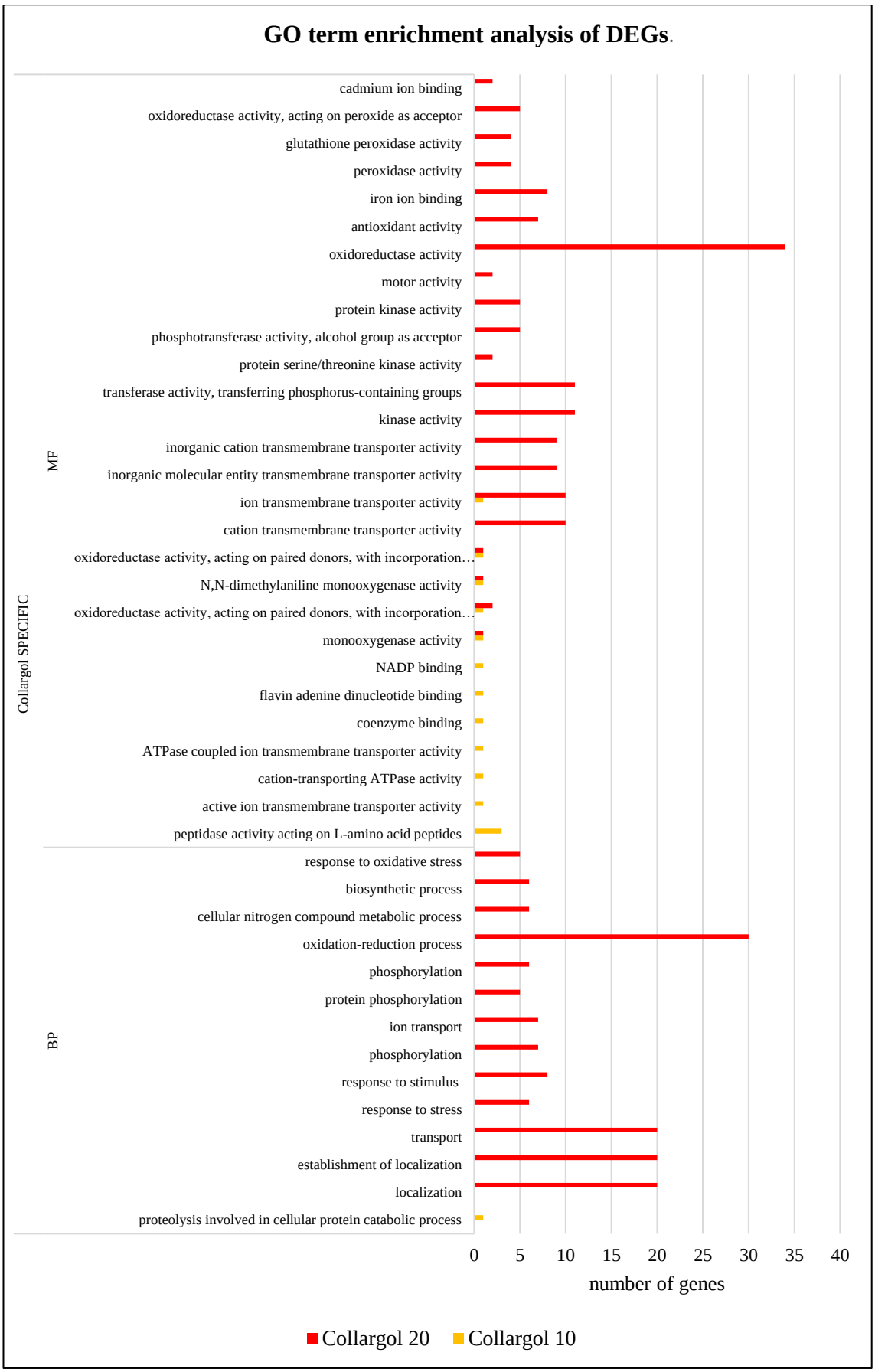

Figure 10. Collargol-specific GO term enrichment analysis of DEGs. GO terms are divided in molecular function (MF) and biological processes (BP) GO categories.

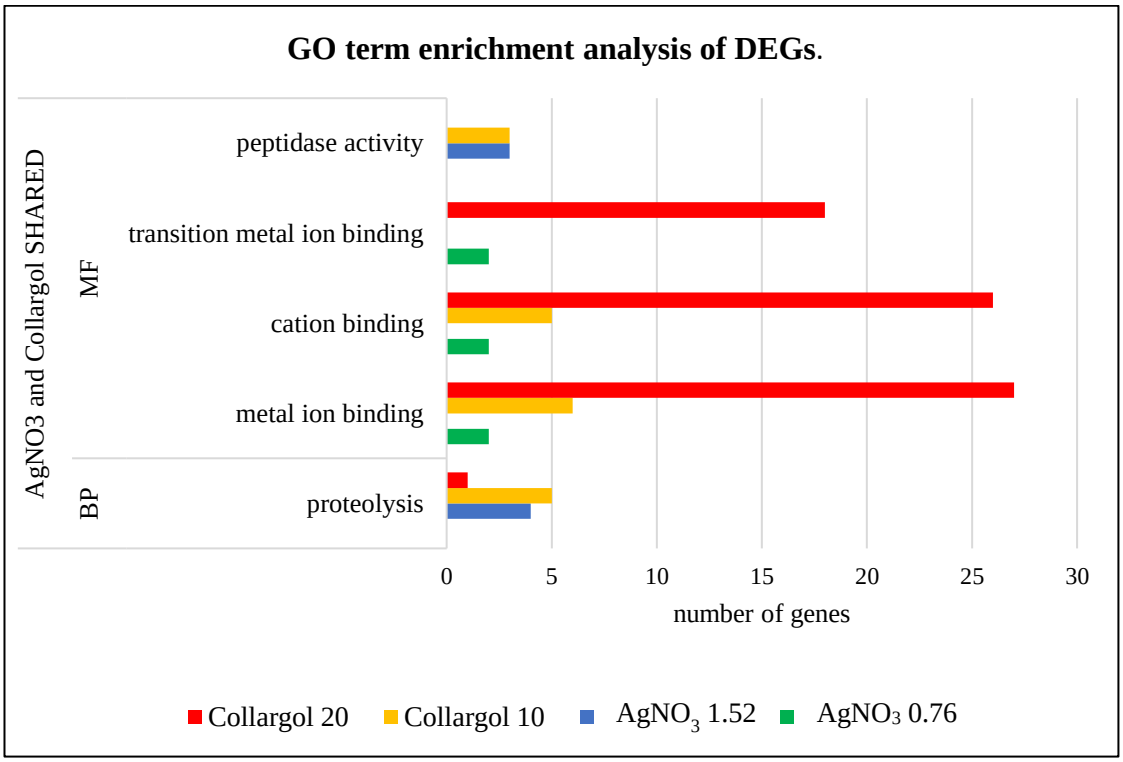

Figure 11. $AgNO_3$ and Collargol shared GO term enrichment analysis of DEGs. GO terms are divided in molecular function (MF) and biological processes (BP) GO categories.

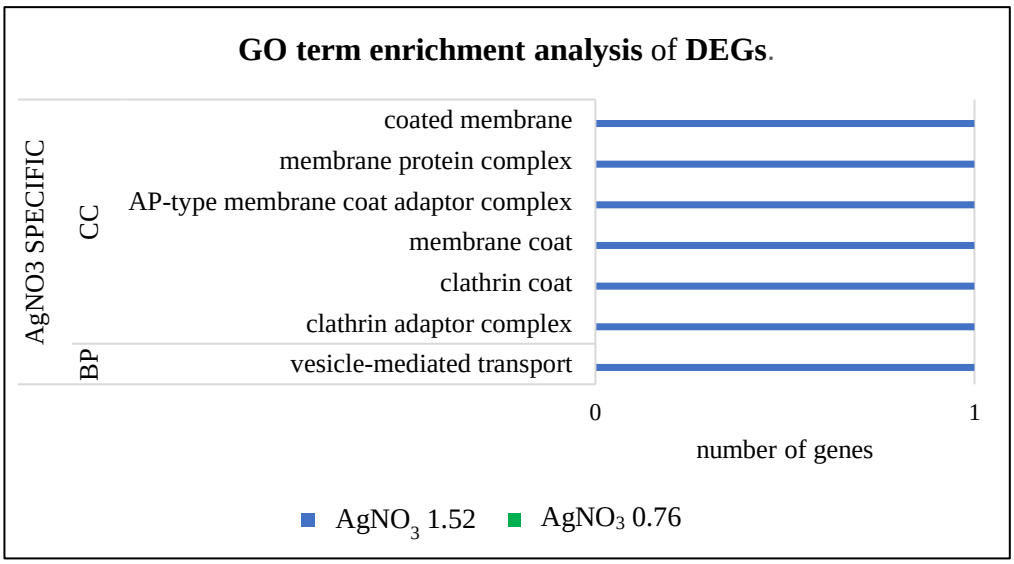

Figure 12. $AgNO_3$-specific specific GO term enrichment analysis of DEGs. GO terms are divided in cellular components (CC) and biological processes (BP) GO categories.

.

1.3.4 Generation of oxidative stress by AgNPs

Oxidative stress is a cellular damage mechanism caused by a high concentration of free radicals, including the so-called reactive oxygen species (ROS). It occurs when the formation of free radicals is higher than their elimination. All organisms have mechanisms to detoxify the oxidants or to repair the damage caused by ROS, including superoxide dismutases, catalases, peroxidases, glutathione, thioredoxin and heat shock proteins (Koduru et al. 2018), which are quite conserved from prokaryotes to eukaryotes. The expression of the genes coding these proteins (oxidative stress genes) is induced by changes in the concentration of ROS (Espinosa-Diez et al. 2015).

These results suggest that AgNPs induce oxidative stress in the cells in a concentration dependent way, since, thioredoxin and glutathione reductase family proteins and GPX are up-regulated compared to untreated cells, especially at the highest AgNPs concentration (Figure 13, Table 5). *Tetrahymena* haemoglobin is a small oxygen-binding hemoprotein evolved with a truncated structure. Various biochemical functions other than the more conventional oxygen transport or storage have been proposed for this primitive or ancient hemoglobin, but the precise in vivo activity is still unclear (Wittenberg et al. 2002). The HEM1 gene is not only upregulated under AgNPs stress, but also by $AgNO_3$ 1. 52 mg Ag/L (Figure 13, Table 5), thus indicating that this gene plays an important role in the oxidative stress response, more than what has been described so far.

Another route could be the activation of an inflammatory response, or a response to stimulus. Although the exact mechanism whereby NPs induce pro-inflammatory effects is not known, it has been suggested that phagocytized NPs can induce an inflammatory response, consequently leading to generation of reactive oxygen species and reactive nitrogen species. The oxidative stress results in the release of pro-inflammatory mediators or cytokines in higher organisms.

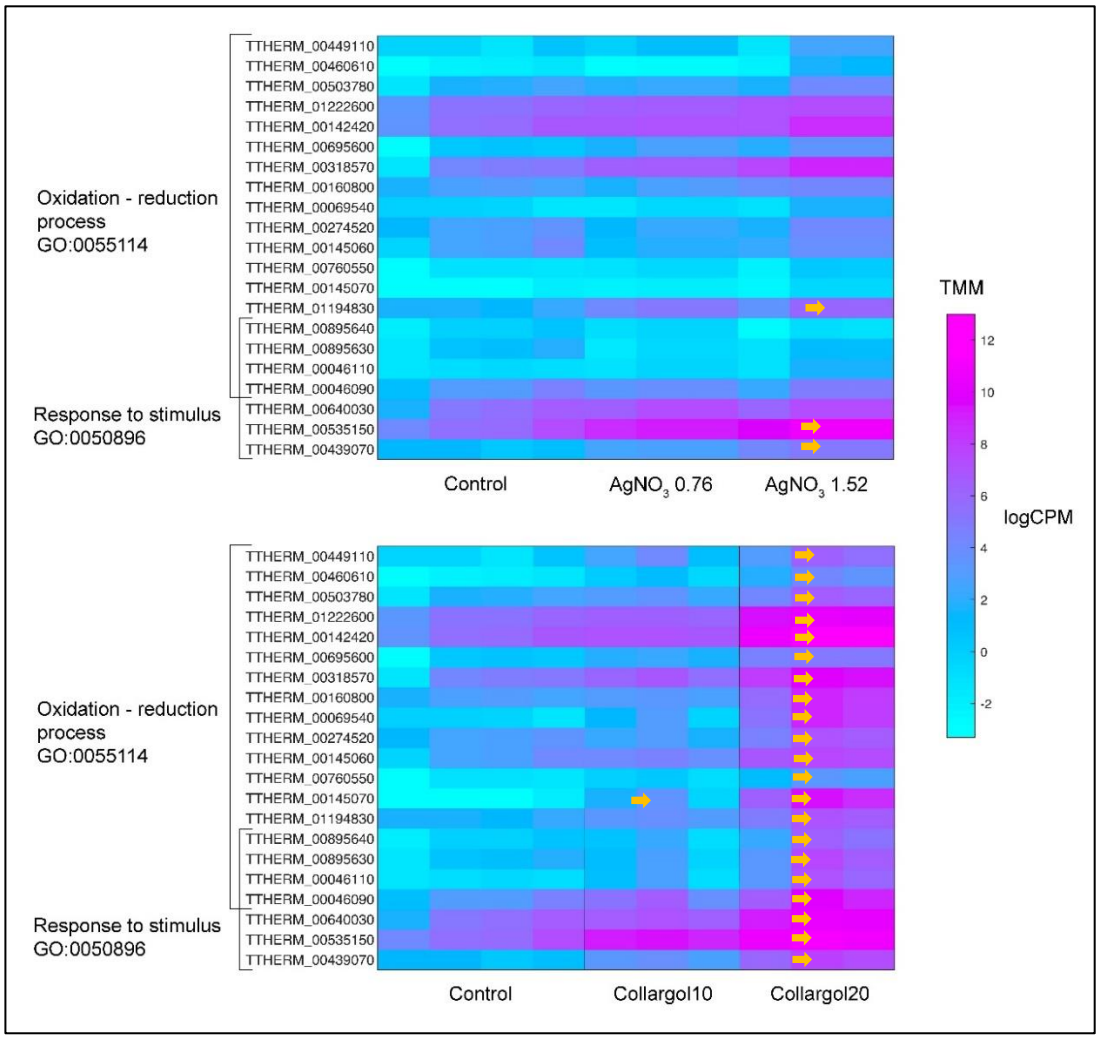

Figure 13. Heatmaps of DEGs of two top scored Biological Processes between different treatment groups: Oxidation–reduction process and Response to stimulus. CPM values are used to generate the heatmaps. Yellow arrows indicate genes that are significantly upregulated with at least 4-fold change. The colours range indicates the gene expression levels from purple (high expression) to light blue (low expression) The genes common names are listed in Table 5.

Table 5. Named DEGs in two of the top scoring Biological Processes displayed in the heatmaps in Figure 13. Blue box = Oxidation–reduction process GO:0055114. Black box = Response to stimulus GO:0050896.

TTHERM_00449110	Catalytic LigB subunit of aromatic ring-opening dioxygenase family protein
TTHERM_00460610	Catalytic LigB subunit of aromatic ring-opening dioxygenase family protein
TTHERM_00503780	Catalytic LigB subunit of aromatic ring-opening dioxygenase family protein
TTHERM_01222600	thioredoxin and glutathione reductase family protein
TTHERM_00142420	thioredoxin and glutathione reductase family protein
TTHERM_00695600	thioredoxin and glutathione reductase family protein
TTHERM_00318570	citrate synthase
TTHERM_00160800	oxidoreductase, FAD/FMN-binding family protein
TTHERM_00069540	oxidoreductase, FAD/FMN-binding family protein
TTHERM_00274520	oxidoreductase, aldo/keto reductase family protein
TTHERM_00145060	Oxidoreductase, zinc-binding dehydrogenase family protein
TTHERM_00760550	Oxidoreductase, zinc-binding dehydrogenase family protein
TTHERM_00145070	Oxidoreductase, zinc-binding dehydrogenase family protein
TTHERM_01194830	BBC23 AhpC/TSA family protein
TTHERM_00895640	GPX4 (Glutathione PeroXidase)
TTHERM_00895630	GPX6 (Glutathione PeroXidase)
TTHERM_00046110	GPX7 (Glutathione PeroXidase)
TTHERM_00046090	GPX8 (Glutathione PeroXidase)
TTHERM_00640030	conserved hypothetical protein
TTHERM_00535150	HEM1 (HEMoglobin 1)
TTHERM_00439070	protozoan/cyanobacterial globin family protein

Nevertheless, more than half of the significant DEGs are not associated with any gene ontology (GO) term nor to a Kyoto Encyclopedia of Genes and Genomes (KEGG) value and are annotated in the TGD (Stover et al. 2006) as hypothetical or putative proteins, without identified related proteins in other organisms (Figure 14 and Table 6). This means that the effects conveyed by AgNPs do not only activate the regular and known response to stress, response to stimulus, oxidation-reduction and transport pathways (just to name some process) but it triggers also other proteins which are not characterized yet. These results open the way to the discovery of new mechanisms of stress response by metals. Considering the fact that *T. thermophila* is a model organism easily manipulated by gene transfection and reverse genetics, the investigation of new gene function is challenging but possible.

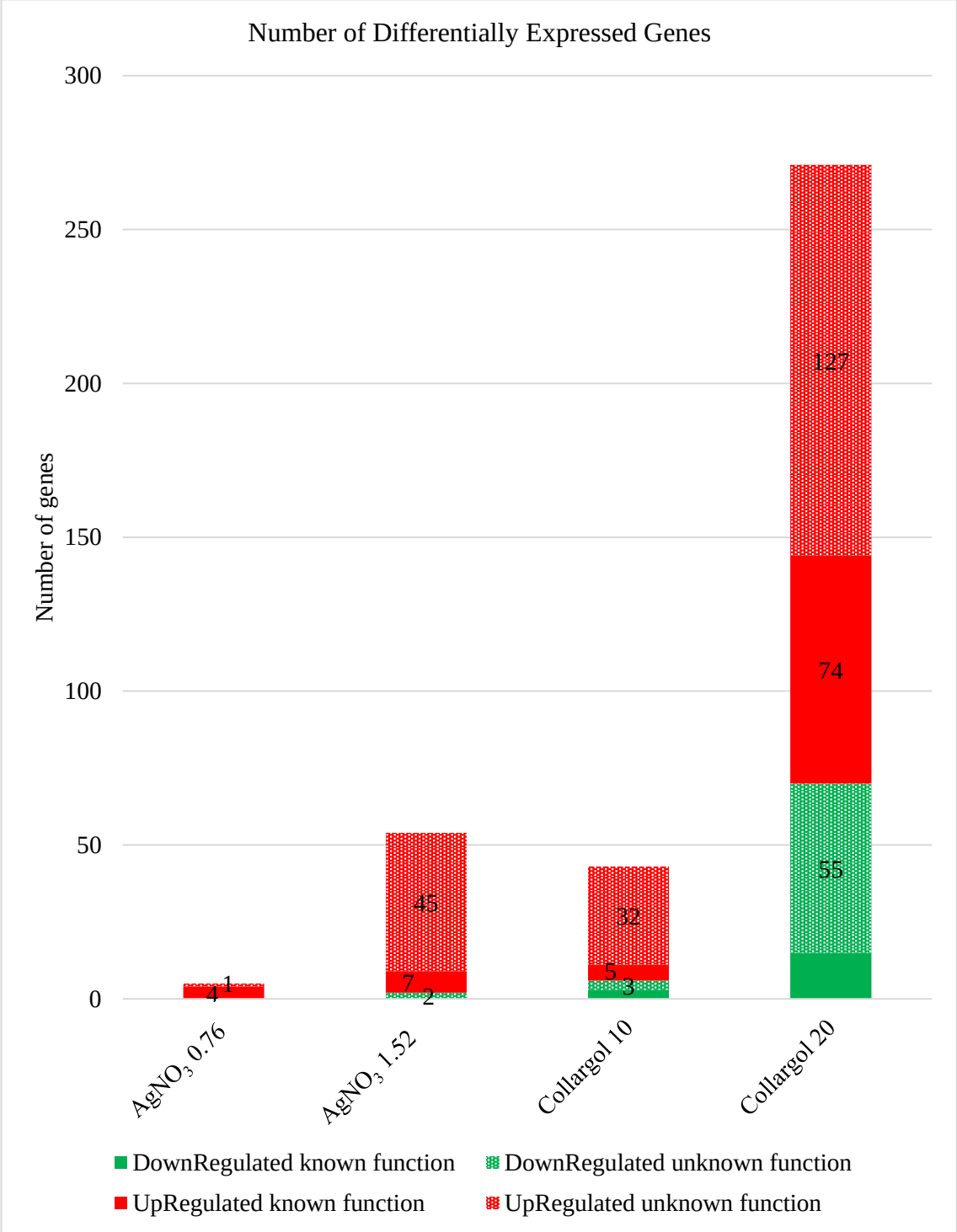

Figure 14. Number of DEGs with known and unknown function.

Table 6. Number of DEGs with known and unknown function.

				Number of DEGs		
$AgNO_3$	0,76	DownReguated	unknown function	0	0	5
			known function	0		
		UpRegulated	unknown function	1	5	
			known function	4		
	1,52	DownReguated	unknown function	2	2	54
			known function	0		
		UpRegulated	unknown function	45	52	
			known function	7		
Collargol	10	DownReguated	unknown function	3	6	43
			known function	3		
		UpRegulated	unknown function	32	37	
			known function	5		
	20	DownReguated	unknown function	55	70	271
			known function	15		
		UpRegulated	unknown function	127	201	
			known function	74		

1.3.5 Gene expression validation

To validate the expression data obtained from RNA-Seq, 8 mRNAs that showed different expression patterns and are known to be involved in important biological functions were selected for further analysis using RT-qPCR (Figure 15). The qPCR results showed a strong correlation with the RNA-Seq analysis (R^2 = 0.9506, Figure 17). For each gene, the expression count values of RNA-Seq exhibited an expression profile very similar to that obtained by qPCR for all tested treatments (Figure 16).

17S rRNA and hsp705 were used as housekeeping genes. I selected *hsp705* as a control housekeeping gene not only due to my results in DGE analysis, but also in agreement to Juganson et al., 2017, which stated that there was no change in *hsp705* expression in *T.*

thermophila strain CU428 after 24 h incubation with Collargol and $AgNO_3$. Hsp703, MTT5, MTT1 were also previously investigated and by this qPCR analysis I could confirm both the previous data by Juganson et al., 2017 and the RNA-seq data of the present study. Both Ag compounds induced MTT5 up-regulation in a significant way. Moreover, MTT1 and MTT4 were up-regulated under these conditions, but with a higher fold change in the AgNPs stressed samples. The 5 *T. thermophila* metallothioneins (MTT) are usually divided in two groups according to the metal binding preferences that they show. MTT4 responds better to copper, while MTT1 and MTT5 (cadmiun induced) respond to a more general stress (Diaz et al. 2007; Espart et al. 2015).

Cathepsin 12 (CTH12) DEGs validation confirms that its expression in down-regulated in cells exposed to Collargol 20. *T. thermophila* has 125 CTH genes. Two of them, CTH 12 and CTH 7, are among the DEGs in Collargol 20: cth12 is downregulated and cth7 is upregulated. Cathepsins are proteases that, in response to certain signals, are released from the lysosomes into the cytoplasm where they trigger apoptotic cell death via various pathways (Chwieralski, Welte, and Bühling 2006). CTH12 is functionally associated to the proteolysis biological process together with other DEGs. Some of them are up-regulated others down-regulated by the presence of AgNPs.

The RPT6 and RPN7 genes, encode components of the proteasome regulatory subunit N7 as it is shown in the schematic representation resulting from the KEGG Mapper – Search Pathway tool (Kanehisa et al. 2016) (Figure 18). These genes are both up-regulated only in Collargol 20 treated cells, suggesting that such an induction in proteasome regulatory subunit expression is justified by the oxidative damage caused by AgNPs that may produce protein fragments that need to be removed, as this has been hypothesized for *E. crassus* (Pan, Zhang, and Lin 2018).

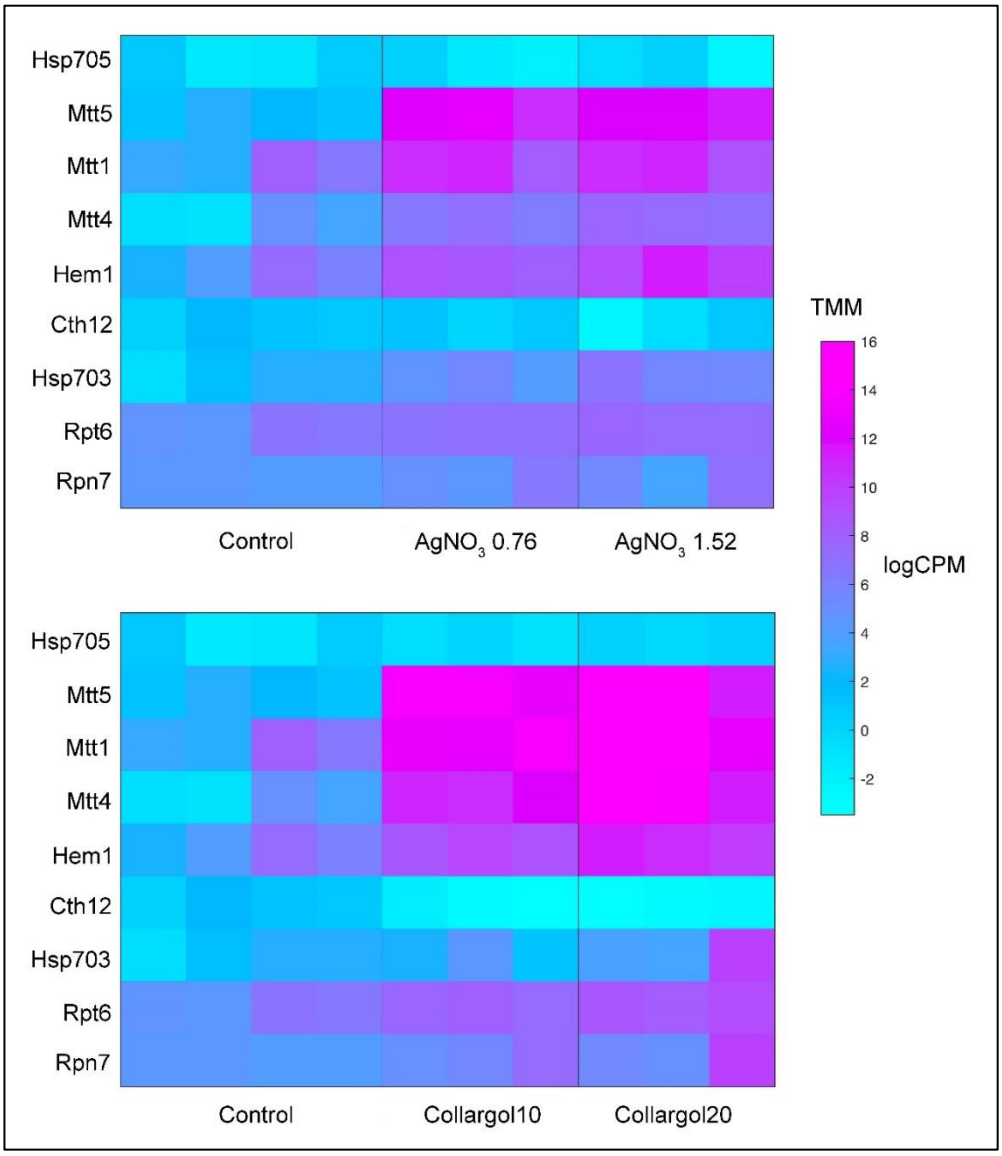

Figure 15. Heatmap illustrating the expression level of several DEGs in all samples exposed to the Ag compounds based on RNA-Seq.

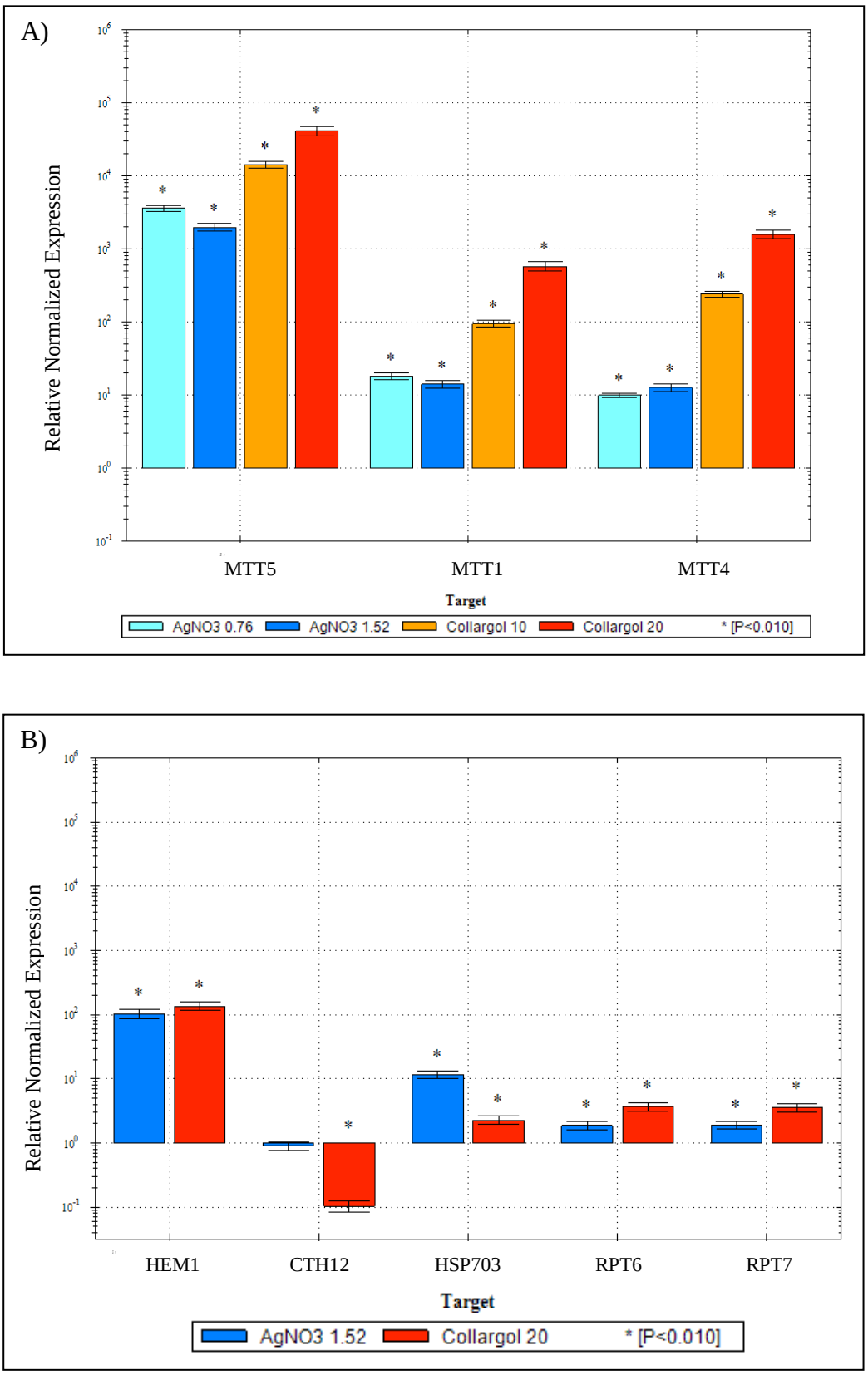

Figure 16. The mRNA relative expression levels detected by qPCR. Error bars indicate ± s.d. of biological triplicates. A) expression profile of 3 genes differentially expressed in all the treatments. B) expression profile of 5 genes differentially expressed in the two treatments at highest Ag compounds concentration.

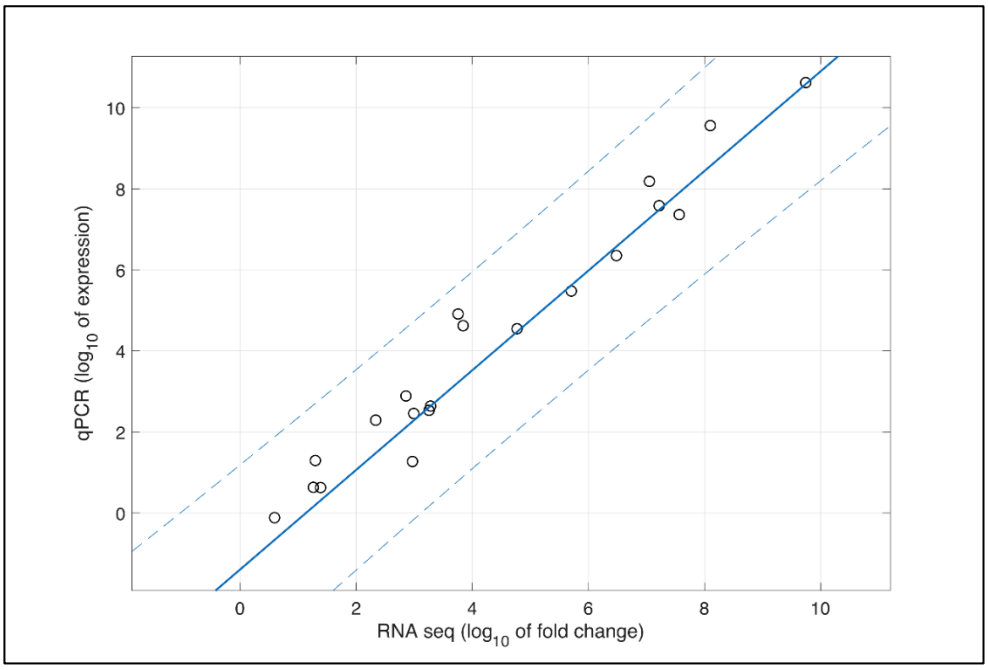

Figure 17. Correlation between qPCR and RNA sequencing results for the 8 selected genes. Each point represents a value of expression. $R^2 = 0.9587$, with prediction bounds of 95%.

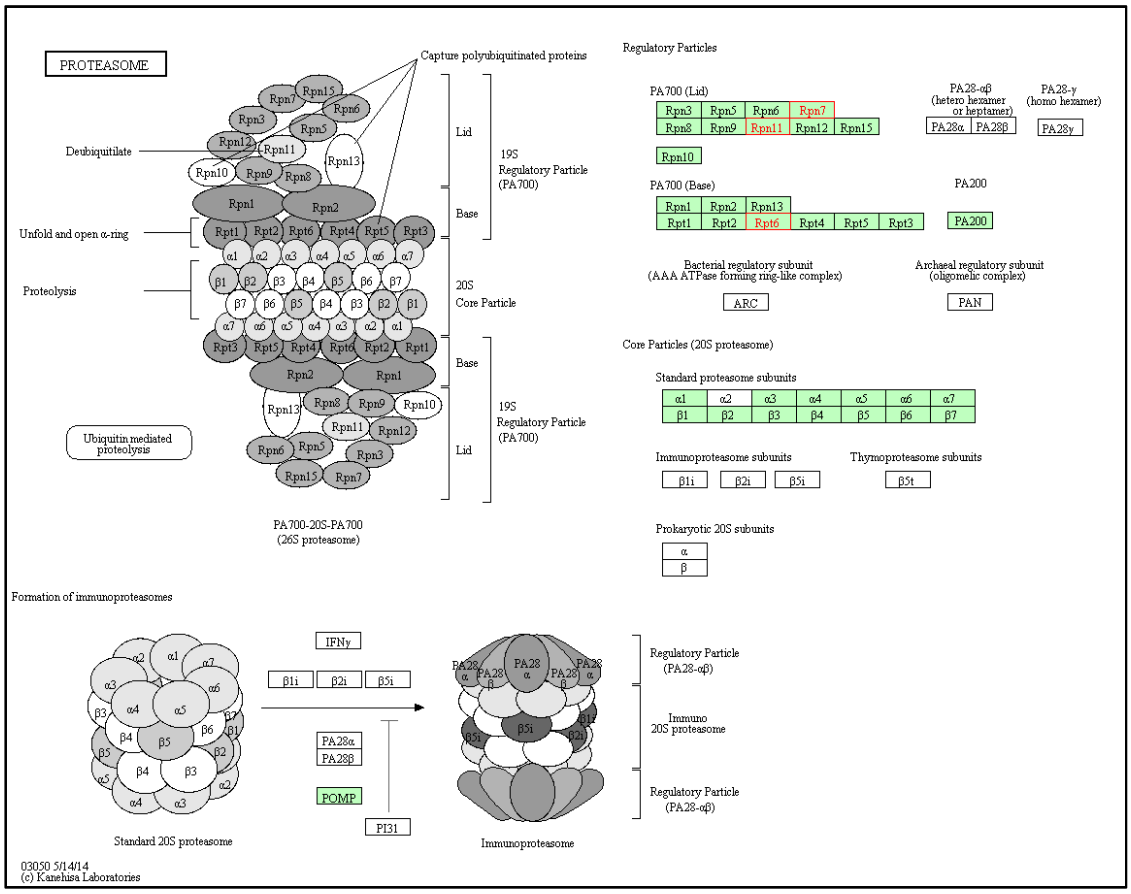

Figure 18. Schematic representation resulting from the KEGG Mapper – Search Pathway tool (Kanehisa et al. 2016) which perform the enrichment of DEGs resulting from the treatment with Collargol 20 mg Ag/L. The enriched genes are marked in red.

1.4 Conclusions

This research provides new evidence that AgNPs are toxic not only due to the released soluble silver ions as expected, but also to their intrinsic physicochemical features.

In this work $AgNO_3$ was used as an ionic silver control, at concentrations equal to the dissolved silver concentration in the water dispersion of AgNPs. In addition to several similarities in affected genes, many genes specifically affected by AgNPs were discovered, including new genes not yet annotated. This result is relevant to environmental safety, considering the increasing presence of NPs in the environment. For the first time we have the complete expression profile of a unicellular eukaryote induced by AgNPs, with the possibility to compare the effect of the silver ions dispersed in solution with the effect of AgNPs.

These results also validated the protocol of DEGs analysis as very suitable for detecting genes involved in stress response (both inhibited and induced).

Genes specifically induced respectively by Collargol and $AgNO_3$ can be further studied to identify their transcriptional promoters, which would allow the development of biosensors by fusing the promoters to reporter genes.

In our work we used well characterized and standardized AgNPs to provide a good reference for future work. Recent studies highlight the capacity of many organisms, specifically bacteria to produce NPs when exposed to soluble silver ions (Koduru et al. 2018). For a future study it would be useful to compare the results of my work with those obtained by the exposure of the same model organism to biologically produced AgNPs.

1.5 References

Akter, Mahmuda, Md Tajuddin Sikder, Md Mostafizur Rahman, A. K.M.Atique Ullah, Kaniz Fatima Binte Hossain, Subrata Banik, Toshiyuki Hosokawa, Takeshi Saito, and Masaaki Kurasaki. 2018. “A Systematic Review on Silver Nanoparticles-Induced Cytotoxicity: Physicochemical Properties and Perspectives.” *Journal of Advanced Research* 9. Cairo University: 1–16. doi:10.1016/j.jare.2017.10.008.

Andrews S. 2010. “FastQC: A Quality Control Tool for High Throughput Sequence

Data.” http://www.bioinformatics.babraham.ac.uk/projects/fastqc.

Anjum, Naser A., Sarvajeet S. Gill, Armando C. Duarte, Eduarda Pereira, and Iqbal Ahmad. 2013. “Silver Nanoparticles in Soil-Plant Systems.” *Journal of Nanoparticle Research*. doi:10.1007/s11051-013-1896-7.

AshaRani, P V, Grace Low Kah Mun, Manoor Prakash Hande, and Suresh Valiyaveettil. 2009. “Cytotoxicity and Genotoxicity of Silver Nanoparticles in Human Cells.” *ACS Nano* 3 (2): 279–90. doi:10.1021/nn800596w.

Ashkarran, Ali Akbar, Mahdi Ghavami, Hossein Aghaverdi, Pieter Stroeve, and Morteza Mahmoudi. 2012. “Bacterial Effects and Protein Corona Evaluations: Crucial Ignored Factors in the Prediction of Bio-Efficacy of Various Forms of Silver Nanoparticles.” *Chemical Research in Toxicology*. doi:10.1021/tx300083s.

Aueviriyavit, Sasitorn, Duangkamol Phummiratch, and Rawiwan Maniratanachote. 2014. “Mechanistic Study on the Biological Effects of Silver and Gold Nanoparticles in Caco-2 Cells - Induction of the Nrf2/HO-1 Pathway by High Concentrations of Silver Nanoparticles.” *Toxicology Letters*. doi:10.1016/j.toxlet.2013.09.020.

Benn, Troy, Bridget Cavanagh, Kiril Hristovski, Jonathan D. Posner, and Paul Westerhoff. 2010. “The Release of Nanosilver from Consumer Products Used in the Home.” *Journal of Environment Quality*. doi:10.2134/jeq2009.0363.

Blinova, Irina, Jukka Niskanen, Paula Kajankari, Liina Kanarbik, Aleksandr Käkinen, Heikki Tenhu, Olli Pekka Penttinen, and Anne Kahru. 2013. “Toxicity of Two Types of Silver Nanoparticles to Aquatic Crustaceans Daphnia Magna and Thamnocephalus Platyurus.” *Environmental Science and Pollution Research* 20 (5): 3456–63. doi:10.1007/s11356-012-1290-5.

Bondarenko, Olesja, Angela Ivask, Aleksandr Käkinen, Imbi Kurvet, and Anne Kahru. 2013. “Particle-Cell Contact Enhances Antibacterial Activity of Silver Nanoparticles.” *PLoS ONE*. doi:10.1080/13683500.2017.1360846.

Bondarenko, Olesja, Katre Juganson, Angela Ivask, Kaja Kasemets, Monika Mortimer, and Anne Kahru. 2013. “Toxicity of Ag, CuO and ZnO Nanoparticles to Selected Environmentally Relevant Test Organisms and Mammalian Cells in Vitro: A Critical Review.” *Archives of Toxicology* 87 (7): 1181–1200. doi:10.1007/s00204-013-1079-4.

Bouwmeester, Hans, Jenneke Poortman, Ruud J. Peters, Elly Wijma, Evelien Kramer, Sunday Makama, Kinarsashanti Puspitaninganindita, Hans J.P. Marvin, Ad A.C.M. Peijnenburg, and Peter J.M. Hendriksen. 2011. “Characterization of Translocation

of Silver Nanoparticles and Effects on Whole-Genome Gene Expression Using an in Vitro Intestinal Epithelium Coculture Model." *ACS Nano*. doi:10.1021/nn2007145.

Brobbey, Kofi J., Janne Haapanen, Marianne Gunell, Jyrki M. Mäkelä, Erkki Eerola, Martti Toivakka, and Jarkko J. Saarinen. 2017. "One-Step Flame Synthesis of Silver Nanoparticles for Roll-to-Roll Production of Antibacterial Paper." *Applied Surface Science*. doi:10.1016/j.apsusc.2017.05.143.

Burdușel, Alexandra-Cristina, Oana Gherasim, Alexandru Mihai Grumezescu, Laurențiu Mogoantă, Anton Ficai, and Ecaterina Andronescu. 2018. "Biomedical Applications of Silver Nanoparticles: An Up-to-Date Overview." *Nanomaterials* 8 (9): 681. doi:10.3390/nano8090681.

Buzea, Cristina, Ivan I. Pacheco, and Kevin Robbie. 2010. "Nanomaterials and Nanoparticles: Sources and Toxicity." *Biointerphases*. doi:10.1116/1.2815690.

Casals, E., E. Gonzalez, and V. F. Puntes. 2012. "Reactivity of Inorganic Nanoparticles in Biological Environments: Insights into Nanotoxicity Mechanisms." *Journal of Physics D: Applied Physics*. doi:10.1088/0022-3727/45/44/443001.

Cassidy-Hanley, Donna M. 2012. "Tetrahymena in the Laboratory: Strain Resources, Methods for Culture, Maintenance, and Storage." *Methods in Cell Biology* 109 (January). Academic Press: 237–76. doi:10.1016/B978-0-12-385967-9.00008-6.

Chen, Yunshun, Aaron T L Lun, and Gordon K Smyth. 2016. "From Reads to Genes to Pathways: Differential Expression Analysis of RNA-Seq Experiments Using Rsubread and the EdgeR Quasi-Likelihood Pipeline." *F1000Research*. doi:10.12688/f1000research.8987.2.

Chwieralski, C. E., T. Welte, and F. Bühling. 2006. "Cathepsin-Regulated Apoptosis." *Apoptosis*. doi:10.1007/s10495-006-3486-y.

Diaz, Silvia, Francisco Amaro, Daniel Rico, Virginia Campos, Laura Benitez, Ana Martín-González, Eileen P. Hamilton, Eduardo Orias, and Juan C. Gutiérrez. 2007. "Tetrahymena Metallothioneins Fall into Two Discrete Subfamilies." *PLoS ONE*. doi:10.1371/journal.pone.0000291.

Dubey, Poornima, Ishita Matai, S. Uday Kumar, Abhay Sachdev, Bharat Bhushan, and P. Gopinath. 2015. "Perturbation of Cellular Mechanistic System by Silver Nanoparticle Toxicity: Cytotoxic, Genotoxic and Epigenetic Potentials." *Advances in Colloid and Interface Science* 221. Elsevier B.V.: 4–21. doi:10.1016/j.cis.2015.02.007.

Durán, Nelson, Marcela Durán, Marcelo Bispo de Jesus, Amedea B. Seabra, Wagner J.

Fávaro, and Gerson Nakazato. 2016. “Silver Nanoparticles: A New View on Mechanistic Aspects on Antimicrobial Activity.” *Nanomedicine: Nanotechnology, Biology, and Medicine*. doi:10.1016/j.nano.2015.11.016.

Dutta, Partha P., Manobjyoti Bordoloi, Kabita Gogoi, Sonali Roy, Bardwi Narzary, Dibya R. Bhattacharyya, Pradyumna K. Mohapatra, and Bhaskar Mazumder. 2017. “Antimalarial Silver and Gold Nanoparticles: Green Synthesis, Characterization and in Vitro Study.” *Biomedicine and Pharmacotherapy*. doi:10.1016/j.biopha.2017.04.032.

Eisen, Jonathan A., Robert S. Coyne, Martin Wu, Dongying Wu, Mathangi Thiagarajan, Jennifer R. Wortman, Jonathan H. Badger, et al. 2006. “Macronuclear Genome Sequence of the Ciliate Tetrahymena Thermophila, a Model Eukaryote.” *PLoS Biology* 4 (9): 1620–42. doi:10.1371/journal.pbio.0040286.

Espart, Anna, Maribel Marín, Selene Gil-Moreno, Òscar Palacios, Francisco Amaro, Ana Martín-González, Juan C. Gutiérrez, Mercè Capdevila, and Sílvia Atrian. 2015. “Hints for Metal-Preference Protein Sequence Determinants: Different Metal Binding Features of the Five Tetrahymena Thermophila Metallothioneins.” *International Journal of Biological Sciences*. doi:10.7150/ijbs.11060.

Espinosa-Diez, Cristina, Verónica Miguel, Daniela Mennerich, Thomas Kietzmann, Patricia Sánchez-Pérez, Susana Cadenas, and Santiago Lamas. 2015. “Antioxidant Responses and Cellular Adjustments to Oxidative Stress.” *Redox Biology*. doi:10.1016/j.redox.2015.07.008.

Esteban, G, C Tellez, and LM Bautista. 1991. “Dynamics of Ciliated Protozoa Communities in Activated-Sludge Process.” *Water Research*, no. 25: 967–72.

Fabrega, Julia, Samuel N. Luoma, Charles R. Tyler, Tamara S. Galloway, and Jamie R. Lead. 2011. “Silver Nanoparticles: Behaviour and Effects in the Aquatic Environment.” *Environment International*. doi:10.1016/j.envint.2010.10.012.

Fan, Qichang, and M C Yao. 2000. “A Long Stringent Sequence Signal for Programmed Chromosome Breakage in Tetrahymena Thermophila.” *Nucleic Acids Research*.

Foldbjerg, Rasmus, Ping Olesen, Mads Hougaard, Duy Anh Dang, Hans Jürgen Hoffmann, and Herman Autrup. 2009. “PVP-Coated Silver Nanoparticles and Silver Ions Induce Reactive Oxygen Species, Apoptosis and Necrosis in THP-1 Monocytes.” *Toxicology Letters*. doi:10.1016/j.toxlet.2009.07.009.

Frankel J. 2007. “Tetrahymena.” *Encyclopedia of Life Sciences*.

Frankel, Joseph. 1999. “Chapter 2 Cell Biology of Tetrahymena Thermophila.”

Methods in Cell Biology. doi:10.1016/S0091-679X(08)61528-9.

Gopinath, P., Sonit Kumar Gogoi, Pallab Sanpui, Anumita Paul, Arun Chattopadhyay, and Siddhartha Sankar Ghosh. 2010. "Signaling Gene Cascade in Silver Nanoparticle Induced Apoptosis." *Colloids and Surfaces B: Biointerfaces*. doi:10.1016/j.colsurfb.2010.01.033.

Götz, Stefan, Juan Miguel García-Gómez, Javier Terol, Tim D. Williams, Shivashankar H. Nagaraj, María José Nueda, Montserrat Robles, Manuel Talón, Joaquín Dopazo, and Ana Conesa. 2008. "High-Throughput Functional Annotation and Data Mining with the Blast2GO Suite." *Nucleic Acids Research*. doi:10.1093/nar/gkn176.

Grabherr, Manfred G., Brian J. Haas, Moran Yassour, Joshua Z. Levin, Dawn A. Thompson, Ido Amit, Xian Adiconis, et al. 2011. "Full-Length Transcriptome Assembly from RNA-Seq Data without a Reference Genome." *Nature Biotechnology*. doi:10.1038/nbt.1883.

Guo, Dawei, Yun Zhao, Yu Zhang, Qing Wang, Zhihai Huang, Qi Ding, Zhirui Guo, Xuefeng Zhou, Lingying Zhu, and Ning Gu. 2014. "The Cellular Uptake and Cytotoxic Effect of Silver Nanoparticles on Chronic Myeloid Leukemia Cells." *Journal of Biomedical Nanotechnology*. doi:10.1166/jbn.2014.1625.

Han, Hye Ji, Taekyung Yu, Woo Sik Kim, and Sang Hyuk Im. 2017. "Highly Reproducible Polyol Synthesis for Silver Nanocubes." *Journal of Crystal Growth*. doi:10.1016/j.jcrysgro.2016.09.038.

He, Ruiyun, Feng Ren, and Feng Chen. 2017. "Embedded Silver Nanoparticles in KTP Crystal Produced by Ion Implantation." *Materials Letters*. doi:10.1016/j.matlet.2017.01.119.

Hobman, Jon L., and Lisa C. Crossman. 2015. "Bacterial Antimicrobial Metal Ion Resistance." *Journal of Medical Microbiology*. doi:10.1099/jmm.0.023036-0.

Holl, Mark M. Banaszak. 2009. "Nanotoxicology: A Personal Perspective." *WIREs Nanomed Nanobiotechnol* 1: 353–59.

Horikoshi, Satoshi, and Nick Serpone. 2013. "Introduction to Nanoparticles." In *Microwaves in Nanoparticle Synthesis: Fundamentals and Applications*. doi:10.1002/9783527648122.ch1.

Ivask, Angela, Katre Juganson, Olesja Bondarenko, Monika Mortimer, Villem Aruoja, Kaja Kasemets, Irina Blinova, Margit Heinlaan, Vera Slaveykova, and Anne Kahru. 2014. "Mechanisms of Toxic Action of Ag, ZnO and CuO Nanoparticles to Selected Ecotoxicological Test Organisms and Mammalian Cells in Vitro: A Comparative Review." *Nanotoxicology* 8 (SUPPL. 1): 57–71.

doi:10.3109/17435390.2013.855831.

Jemec, Anita, Anne Kahru, Annegret Potthoff, Damjana Drobne, and Margit Heinlaan. 2016. “An Interlaboratory Comparison of Nanosilver Characterisation and Hazard Identification : Harmonising Techniques for High Quality Data.” *Environment International* 87: 20–32. doi:10.1016/j.envint.2015.10.014.

Johnston, Helinor J., Gary Hutchison, Frans M. Christensen, Sheona Peters, Steve Hankin, and Vicki Stone. 2010. “A Review of the in Vivo and in Vitro Toxicity of Silver and Gold Particulates: Particle Attributes and Biological Mechanisms Responsible for the Observed Toxicity.” *Critical Reviews in Toxicology*. doi:10.3109/10408440903453074.

Juganson, Katre, Monika Mortimer, Angela Ivask, Kaja Kasemets, and Anne Kahru. 2013. “Extracellular Conversion of Silver Ions into Silver Nanoparticles by Protozoan Tetrahymena Thermophila.” *Environmental Sciences: Processes and Impacts* 15 (1): 244–50. doi:10.1039/c2em30731f.

Juganson, Katre, Monika Mortimer, Angela Ivask, Sandra Pucciarelli, Cristina Miceli, Kaja Orupõld, and Anne Kahru. 2017. “Mechanisms of Toxic Action of Silver Nanoparticles in the Protozoan Tetrahymena Thermophila: From Gene Expression to Phenotypic Events.” *Environmental Pollution* 225: 481–89. doi:10.1016/j.envpol.2017.03.013.

Kahru, Anne, and Henri Charles Dubourguier. 2010. “From Ecotoxicology to Nanoecotoxicology.” *Toxicology*. doi:10.1016/j.tox.2009.08.016.

Kahru, Anne, Henri Charles Dubourguier, Irina Blinova, Angela Ivask, and Kaja Kasemets. 2008. “Biotests and Biosensors for Ecotoxicology of Metal Oxide Nanoparticles: A Minireview.” *Sensors* 8 (8): 5153–70. doi:10.3390/s8085153.

Kanehisa, Minoru, Yoko Sato, Masayuki Kawashima, Miho Furumichi, and Mao Tanabe. 2016. “KEGG as a Reference Resource for Gene and Protein Annotation.” *Nucleic Acids Research*. doi:10.1093/nar/gkv1070.

Käosaar, Sandra, Anne Kahru, Paride Mantecca, and Kaja Kasemets. 2016. “Profiling of the Toxicity Mechanisms of Coated and Uncoated Silver Nanoparticles to Yeast Saccharomyces Cerevisiae BY4741 Using a Set of Its 9 Single-Gene Deletion Mutants Defective in Oxidative Stress Response, Cell Wall or Membrane Integrity and Endocytosis.” *Toxicology in Vitro*. doi:10.1016/j.tiv.2016.05.018.

Khatoon, Umme Thahira, G. V.S. Nageswara Rao, Krishna M. Mohan, Almira Ramanaviciene, and Arunas Ramanavicius. 2017. “Antibacterial and Antifungal Activity of Silver Nanospheres Synthesized by Tri-Sodium Citrate Assisted

Chemical Approach." *Vacuum*. doi:10.1016/j.vacuum.2017.10.003.

Kittler, S., C. Greulich, J. Diendorf, M. Köller, and M. Epple. 2010. "Toxicity of Silver Nanoparticles Increases during Storage Because of Slow Dissolution under Release of Silver Ions." *Chemistry of Materials*. doi:10.1021/cm100023p.

Koduru, Janardhan Reddy, Suresh Kumar Kailasa, Jigna R. Bhamore, Ki Hyun Kim, Tanushree Dutta, and Kowsalya Vellingiri. 2018. "Phytochemical-Assisted Synthetic Approaches for Silver Nanoparticles Antimicrobial Applications: A Review." *Advances in Colloid and Interface Science* 256. Elsevier B.V.: 326–39. doi:10.1016/j.cis.2018.03.001.

Koppelhus, U, P Hellung-Larsen, and V Leick. 1994. "Physiological Parameters Affecting the Chemosensory Response of Tetrahymena." *The Biological Bulletin* 187 (1). The University of Chicago Press: 1–7. doi:10.2307/1542159.

Lankoff, Anna, Wiggo J. Sandberg, Aneta Wegierek-Ciuk, Halina Lisowska, Magne Refsnes, Bozena Sartowska, Per E. Schwarze, Sylwia Meczynska-Wielgosz, Maria Wojewodzka, and Marcin Kruszewski. 2012. "The Effect of Agglomeration State of Silver and Titanium Dioxide Nanoparticles on Cellular Response of HepG2, A549 and THP-1 Cells." *Toxicology Letters*. doi:10.1016/j.toxlet.2011.11.006.

Lesniak, Anna, Anna Salvati, Maria J. Santos-Martinez, Marek W. Radomski, Kenneth A. Dawson, and Christoffer Åberg. 2013. "Nanoparticle Adhesion to the Cell Membrane and Its Effect on Nanoparticle Uptake Efficiency." *Journal of the American Chemical Society*. doi:10.1021/ja309812z.

Livak, Kenneth J., and Thomas D. Schmittgen. 2001. "Analysis of Relative Gene Expression Data Using Real-Time Quantitative PCR and the 2-ΔΔCT Method." *Methods*. doi:10.1006/meth.2001.1262.

Marioni, John C., Christopher E. Mason, Shrikant M. Mane, Matthew Stephens, and Yoav Gilad. 2008. "RNA-Seq: An Assessment of Technical Reproducibility and Comparison with Gene Expression Arrays." *Genome Research*. doi:10.1101/gr.079558.108.

Miao Laboratory. 2017. "TetraFGD." http://tfgd.ihb.ac.cn.

Mortimer, Monika, Alexander Gogos, Nora Bartolomé, Anne Kahru, Thomas D. Bucheli, and Vera I. Slaveykova. 2014. "Potential of Hyperspectral Imaging Microscopy for Semi-Quantitative Analysis of Nanoparticle Uptake by Protozoa." *Environmental Science and Technology*. doi:10.1021/es500898j.

Mortimer, Monika, Anne Kahru, and Vera I. Slaveykova. 2014. "Uptake, Localization and Clearance of Quantum Dots in Ciliated Protozoa Tetrahymena Thermophila."

Environmental Pollution. doi:10.1016/j.envpol.2014.03.021.

Mortimer, Monika, Kaja Kasemets, and Anne Kahru. 2010. "Toxicity of ZnO and CuO Nanoparticles to Ciliated Protozoa Tetrahymena Thermophila." *Toxicology* 269 (2–3). Elsevier Ireland Ltd: 182–89. doi:10.1016/j.tox.2009.07.007.

Mortimer, Monika, Elijah J. Petersen, Bruce A. Buchholz, Eduardo Orias, and Patricia A. Holden. 2016. "Bioaccumulation of Multiwall Carbon Nanotubes in Tetrahymena Thermophila by Direct Feeding or Trophic Transfer." *Environmental Science and Technology*. doi:10.1021/acs.est.6b01916.

Nadagouda, Mallikarjuna N., Thomas F. Speth, and Rajender S. Varma. 2011. "Microwave-Assisted Green Synthesis of Silver Nanostructures." *Accounts of Chemical Research*. doi:10.1021/ar1001457.

Nowack, Bernd, and Nicole C. Mueller. 2008. "Exposure Modeling of Engineered Nanoparticles in the Environment." *EMPA Activities*. doi:10.1021/es7029637.

Nusblat, Alejandro D., Lydia J. Bright, and Aaron P. Turkewitz. 2012. "Conservation and Innovation in Tetrahymena Membrane Traffic: Proteins, Lipids, and Compartments." *Methods in Cell Biology*. doi:10.1016/B978-0-12-385967-9.00006-2.

Oliveros, J.C. 2015. "Venny. An Interactive Tool for Comparing Lists with Venn's Diagrams." http://bioinfogp.cnb.csic.es/tools/venny/index.html.

Orias, Eduardo, Marcella D. Cervantes, and Eileen P. Hamilton. 2011. "Tetrahymena Thermophila, a Unicellular Eukaryote with Separate Germline and Somatic Genomes." *Res Microbiol.* 162 (6): 578–86. doi:10.1016/j.dcn.2011.01.002.The.

Pan, Yongbo, Wenjing Zhang, and Senjie Lin. 2018. "Transcriptomic and MicroRNAomic Profiling Reveals Molecular Mechanisms to Cope with Silver Nanoparticle Exposure in the Ciliate Euplotes Vannus." *Environmental Science: Nano*. doi:10.1039/C8EN00924D.

Prescott, David M. 1994. "The DNA of Ciliated Protozoa." *MICROBIOLOGICAL REVIEWS* 58 (2): 233–67. doi:10.1007/BF00326311.

Rai, Mahendra, Alka Yadav, and Aniket Gade. 2009. "Silver Nanoparticles as a New Generation of Antimicrobials." *Biotechnology Advances*. doi:10.1016/j.biotechadv.2008.09.002.

Robinson, Mark D., Davis J. McCarthy, and Gordon K. Smyth. 2009. "EdgeR: A Bioconductor Package for Differential Expression Analysis of Digital Gene Expression Data." *Bioinformatics* 26 (1): 139–40. doi:10.1093/bioinformatics/btp616.

Salata, Oleg V. 2004. “Applications of Nanoparticles in Biology and Medicine.” *Journal of Nanobiotechnology*. doi:10.1186/1477-3155-2-3.

Simon, Dana F., Rute F. Domingos, Charles Hauser, Colin M. Hutchins, William Zerges, and Kevin J. Wilkinson. 2013. “Transcriptome Sequencing (RNA-Seq) Analysis of the Effects of Metal Nanoparticle Exposure on the Transcriptome of Chlamydomonas Reinhardtii.” *Applied and Environmental Microbiology* 79 (16): 4774–85. doi:10.1128/AEM.00998-13.

Singh, Tej, Kumari Jyoti, Amar Patnaik, Ajeet Singh, Ranchan Chauhan, and S. S. Chandel. 2017. “Biosynthesis, Characterization and Antibacterial Activity of Silver Nanoparticles Using an Endophytic Fungal Supernatant of Raphanus Sativus.” *Journal of Genetic Engineering and Biotechnology*. doi:10.1016/j.jgeb.2017.04.005.

Sotiriou, Georgios A., and Sotiris E. Pratsinis. 2011. “Engineering Nanosilver as an Antibacterial, Biosensor and Bioimaging Material.” *Current Opinion in Chemical Engineering*. doi:10.1016/j.coche.2011.07.001.

Stover, Nicholas A, Cynthia J Krieger, Gail Binkley, Qing Dong, Dianna G Fisk, Robert Nash, Anand Sethuraman, Shuai Weng, and J Michael Cherry. 2006. “Tetrahymena Genome Database (TGD): A New Genomic Resource for Tetrahymena Thermophila Research.” *Nucleic Acids Res. 34 (Database Issue): D500-3.*

Verma, Shweta, B. Tirumala Rao, A. P. Srivastava, D. Srivastava, R. Kaul, and B. Singh. 2017. “A Facile Synthesis of Broad Plasmon Wavelength Tunable Silver Nanoparticles in Citrate Aqueous Solutions by Laser Ablation and Light Irradiation.” *Colloids and Surfaces A: Physicochemical and Engineering Aspects*. doi:10.1016/j.colsurfa.2017.05.003.

Vindimian, E. 2001. “MSExcel Macro REGTOX EV7.0.5.Xls.” http://www.normalesup.org/~vindimian/en_download.html.

Wiesner, Mark R., Gregory V. Lowry, Kimberly L. Jones, Michael F. Hochella, Richard T. Digiulio, Elizabeth Casman, and Emily S. Bernhardt. 2009. “Decreasing Uncertainties in Assessing Environmental Exposure, Risk, and Ecological Implications of Nanomaterials.” *Environmental Science and Technology*. doi:10.1021/es803621k.

Wittenberg, Jonathan B., Martino Bolognesi, Beatrice A. Wittenberg, and Michel Guertin. 2002. “Truncated Hemoglobins: A New Family of Hemoglobins Widely Distributed in Bacteria, Unicellular Eukaryotes, and Plants.” *Journal of Biological*

Chemistry 277 (2): 871–74. doi:10.1074/jbc.R100058200.

Wloga, Dorota, and Joseph Frankel. 2012. “From Molecules to Morphology: Cellular Organization of Tetrahymena Thermophila.” *Methods in Cell Biology*. doi:10.1016/B978-0-12-385967-9.00005-0.

Xiong, Jie, Yuming Lu, Jinmei Feng, Dongxia Yuan, Miao Tian, Yue Chang, Chengjie Fu, Guangying Wang, Honghui Zeng, and Wei Miao. 2013. “Tetrahymena Functional Genomics Database (TetraFGD): An Integrated Resource for Tetrahymena Functional Genomics.” *Database* 2013: 6–11. doi:10.1093/database/bat008.

Yao, Meng-Chao, and Ju-Lan Chao. 2005. “RNA-Guided DNA Deletion in Tetrahymena: An RNAi-Based Mechanism for Programmed Genome Rearrangements.” *Annual Review of Genetics*. doi:10.1146/annurev.genet.39.073003.095906.

Yao, Meng Chao, Judy Choi, Shozo Yokoyama, Charles F. Austerberry, and Ching Ho Yao. 1984. “DNA Elimination in Tetrahymena: A Developmental Process Involving Extensive Breakage and Rejoining of DNA at Defined Sites.” *Cell*. doi:10.1016/0092-8674(84)90236-8.

Yao, Meng Chao, Ching Ho Yao, and Bob Monks. 1990. “The Controlling Sequence for Site-Specific Chromosome Breakage in Tetrahymena.” *Cell*. doi:10.1016/0092-8674(90)90142-2.

Youngs, Wiley J., Amanda R. Knapp, Patrick O. Wagers, and Claire A. Tessier. 2012. “Nanoparticle Encapsulated Silver Carbene Complexes and Their Antimicrobial and Anticancer Properties: A Perspective.” *Dalton Transactions*. doi:10.1039/c1dt11100k.

Yu, Guo Liang, and Elizabeth H. Blackburn. 1991. “Developmentally Programmed Healing of Chromosomes by Telomerase in Tetrahymena.” *Cell*. doi:10.1016/0092-8674(91)90077-C.

This material is the subject of a manuscript in preparation in which the first name will be of the author of this thesis. Collaborators from the three below mentioned institutions will be included as coauthors.

1 School of Biosciences and Veterinary Medicine, University of Camerino, Italy
2 Laboratory of Environmental Toxicology, National Institute of Chemical Physics and Biophysics, Tallinn, Estonia
3 Institute of Hydrobiology, Chinese Academy of Sciences, Wuhan, China

Chapter 2

2.0 Isolation of *Euplotes crassus* micronuclear chromosomes by Pulsed Field Gel Electrophoresis

2.1 Introduction and aims

Ciliates have served as model organisms in many research fields, including cytology, zoology, evolutionary biology and genetics. In addition, they provide novel insight into epigenetic regulation due to their nuclear dimorphism (Nanney and Caughey 1953; Hammerschmidt et al. 1996). As a group of unicellular eukaryotes, they display a high level of diversity not only in morphology but also in structure, such as genome size, gene copy numbers, genome rearrangement and in their mechanisms of epigenetic regulation (Y. Wang et al. 2017).

Ciliated protozoans are characterized by nuclear dimorphism, having two types of nuclei in the same cytoplasm. The polyploid transcriptionally active, somatic macronucleus (MAC), provides most gene expression during vegetative growth. In contrast, the diploid germline micronucleus (mic), which is organized in the form of conventional eukaryotic chromosomes, is transcriptionally inert during vegetative growth, ,but becomes transcriptionally active during conjugation (Prescott 1994).

Within the past decade, micronuclear, macronuclear and mitochondrial genome sequences of several ciliates have been reported (Aury et al. 2006; Eisen et al. 2006; de Graaf et al. 2009; Arnaiz et al. 2012; Swart et al. 2013; Chen et al. 2014; Hamilton et al. 2016; Slabodnick et al. 2017). Genome studies have made a major impact on ciliate research (Y. Wang et al. 2017). More extensive investigations should be carried out on not-yet model ciliates, since it would be valuable to investigate the functional and evolutionary relationships among DNA elimination events in different, deeply divergent groups of ciliates (Vogt et al. 2013). Our laboratory for years has focused its attention on marine *Euplotes* species, particularly on the Antarctic *E. focardii* that is strictly adapted to the cold environment. This has made it possible to investigate the molecular characteristics of cold adaptations (Pucciarelli et al. 2009; Yang, De Santi, et al. 2013; Yang, Yang, et al. 2013; Yang et al. 2017).

During asexual division, both nuclei divide and *Euplotes* secures its immediate survival by binary fission, producing standardized progenies of genotypes. Whereas, when cells of different mating types are mixed, under certain circumstances, they undergo sexual conjugation providing recombination genetic variety and physiological plasticity to face new environmental conditions (Dini 1984).

Indeed, following mating, the ciliated protozoa undergo extensive changes in their genome, the old MAC is destroyed, and a new MAC is generated from a mitotic copy of

the mic. It is during this transformation of a copy of the mic into the new MAC that numerous genomic rearrangements occur, (Klobutcher and Jahn 1991) deleting large portions of germline DNA.

MAC generation/development begins with rounds of total DNA replication resulting in the formation of polytene chromosomes(Klobutcher et al. 1998). The polytene chromosomes are then fragmented and up to 95% of the mic genome complexity is eliminated. The remaining DNA molecules undergo additional replication resulting in the mature MAC genome (Klobutcher, Huff, and Gonye 1988; Klobutcher et al. 1998). As a result of the chromosome fragmentation and DNA amplification events, the mature MAC contains 24,000-30,000 short linear DNA molecules (Lobanov et al. 2017 and unpublished data), with an average size of ~ 2 kbp, each highly amplified in differential copy number (1,000 as average) (Tausta et al. 1991).

Two classes of DNA sequences involved in breakage and rejoining events have been defined in *E. crassus*. Three related families of transposable elements, Tecl, Tec2, and Tec3 are excised during MAC development (Baird et al. 1989; Jahn, Krikau, and Shyman 1989; Doak et al. 1994; Jacobs et al. 2003). The second class consists of short (31-374 bp) unique segments of DNA that have been termed "internal eliminated sequences" (IESs) (Baird et al. 1989). *E. crassus* IESs and Tec elements display some similarities. Both are bounded by a direct repeat of the dinucleotide 5'-TA-3', and excision has been shown to be precise such that one copy of the 5'-TA-3' repeat is retained in the resulting MAC DNA molecule (Tausta et al. 1991). The Tec elements are excised early in the polytenization process (Jahn, Krikau, and Shyman 1989), while the IESs are removed later (Tausta and Klobutcher 1990). Once excised, Tec elements and IESs assume free circular forms with an unusual heteroduplex junction region, as shown in Figure 19 (Klobutcher, Turner, and La Plante 1993; Jaraczewski, Frels, and Jahn 1994). Tecl and Tec2 elements are 5.3 kbp in length with 700 to 725 bp terminal inverted repeats. Each element is present in 30,000 copies, and 50% of them interrupt "macronuclear-destined sequences" (MDSs) (Jaraczewski and Jahn 1993). Tec3 elements are present in 20 to 30 copies in the micronuclear genome have long inverted terminal repeats and contain a degenerate open reading frame encoding a tyrosine-type recombinase (Jacobs et al. 2003). Moreover, multiple classes of IESs exist (Klobutcher 1995). Some smaller IESs are excised later in macronuclear development, and their sequence resembles the telomeric repeat sequence of the organism (Klobutcher 1995; Hale et al. 1996).

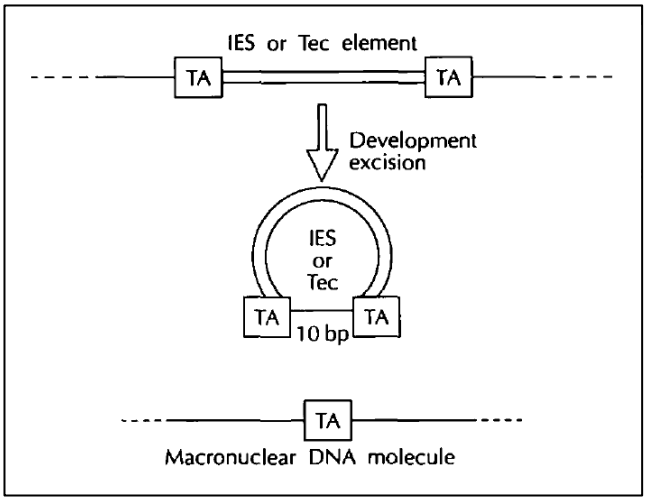

Figure 19. Excision of lESs and Tec elements in *E. crassus*. In the top of the figure is shown an IES or Tec element in its mic chromosomal context with terminal 5'-TA-3'direct repeats. After the excision, a MAC DNA molecule that retains one copy of the element direct repeat is generated. The free circular element produced by the excision has both copies of the direct repeat plus 10 bp that match MAC DNA molecule sequence. From Klobutcher and Jahn 1991.

E. crassus, displays some differences in the chromosome fragmentation and telomere addition process relative to the other ciliates (Klobutcher 1999). In *T. thermophila,* a *cis*-acting sequence elements termed "chromosome breakage sequence" (Cbs) has been demonstrated to be necessary and sufficient for chromosome breakage (Yao, Yao, and Monks 1990). The Cbs element resides between what will become the ends of two separate MAC chromosomes, and telomeres are ultimately added 4-22 bp from the ends of the Cbs. In *E. crassus*, instead, chromosome fragmentation and telomere addition are precise and reproducible. The likely *cis*-acting sequence specifying fragmentation can reside either near the end of the MDS, or in the flanking DNA. A 10 bp consensus sequence termed "*Euplotes* Cbs" (E-Cbs) has been identified (Baird and Klobutcher 1989; Klobutcher et al. 1998; Klobutcher 1999). When the E-Cbs resides within the MDSs, the highly conserved core TTGAA sequence is located 17 bp from the site of telomere addition; when the E-Cbs is located in the flanking DNA, it is in inverted orientation with the core TTGAA positioned 11 bp from the telomere addition site (Möllenbeck and Klobutcher 2002).

De novo telomere formation is tightly coupled to chromosome fragmentation and is known to be mediated by the telomerase enzyme (Yu and Blackburn 1991; Klobutcher 1999). While the telomerase of vegetative cells can only add telomeric repeats to telomeric ends, a telomerase complex has been shown to be present in exconjugant cells

that adds telomeric DNA sequences de novo to non-telomeric ends (Greene and Shippen 1998).

Despite the genome downsizing via DNA elimination required for the constitution of functional genes in the MAC, this nucleus contains a greater quantity of DNA than the mic: >95% of whole cell DNA in this organism is MAC (Klobutcher et al. 1981; Vogt et al. 2013).

Every nanochromosome molecule (Figure 20) is flanked by short non-translated regions (5' leader and a 3' trailer) and bounded by telomeres (C4A4 repeats). A 3’ overhang is also present on both strands (Klobutcher et al. 1981). The 5' leaders have been hypothesized to contain sequences needed for transcriptional regulation, for specification of transcription start sites, and for origins of replication (Prescott 1994).

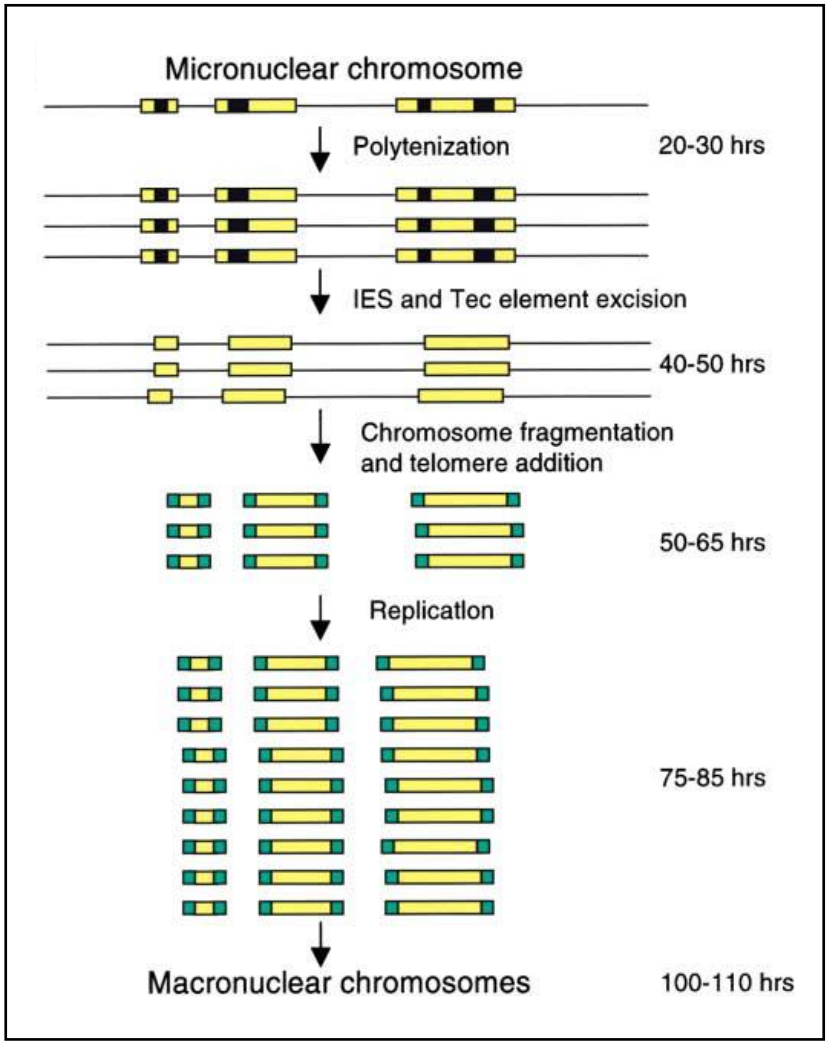

Figure 20. Types of DNA processing and their developmental timing in the sexual phase of the *E. crassus* life cycle. Developmental timing of events, where time of mixing of two different mating types is 0 h and other events are referred to as time post mixing. From Karamysheva et al. 2003.

Euplotes has two translational peculiarities that can distinguish it from other ciliates: stop codon usage and +1or +2 programmed ribosomal frameshift (PRF). The stop codon UGA is used in *Tetrahymena* and *Paramecium*, while in *Euplotes* it is reassigned as the cysteine or selenocysteine codon (Turanov et al. 2009; Lobanov et al. 2017). The stop codons UAA and UAG in *Tetrahymena* and *Paramecium* encode glutamine while *Euplotes* uses both as stop codons (Salim, Ring, and Cavalcanti 2008). *Euplotes* species are so far the only ciliates reported to require +1 or +2 programmed ribosomal frameshift: a number of genes of euplotids have been reported to require this frameshift to express a functional protein (Jahn et al. 1993; Aigner et al. 2000; Doak et al. 2003; R. Wang et al. 2016; Lobanov et al. 2017). It has been hypothesized that frameshifting has evolved as a consequence of TGA-codon reassignment from stop to cysteine, thus weakening release-factor recognition of the remaining stop codons, TAA and TAG (Klobutcher and Farabaugh 2002; Vallabhaneni et al. 2009).

Although in the recent years some *Euplotes* macronuclear genomes were sequenced (Lobanov, Hatfield, and Gladyshev 2009; Lobanov et al. 2017; R. Wang et al. 2018) and most of them are currently under improvement in annotation, *Euplotes* mic sequences are still not available. This gap is significant for our research, compared to other model ciliates. Also, molecular genetic tools in *Euplotes* species are far less powerful and the attempts to improve them will take advantages from an annotated genome.

To address this gap in research, we developed a technique to isolate *E. crassus* micronuclear chromosomes with the more long-term objective to sequence and annotate them. We used the advantage that micronuclear DNA has a high molecular weight compared to the MAC DNA. The entire genome size of *E. crassus* is estimated to be 1.7 x 10^9 bp (Klobutcher, L. A. 1986), since there are many chromosomes, the molecular weight of any one mic chromosome would be smaller, but still a lot more than a MAC chromosome. Thus, it appeared possible to purify mic from MAC DNA by Pulsed Field Gel Electrophoresis. We focused the attention on *E. crassus* because it is a marine species more easily grown in large cultures with respect to *E. focardii* and some information, as above reported is available on the mic genome. This work was supported by The Marine Microbiology Initiative (MMI, funded by Gordon and Betty Moore foundation) and developed in collaboration with the University of Bern and the University of Connecticut.

2.2 Results

2.2.1 *E. crassus* micronuclear chromosomes isolation by PFGE

We managed to optimize the *E. crassus* micronuclear chromosomes isolation protocol by PFGE. Different experimental conditions and outcomes which lead us in making progress are reported in Table 7. We adjusted the number of *E. crassus* cells per plug (150,000), the run time and the switch time. We added antibiotics to decrease the bacterial contamination. The gel cuts were done using the Lambda (λ) ladder (Bio-Rad) (size range: 48.5–1,000 kbp) as an indicator of DNA dimensions to discard (see Figure 21 and Figure 22). Moreover, since we did not want to lose the shortest mic chromosomes, we experimentally determined in which part of the gel the mic DNA was, actually, migrating through a technique called "IES retention PCR" described in the next chapter. Eventually, we estimated the yield that we could get from each run.

Table 7. Summary of PFGE runs:

Run	Ab	Number of *E. crassus* cells	Run time	Switch time	Gel cut	mic DNA quantity (µg)	IES retention PCR result
1st	-	400,000	22 h	70s	2nd b	0.2	-
2nd	-	1,800,000	22 h	70s	plugs	10.5	+
70s (1)	-	1,100,000	30 h	70s	plugs	3.9	+
					2nd b	0.7	-
70s (2)	Amp	1,650,000	30 h	70s	plugs	17.8	+
90s	Amp	1,650,000	30 h	90s	plugs	2.3	+
					2nd b	2	+
80s	Amp and Kan	1,650,000	30 h	80s	plugs	1	+
					2nd b	0	-
70s (3&4)	Amp	3,900,000	30 h	70s	plugs	10.9 *	+

Ab = antibiotic used;
Amp = ampicillin;
Kan = kanamycin;
2nd b = 2nd band cut from the gel;
plugs = 1st band cut from the gel, containing the plugs (*E. crassus* cells and low melting agarose assembly polymerized inside plug mold) inserted into the wells of the gel;
*digested with RNase A.

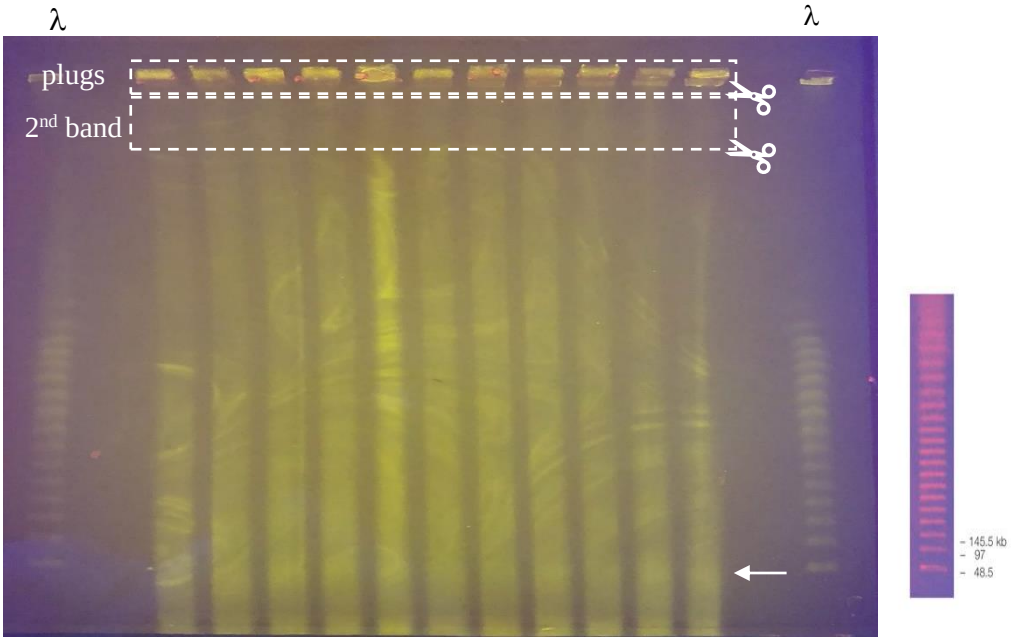

Figure 21. PFGE gel, 70s (1) run, with 1,100,000 *E. crassus* cells. Gel cuts' examples: plugs and 2nd band. The mitochondrial band (arrow) is located just below the one lambda band (48 kbp, de Graaf et al. 2009). Lambda (λ) ladder (Bio-Rad) size range: 48.5–1,000 kbp in 48.5 kbp increments.

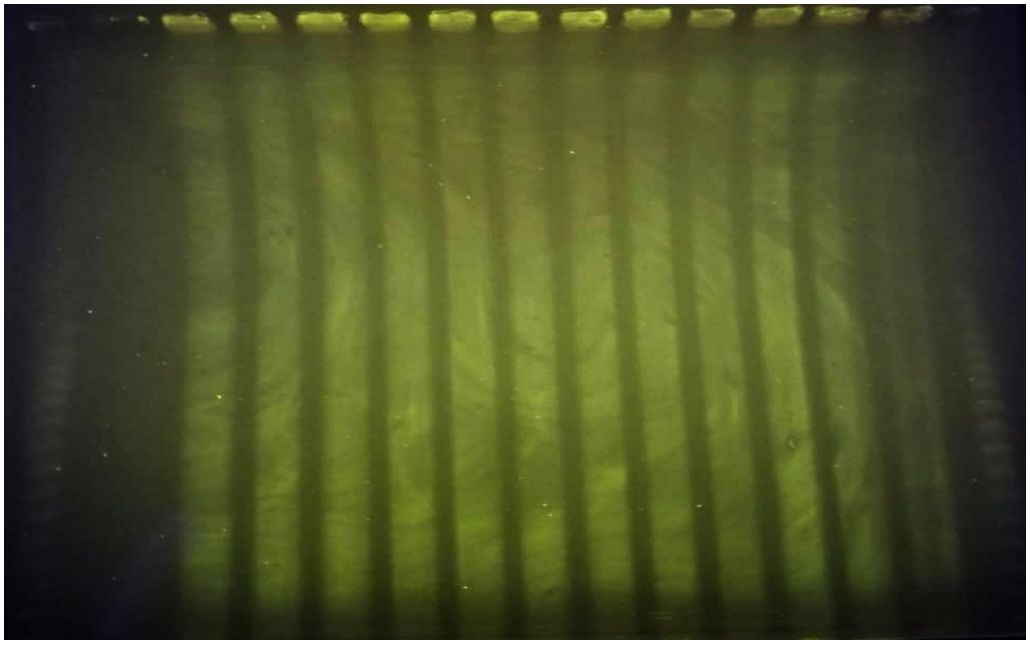

Figure 22. PFGE gel, 70s (3) run, with 3,900,000 *E. crassus* cells. From left to right Lambda (λ) ladder (Bio-Rad), plug 1, plug 2, plug 3, plug 4, plug 5, plug 6, plug 7, plug 8, plug 9, plug 10, plug 11, plug 12, Lambda (λ) ladder (Bio-Rad).

2.2.2 IES PCR and Tec 2 PCR

In the past years partial *E. crassus* mic sequences had been cloned and sequenced (Hale et al. 1996; Doak et al. 2003; Karamysheva et al. 2003), therefore some IESs and Tec elements sequences are known. To check if the DNA that we isolated belonged to the micronucleus, we performed PCR reactions to look for specific mic elements (IES-PCR) using as primers oligonucleotides corresponding to the sequence located externally to the IES that means inside MDSs. If the DNA belongs to the mic it should retain the IES, if it simply belongs to the MAC the size should be shorter, without the IES retention because IESs are eliminated during MAC development

In Figure 23 and Figure 24 are reported the results, obtained for specific mic elements, tested in the DNA samples isolated from the runs performed after antibiotic pretreatment on *E. crassus* culture.

To get a wider analysis, two IESs (named IES 144 and IES 300) assumed to be located on different mic chromosomes, were tested. We tested also other known IESs that are thought to reside in the same mic chromosome together with IES 144, indeed they showed the same PCR retention pattern (results not shown). Moreover, we performed Tec 2 elements retention PCR, in this case using as primers oligonucleotides internal to the Tec elements.

IES PCR results showed the IES retention in all the DNA samples isolated by PFGE, compared to the genomic DNA (gDNA) used as control that should contain the total MAC and mic DNA in their natural ratio 500:1, assuming a diploid mic and an average copy number of 1,000 for a typical MAC DNA molecule. In particular, the PCR with primers outside the 144 bp IES showed a similar pattern in the three runs (70 sec, 80 sec, 90 sec switch time). Whereas, the PCR with primers outside the 300 bp IES showed a different pattern between the run at 70 sec switch time and the one at 90 sec switch time.

Tec 2 PCR showed an amplicon in all the samples except for the DNA extracted from the 2nd band of the run at 70 sec switch time.

‘IES144-’ and ‘IES144+’ gel bands were excised from the ‘plugs 70s’ sample and purified. The expected nucleotide sequence was then confirmed by Sanger Sequencing (BMR Genomics).

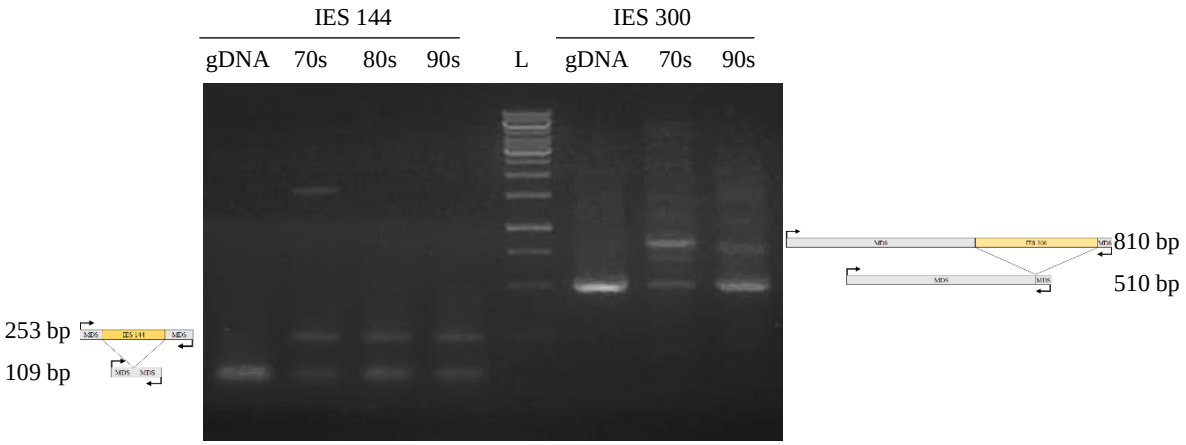

Figure 23. 1% agarose gel with IES PCR products separation. IESs retention is visible in all the DNA samples isolated by PFGE, compared to the gDNA sample.
IES 144 = primers outside the 144 bp IES; IES 300 = primers outside the 300 bp IES; gDNA = E. crassus genomic DNA as PCR template; 70s = plugs gel cut from 70s (3) run as PCR template; 80s = plugs gel cut from 80s run as PCR template; 90s = plugs gel cut from 90s run as PCR template; L = 1 kb ladder (Thermo Scientific).

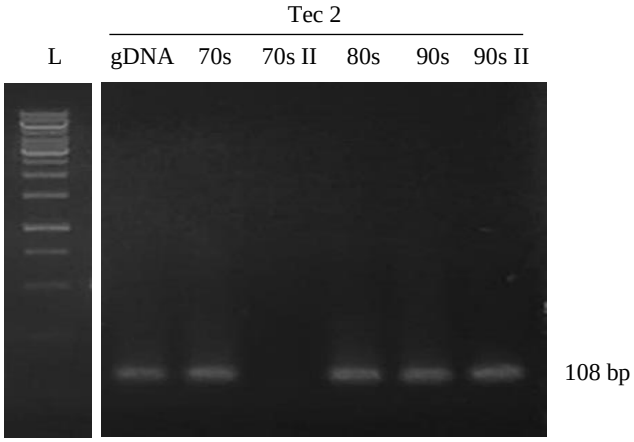

Figure 24. 1 % agarose gel with Tec 2 PCR products separation. A Tec 2 amplicon is present in all the samples except for the 70s II sample.
Tec 2 = primers internal to the Tec elements; L = 1 kb ladder (Thermo Scientific); gDNA = E. crassus genomic DNA as PCR template; 70s = plugs gel cut from 70s (1) run as PCR template; 70s II = 2nd band cut from 70s (1) run as PCR template; 80s = plugs gel cut from 80s run as PCR template; 90s = plugs gel cut from 90s run as PCR template; 90s II = 2nd band cut from 90s run as PCR template.

2.2.3 Quantitative PCR

In order to estimate the enrichment of the mic DNA with respect to the MAC DNA in the samples, a quantitative PCR (qPCR), with a relative quantification analysis, was performed using primers design on the internal part of the IES 144 sequence, since IES presence is mic specific. As control we designed primers on *P0* gene sequence, which encodes for the ribosomal P0 protein that is constitutively expressed, therefore it should be a valid housekeeping gene. Nevertheless, we need to keep in mind that the genomic DNA sample contains a small percentage of mic DNA (estimated to be around the0.2%) and that the mic DNA, as well, contains diploid *P0* gene copies in its chromosomes, whether they are interrupted by mic specific elements or not.

An internal region of the IES 144 and a region of *P0* were amplified in both the DNA isolated by PFGE in the '70s (2)'run, '90s'run, and in the gDNA sample.

The specificity of each primer set and annealing temperature to optimize PCR conditions and the fluorescence signal specificity of PCR amplification were confirmed through assessment of the product melting curves and the efficiency was 108.8 % for IES 144 and 102.3 % for p0, with $r^2 = 0.99$.

A significant enrichment of the micronuclear DNA was shown by the CFX Connect Real-Time PCR Detection System (Bio-Rad) in the sample with a switch time of 70 sec, compared to the sample with a switch time of 90 sec, the 2nd gel slice of the run with 90 sec switch time and the gDNA used as control (see Figure 25).

The data of the run with 80 sec switch time were not included in the analysis, because there was not significant difference compared to the sample with a switch time of 90 sec.

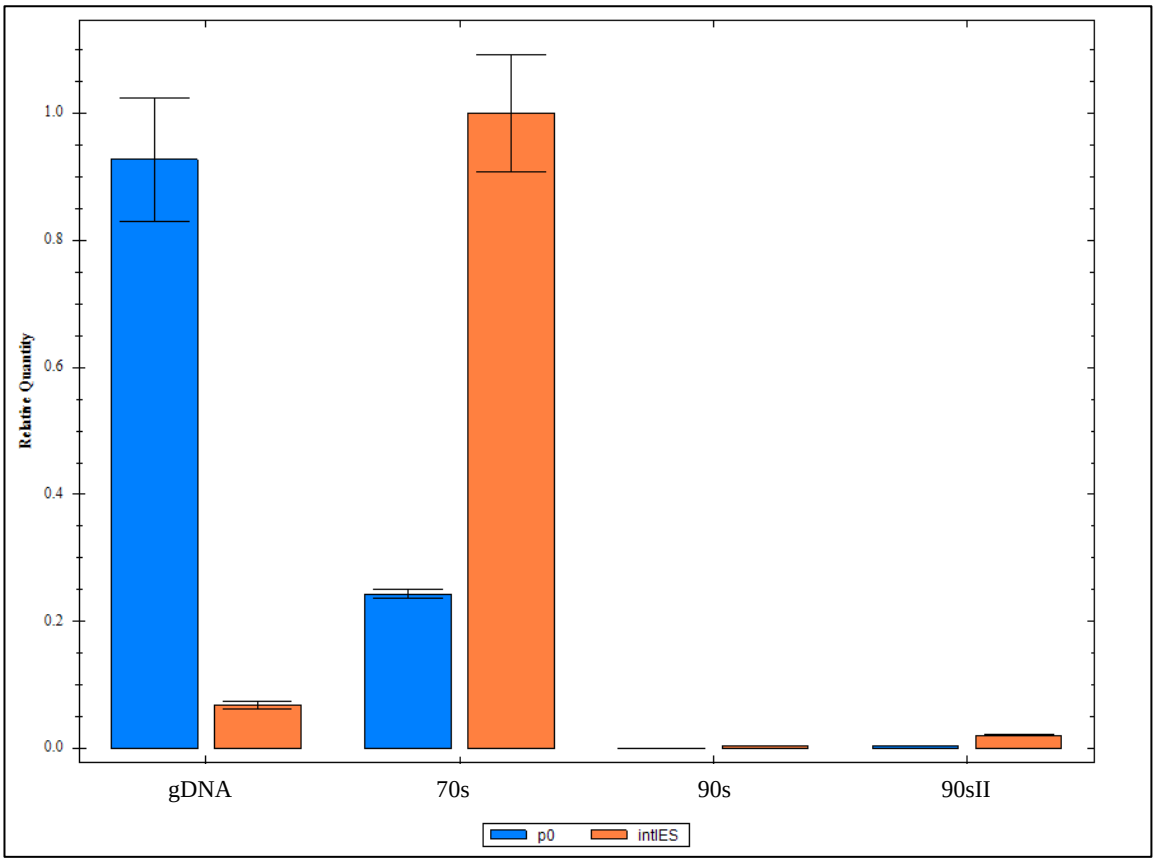

Figure 25. qPCR result. IES presence is detected in a significant amount in the 70s sample, compared to 90s and 90sII samples and to the gDNA sample.
p0 = primers internal to the P0 gene sequence; intIES = primers internal to the 144 bp IES; gDNA = E. crassus genomic DNA as qPCR template; 70s = plugs gel cut from 70s (3) run as qPCR template; 90s = plugs gel cut from 90s run as qPCR template; 90sII = 2nd band cut from 90s run as qPCR template.

2.2.4 Illumina sequencing results

Since, according to the qPCR results the DNA sample was enriched for the mic DNA we proceeded with a pilot Illumina sequencing for the 'plug 70s' sample, at the Bern University facility. The data reads produced from the sequencing were assembled, using the SPAdes assembler version 3.10.1 (Bankevich et al. 2012), and cleaned until 47,640 scaffolds were obtained. This assembly contains 120,968,437 bp, with a mean scaffold length of 2,539 bp, a maximum scaffold length of 2,307,465 bp and a N50 of 4,980. In addition, this assembly contains 3,536 telomers into 2,194 scaffolds. The assembly showed only 6% of bacterial contamination.

The comparison with the annotated *E. crassus* MAC genome showed that only 6,004 MAC chromosomes mapped to the obtained sequences of the mic assembly. Considering only scaffolds that mapped with at least two MAC nodes (2,771), we could count 776 sequences longer than 30 bp which could be considered IESs or Tec c

elements. Nevertheless, we could not find any match for known Tec sequences nor for known IESs sequences, whose presence had been confirmed by PCRs and Sanger sequencing.

2.3 Discussion

IES retention in all the DNA samples isolated by PFGE demonstrated an increase in the proportion of the mic chromosomes present, further confirmed by the quantitative PCR. In the first trials, the DNA samples isolated from the PFGE runs showed on the gel neither the amplicon of the retained IES nor the amplicon of the excised IES. Maybe it was caused by an overestimation of the DNA quantity due to a bacterial DNA contamination (results not shown). This issue was solved by pretreating the *E. crassus* culture with ampicillin.

Conversely, Tec 2 presence in all the samples except for the DNA extracted from the 2nd gel slice of the run at 70 sec is an indicator of concentration of mic chromosomes in the plugs. Indeed, the presence of Tec 2 in the DNA extracted from the 2nd gel slice of the run at 90 sec is an indication of dispersion of mic chromosomes in the gel. This data was confirmed by the qPCR, which showed almost no mic chromosomes in the DNA extracted from the plugs at 90 sec switch time and a small quantity in the DNA extracted from the highest gel slice of the same run.

However, we also need to consider that *P0* may not the best control to check for mic samples purity (although it was the best we could have). In fact, thanks to the Illumina sequence results, we realized that the *P0* mic gene does not contain any IES. This means that the primers that we designed have amplified, not only the polyploid copies of *P0* gene in the MAC chromosomes, but also the diploid copies that are in the mic chromosomes, much less in copy number, but not totally irrelevant. Thus, in the graph in Figure 25 the value related to *P0* does not only represents the MAC chromosomes in our samples, but also includes the P0 genes of the mic DNA.

As positive result, there was a considerable reduction of MAC chromosomes in the sample of the run with a switch time of 70 sec, that indicates that we selected a good switch time for mic enrichment.

Illumina sequencing results were quite poor, the mean scaffold length of 2,539 bp and the N50 of 4,980 are shorter than the expected ones, suggesting a highly fragmented assembly. In addition, the number of telomeres indicates the MAC contamination. Moreover, the results are not consistent with PCR and qPCR results, since we could not find IES sequences in silico which presence were confirmed by PCR and Sanger sequencing. The most likely interpretation in this circumstance is that Illumina sequencing technology features do not allow a proper assembly of the mic genome sequences due to the germline genome complexity that includes a high number of repeated regions which cannot be well assembled by the short size reads produced (almost 100 bs long on average). The intricacy of the mic DNA sequence may be increased by the presence of some scrambled genes, as were found in the related ciliates *Oxythricha* and *Stylonychia*. These scrambled genes in the mic are characterized by MDSs not in the same order of the MAC DNA (that is the order that permits the coding of the gene). The correct order for coding is obtained by rearrangements during MAC development (Landweber, Kuo, and Curtis 2000). In addition to this difficulty, in our Illumina sequenced DNA sample also some contaminant MAC DNA is still present with sequences corresponding to MDSs of the mic but potentially in a different order.

The contamination of the MAC DNA in the plug may also be related to a process of tangling of the mic sequences that are contained in the mic with exactly the same sequence, without IESs, such as the *P0* gene. If they tangle with the corresponding mic sequences, they do not run correctly outside of the plugs.

In the light of all the previous considerations, we planned in a future experiment to repeat the sequencing using third generation sequencing technology as Pacific biosciences SMRT sequencing (PacBio), with a real-time sequencing approach that skips the fragmentation and amplification steps of the Illumina procedure and in turn produce reads exceeding several kilobases by which should resolve most of the repetitive regions (Kchouk, Gibrat, and Elloumi 2017) and hopefully the other assembly problems.

2.4 Conclusions

We succeeded in the development of a protocol for *E. crassus* mic chromosomes enrichment and isolation. Now we need to proceed with the sequencing of the sample

using a more suitable NGS technology to reach our goal. The protocol we have set is very suitable for purifying DNA for PacBio sequencing because the DNA is maintained in the agar plugs and require only a simple agar digestion and soft extraction that limit the DNA fragmentation.

We also plan to test an additional purification step from the putative MAC molecules potentially tangled with the mic chromosomes, by denaturing the isolated DNA sample in the plugs, stabilizing the single strands molecules with formamide and allowing the separation through another electrophoresis on low melting gel.

Once well assembled and annotated, the germline (mic) genome of *E. crassus* will be valuable to investigate the functional and evolutionary relationships among DNA elimination events in different groups of ciliates, to develop and enhance molecular genetic tools in the *Euplotes* system and to use it more easily as marine model organism for environmental and toxicological studies.

2.5 Experimental procedures

2.5.1 *E. crassus* culture

E. crassus cells (60-80 μm in size) of strain DP1, kindly supplied by prof. L. A. Klobutcher (UConn Health, USA), were grown in sterilized sea water at 24°C. *Escherichia coli* (HT115 transformed with L4440 vector) were used as the only food source.

1 L culture of *E. coli* was grown in Luria Broth to saturation without antibiotic selection. For 1 L of *E. crassus*, *E. coli* from 100 ml of culture were pelleted (4,000 rpm for 10 min at 4°C). The remaining bacteria were stored at 4°C and used to feed *E. crassus* as necessary. After discarding most of the medium, the bacteria were resuspended before addition to the *E. crassus*.

Cells typically consume all the bacteria after 3-4 days at 24°C with the aeration system, reaching a density of around 3,000 cells/ml.

2.5.2 *E. crassus* micronuclear chromosomes isolation by PFGE

Starved *E. crassus* cells (150,000 per plug) were harvested by centrifugation in pear-shaped glass centrifuge tubes at 400 rcf for 3 min (cells were filtered with 70 μm filter).

In the last three PFGE run cells were also treated overnight with ampicillin 100 μg/ml, before being harvested. The 80 sec run was with ampicillin 100 μg/ml and kanamycin 50 μg/ml. Cells were washed with sterilized sea water and centrifuged at 400 rcf for 3 min.

Cells were transferred in an Eppendorf tube and centrifuged at 400 rcf for 3 min to remove as much as possible of the sea water, then resuspended in 560 μl of 1X TE buffer. 560 μl of cells were mixed with 560 μl of 2% Certified Low-Melt Agarose (Bio-Rad) in 1X TE buffer, then quickly transferred into the wells of the plug mold to produce the plugs (80 μl in each well). Plugs were set at 4°C for at least 30 min and then placed in 5 ml cells lysis buffer (1% N-Lauroylsarcosine sodium salt, 1% SDS, 1 mg/ml Proteinase K, 0.5 M EDTA pH 8.0) at 60°C overnight.

The plugs were washed three times in 0.5 M EDTA pH 8.0 for 10 min each, then inserted into the wells of the 1% Certified Low-Melt Agarose gel (Bio-Rad). Lambda (λ) ladder (Bio-Rad) was regenerated in 500 μl of 0.5X TBE buffer for 10 min at 45°C, then chilled in ice, and inserted into the wells of the gel. Gaps and empty wells were filled with 1% Certified Low-Melt Agarose gel (Bio-Rad).

The instrument used for the PFGE was CHEF Mapper XA Pulsed Field Electrophoresis System (Bio-Rad). 2.2 L of 0.5X TBE buffer were poured into the electrophoresis chamber for a pre-run of 30 min at 14°C, with a pump speed of 70. The runs were set with a gradient of 6 V/cm, a time of 22-30 h, an included angle of 120°, an initial switch time of 70-90 sec, a final switch time of 70-90 sec and a linear ramping factor.

When the run was completed the gel was stained with SYBR Safe DNA Gel Stain (Thermo Fisher Scientific) for 60 min and visualized with blue light. The gel was cut in three parts and stored at -20°C. Plugs were isolated and stored at -20°C.

The plugs and the highest gel slice were melted at 65°C for around 30 min. The gel volume was determined and digested with Agarase from *Pseudomonas atlantica* (Sigma) at 40°C overnight and then with RNase A (Thermo Fisher Scientific) 10 μg/ml for 2 h at 37°C.

The DNA was extracted by Phenol/Chloroform, precipitated by 3 M sodium acetate pH 5.2/absolute EtOH, resuspended in 30 μl of ddH_2O, and quantified by NanoDrop™ 1000 UV-Vis Spectrophotometer (Thermo Fisher Scientific).

2.5.3 Genomic DNA extraction

Starved *E. crassus* cells (300,000) were filtered and collected the day after by centrifugation in pear-shaped glass centrifuge tubes. Cells were centrifuged at 400 rcf for 3 min, then washed once with sterilized sea water, and centrifuged again at 400 rcf for 3 min. In order to remove as much of the sea water as possible, cells were centrifuged in an Eppendorf tube at 400 rcf for 3 min, before resuspendeding in 500 µl of NDS (10 mM Tris-HCl pH 7,5, 1% SDS, 20 mg/ml Proteinase K, 0.5 M EDTA pH 8.0). The tube was placed at 50°C overnight.

The DNA was extracted by Phenol/Chloroform and precipitated by 0.4 M LiCl/absolute EtOH.

The sample was pelleted at 4°C for 30 min at maximum speed, resuspended in 100 µl of ddH_2O and 50 µl of PEG-$MgCl_2$ (40% polyethylene glycol, 30 mM $MgCl_2$), and left 10 min at room temperature. The sample was pelleted for 30 min at maximum speed. The pellet was washed twice with 70% EtOH, dried out at room temperature, resuspended in 30 µl of ddH_2O, and quantified by NanoDrop^{TM} 1000 UV-Vis Spectrophotometer (Thermo Fisher Scientific).

2.5.4 IES PCR and Tec 2 PCR

The first micronuclear sequence analysed, was *E. crassus* G1 micronuclear sequence, protein kinase gene, partial CDS (GenBank: M28500.1) (Hale et al. 1996). Primers (Sigma) were designed outside an IES (144 bp):

FW 5'-ATGGACAGGACTAAGACAC-3',

RV 5'-CCATTTGATAATTAGGAAGAAATATACG-3'.

An amplicon of length 109 bp IES- and 253 bp IES+ was expected (Figure 26).

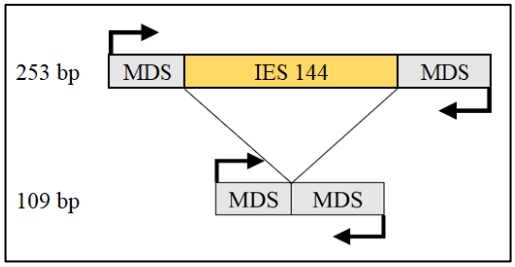

Figure 26. Schematic representation of expected fragments IES 144+ and IES 144-.

The second micronuclear sequence of interest was *Moneuplotes crassus* micronuclear telomerase reverse transcriptase (TERT-2) gene, complete CDS (GenBank: AY267543.1) (Karamysheva et al. 2003). Primers (Sigma) were designed outside an IES (300 bp):

FW 5'-GGATATTGAGAAATGATATGACAGC-3',

RV 5'-TTAGGGTCATTAGCATCCAT-3'.

An amplicon of length 510 bp IES- and 810 bp IES+ was expected (Figure 27).

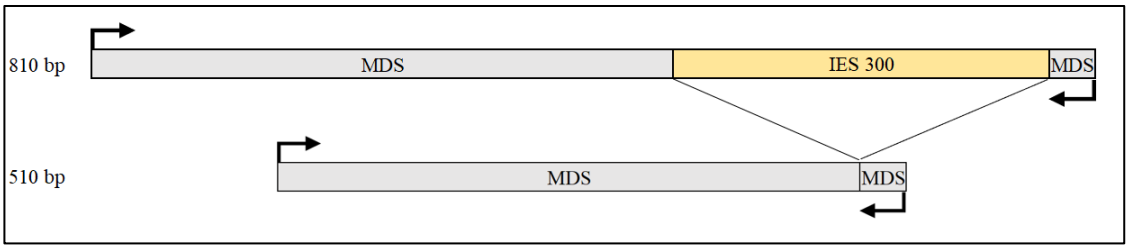

Figure 27. Schematic representation of the expected fragments IES 300+ and IES 300-.

Tec 2 sequences were taken from Doak *et al.*, 2003 and degenerate primers (Sigma) were designed inside 16 Tec 2 elements internal sequences after Clustal omega alignment (GenBank: AF159907.1; AF159908.1; AF159909.1; AF159910.1; AH008187.2; AF159913.1; AF159914.1; AF159915.1; AF159916.1; AF159916.1; AF159918.1; AF159919.1; AF159920.1; AF159921.1; L03359.1; L03360.1):

FW 5'-TATTATGGATGTGAATCAGGTTCTACTYTCM-3',

RV 5'-GATCTTCTGCATCATGTTCATATGATCTTGA-3'.

Expected amplicon length was 108 bp.

PCR was performed using Phusion High-Fidelity DNA Polymerase (Thermo Fisher Scientific) and the following conditions:

95°C	2 min	
95°C	30 sec	35 cycles
54°C	1 min 15 sec	
72°C	1 min 15 sec	
72°C	5 min	
4°C	∞	

The DNA was run on a 1% agarose gel and stained with EtBr.

'IES144-' and 'IES144+' gel bands were excised from the gel and purified by NucleoSpin Gel and PCR Clean-up (Macherey-Nagel) and sent for Sanger Sequencing (BMR Genomics).

2.5.5 Quantitative PCR

Primers (Sigma) for quantitative PCR were designed inside the IES 144 bp in the *E. crassus* G1 micronuclear sequence, protein kinase gene, partial CDS (GenBank: M28500.1) (Hale et al. 1996):
FW 5'-GCAAAATTGATAAAGGGTATAAGAGAATAGTAGAGAC-3',
RV 5'-ATGAATATGGGATATTGAATAAGAAGGATATTTTTATTCTAGG-3'.
Expected amplicon length was 132 bp (Figure 28).

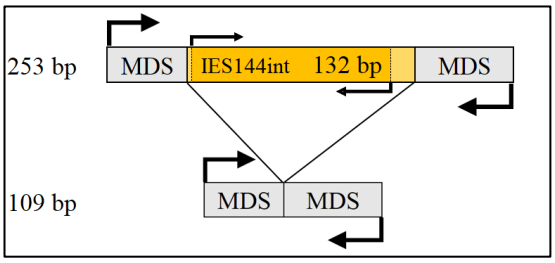

Figure 28. Schematic representation of IES 144 internal amplicon.

The *P0* gene was used as control. We blasted the *E. focardii* acidic ribosomal P0 protein (*P0*) gene, complete CDS (GenBank: DQ003025.1) (Pucciarelli et al. 2005) against the *E. crassus* DP1 genome available in our laboratory (data not yet published) to find the *P0 E. crassus* sequence to design primers.

Primers (Sigma):
FW 5'-TGGTTCACCTTCAACTGGCT-3',
RV 5'-CCCTCTTCGTCCAATGCGATA-3'.
Expected amplicon length was 155 bp.

The PCR was performed in triplicate with 50 ng of template, using SsoAdvanced Universal SYBR Green Supermix, CFX Connect Real-Time PCR Detection System (Bio-Rad) in a final volume of 20 µl, using the following conditions:

98°C 3 min

98°C 15 sec

60°C 30 sec } 40 cycles

Plate Read

Melt Curve 65°C to 95°C: Increment 0.5°C 5 sec

Plate Read

2.5.6 Data analysis

Statistical analyses were performed with CFX Maestro™ Software for Bio-Rad CFX Real-Time PCR Systems. One-way ANOVA were used to assess significant differences ($p < 0.01$).

2.6 References

Aigner, Stefan, Joachim Lingner, Karen J. Goodrich, Cheryl A. Grosshans, Andrej Shevchenko, Matthias Mann, and Thomas R. Cech. 2000. "Euplotes Telomerase Contains an La Motif Protein Produced by Apparent Translational Frameshifting." *The EMBO Journal*. doi:10.1093/emboj/19.22.6230.

Arnaiz, Olivier, Nathalie Mathy, Céline Baudry, Sophie Malinsky, Jean Marc Aury, Cyril Denby Wilkes, Olivier Garnier, et al. 2012. "The Paramecium Germline Genome Provides a Niche for Intragenic Parasitic DNA: Evolutionary Dynamics of Internal Eliminated Sequences." *PLoS Genetics*. doi:10.1371/journal.pgen.1002984.

Aury, Jean Marc, Olivier Jaillon, Laurent Duret, Benjamin Noel, Claire Jubin, Betina M. Porcel, Béatrice Ségurens, et al. 2006. "Global Trends of Whole-Genome Duplications Revealed by the Ciliate Paramecium Tetraurelia." *Nature* 444 (7116): 171–78. doi:10.1038/nature05230.

Baird, Scott E, Gina M Fino, Susan L Tausta, and Lawrence A Klobutcher. 1989. "Micronuclear Genome Organization in Euplotes Crassus: A Transposonlike Element Is Removed during Macronuclear Development." *Mol Cell Biol* 9 (9): 3793–3807. doi:10.1128/MCB.9.9.3793.

Baird, Scott E, and Lawrence A Klobutcher. 1989. "Characterization of Chromosome Fragmentation in Two Protozoans and Identification of a Candidate Fragmentation Sequence in Euplotes Crassus." *Genes & Development*. doi:10.1101/gad.3.5.585.

Bankevich, Anton, Sergey Nurk, Dmitry Antipov, Alexey A. Gurevich, Mikhail

Dvorkin, Alexander S. Kulikov, Valery M. Lesin, et al. 2012. “SPAdes: A New Genome Assembly Algorithm and Its Applications to Single-Cell Sequencing.” *Journal of Computational Biology*. doi:10.1089/cmb.2012.0021.

Chen, Xiao, John R. Bracht, Aaron David Goldman, Egor Dolzhenko, Derek M. Clay, Estienne C. Swart, David H. Perlman, et al. 2014. “The Architecture of a Scrambled Genome Reveals Massive Levels of Genomic Rearrangement during Development.” *Cell* 158 (5). Elsevier Inc.: 1187–98. doi:10.1016/j.cell.2014.07.034.

de Graaf, Rob M., Theo A. van Alen, Bas E. Dutilh, Jan W.P. Kuiper, Hanneke J.A.A. van Zoggel, Minh B. Huynh, Hans Dieter Görtz, Martijn A. Huynen, and Johannes H.P. Hackstein. 2009. “The Mitochondrial Genomes of the Ciliates Euplotes Minuta and Euplotes Crassus.” *BMC Genomics* 10: 514. doi:10.1186/1471-2164-10-514.

Dini, Fernando. 1984. “On the Evolutionary Significance of Autogamy in the Marine Euplotes (Ciliophora: Hypotrichida).” *The American Naturalist* 123 (2): 151–62.

Doak, Thomas G., David J. Witherspoon, Carolyn L. Jahn, and Glenn Herrick. 2003. “Selection on the Genes of Euplotes Crassus Tec1 and Tec2 Transposons: Evolutionary Appearance of a Programmed Frameshift in a Tec2 Gene Encoding a Tyrosine Family Site-Specific Recombinase.” *Eukaryotic Cell*. doi:10.1128/EC.2.1.95-102.2003.

Doak, Thomas G, F P Doerder, Carolyn L Jahn, and Glenn Herrick. 1994. “A Proposed Superfamily of Transposase Genes: Transposon-like Elements in Ciliated Protozoa and a Common ‘D35E’ Motif.” *Proceedings of the National Academy of Sciences of the United States of America*. doi:10.1073/pnas.91.3.942.

Eisen, Jonathan A., Robert S. Coyne, Martin Wu, Dongying Wu, Mathangi Thiagarajan, Jennifer R. Wortman, Jonathan H. Badger, et al. 2006. “Macronuclear Genome Sequence of the Ciliate Tetrahymena Thermophila, a Model Eukaryote.” *PLoS Biology*. doi:10.1371/journal.pbio.0040286.

Greene, Eric C., and Dorothy E. Shippen. 1998. “Developmentally Programmed Assembly of Higher Order Telomerase Complexes with Distinct Biochemical and Structural Properties.” *Genes and Development*. doi:10.1101/gad.12.18.2921.

Hale, Cynthia A, Mary Ellen Jacobs, Heather G Estes, Susmita Ghosh, and Lawrence A Klobutcher. 1996. “Micronuclear and Macronuclear Sequences of a Euplotes Crassus Gene Encoding a Putative Nuclear Protein Kinase.” *Journal of Eukaryotic Microbiology*. doi:10.1111/j.1550-7408.1996.tb05048.x.

Hamilton, Eileen P., Aurélie Kapusta, Piroska E. Huvos, Shelby L. Bidwell, Nikhat Zafar, Haibao Tang, Michalis Hadjithomas, et al. 2016. “Structure of the Germline Genome of Tetrahymena Thermophila and Relationship to the Massively Rearranged Somatic Genome.” *ELife*. doi:10.7554/eLife.19090.001.

Jacobs, Mary Ellen, Adolfo Sánchez-Blanco, Laura A. Katz, and Lawrence A Klobutcher. 2003. “Tec3, a New Developmentally Eliminated DNA Element in Euplotes Crassus.” *Eukaryotic Cell* 2 (1): 103–14. doi:10.1128/EC.2.1.103-114.2003.

Jahn, Carolyn L., Stella Z. Doktor, John S. Frels, John W. Jaraczewski, and Mark F. Krikau. 1993. “Structures of the Euplotes Crassus Tec1 and Tec2 Elements: Identification of Putative Transposase Coding Regions.” *Gene*. doi:10.1016/0378-1119(93)90226-S.

Jahn, Carolyn L, Mark F Krikau, and Susan Shyman. 1989. “Developmentally Coordinated En Masse Excision of a Highly Repetitive Element in E. Crassus.” *Cell*. doi:10.1016/0092-8674(89)90757-5.

Jaraczewski, John W., and Carolyn L. Jahn. 1993. “Elimination of Tec Elements Involves a Novel Excision Process.” *Genes and Development* 7 (1): 95–105. doi:10.1101/gad.7.1.95.

Jaraczewski, John W, John S Frels, and Carolyn L Jahn. 1994. “Developmentally Regulated , Low Abundance Tec Element Transcripts in Euplotes Crassus-Implications for DNA Elimination and Transposition” 22 (21): 4535–42.

Karamysheva, Zemfira, Libin Wang, Timothy Shrode, Janna Bednenko, Leigh Anne Hurley, and Dorothy E. Shippen. 2003. “Developmentally Programmed Gene Elimination in Euplotes Crassus Facilitates a Switch in the Telomerase Catalytic Subunit.” *Cell*. doi:10.1016/S0092-8674(03)00363-5.

Kchouk, Mehdi, Jean Francois Gibrat, and Mourad Elloumi. 2017. “Generations of Sequencing Technologies: From First to Next Generation.” *Biology and Medicine* 09 (03). doi:10.4172/0974-8369.1000395.

Klobutcher, Lawrence A. 1999. “Characterization of in Vivo Developmental Chromosome Fragmentation Intermediates in E. Crassus.” *Molecular Cell*. doi:10.1016/S1097-2765(00)80380-9.

Klobutcher, Lawrence A., Martha E. Huff, and Gregory E. Gonye. 1988. “Alternative Use of Chromosome Fragmentation Sites in the Ciliated Protozoan Oxytricha Nova.” *Nucleic Acids Research*. doi:10.1093/nar/16.1.251.

Klobutcher, Lawrence A. 1995. “Developmentally Excised DNA Sequences in Euplotes Crassus Capable of Forming G Quartets.” *Proc Natl Acad Sci U S A* 92 (6): 1979–83. doi:10.1073/pnas.92.6.1979.

Klobutcher, Lawrence A, and Philip J. Farabaugh. 2002. “Shifty Ciliates: Frequent Programmed Translational Frameshifting in Euplotids.” *Cell* 111 (6): 763–66. doi:10.1016/S0092-8674(02)01138-8.

Klobutcher, Lawrence A, Jed D Gygax, Scott E.Podoloff, Joris R Vermeesch, Carolyn M Price, Christopher M Tebeau, and Carolyn L Jahn. 1998. “Conserved DNA Sequences Adjacent to Chromosome Fragmentation and Telomere Addition Sites in Euplotes Crassus.” *Nucleic Acids Research*. doi:10.1093/nar/26.18.4230.

Klobutcher, Lawrence A, and Carolyn L Jahn. 1991. “Developmentally Controlled Genomic Rearrangements in Ciliated Protozoa.” *Current Opinion in Genetics and Development* 1 (3): 397–403. doi:10.1016/S0959-437X(05)80306-5.

Klobutcher, Lawrence A, Marshal T Swanton, Pierluigi Donini, and David M Prescott. 1981. “All Gene-Sized DNA Molecules in Four Species of Hypotrichs Have the

Same Terminal Sequence and an Unusual 3' Terminus." *Pnas* 78 (5): 3015–19. doi:10.1073/pnas.78.5.3015.

Klobutcher, Lawrence A, Leah R Turner, and Janice La Plante. 1993. "Circular Forms of Developmentally Excised DNA in Euplotes Crassus Have a Heteroduplex Junction." *Genes and Development*. doi:10.1101/gad.7.1.84.

Landweber, Laura F, Tai-Chih Kuo, and Edward A Curtis. 2000. "Evolution and Assembly of an Extremely Scrambled Gene." *Pnas* 97: 3298–3303. doi:10.1073/pnas.97.7.3298.

Lobanov, Alexey V, Dolph L Hatfield, and Vadim N Gladyshev. 2009. "Eukaryotic Selenoproteins and Selenoproteomes." *Biochim Biophys Acta.* 1790 (11): 1424–28.

Lobanov, Alexey V, Stephen M. Heaphy, Anton A. Turanov, Maxim V. Gerashchenko, Sandra Pucciarelli, Raghul R. Devaraj, Fang Xie, et al. 2017. "Position-Dependent Termination and Widespread Obligatory Frameshifting in Euplotes Translation." *Nature Structural and Molecular Biology* 24 (1): 61–68. doi:10.1038/nsmb.3330.

Möllenbeck, Matthias, and Lawrence A Klobutcher. 2002. "De Novo Telomere Addition to Spacer Sequences Prior to Their Developmental Degradation in Euplotes Crassus." *Nucleic Acids Res* 30 (2): 523–31.

Prescott, David M. 1994. "The DNA of Ciliated Protozoa." *MICROBIOLOGICAL REVIEWS* 58 (2): 233–67. doi:10.1007/BF00326311.

Pucciarelli, Sandra, Antonietta La Terza, Patrizia Ballarini, Sabrina Barchetta, Ting Yu, Francesca Marziale, Valerio Passini, Barbara Methé, H. William Detrich, and Cristina Miceli. 2009. "Molecular Cold-Adaptation of Protein Function and Gene Regulation: The Case for Comparative Genomic Analyses in Marine Ciliated Protozoa." *Marine Genomics*. doi:10.1016/j.margen.2009.03.008.

Pucciarelli, Sandra, Francesca Marziale, Graziano Di Giuseppe, Sabrina Barchetta, and Cristina Miceli. 2005. "Ribosomal Cold-Adaptation: Characterization of the Genes Encoding the Acidic Ribosomal P0 and P2 Proteins from the Antarctic Ciliate Euplotes Focardii." *Gene*. doi:10.1016/j.gene.2005.06.007.

Salim, Hannah M W, Karen L. Ring, and Andre R O Cavalcanti. 2008. "Patterns of Codon Usage in Two Ciliates That Reassign the Genetic Code: Tetrahymena Thermophila and Paramecium Tetraurelia." *Protist*. doi:10.1016/j.protis.2007.11.003.

Slabodnick, Mark M, J Graham Ruby, Sarah B Reiff, Estienne C Swart, Sager Gosai, Sudhakaran Prabakaran, Ewa Witkowska, et al. 2017. "The Macronuclear Genome of Stentor Coeruleus Reveals Tiny Introns in a Giant Cell." *Current Biology*. doi:10.1016/j.cub.2016.12.057.

Swart, Estienne C., John R. Bracht, Vincent Magrini, Patrick Minx, Xiao Chen, Yi Zhou, Jaspreet S. Khurana, et al. 2013. "The Oxytricha Trifallax Macronuclear Genome: A Complex Eukaryotic Genome with 16,000 Tiny Chromosomes." *PLoS Biology* 11 (1). doi:10.1371/journal.pbio.1001473.

Tausta, S. Lorraine, and Lawrence A Klobutcher. 1990. "Internal Eliminated Sequenc

Are Removed Prior to Chromosome Fragmentation during Development in Euplotes Crassus." *Nucleic Acids Research*. doi:10.1093/nar/18.4.845.

Tausta, S. Lorraine, Leah R. Turner, Linda K. Buckley, and Lawrence A. Klobutcher. 1991. "High Fidelity Developmental Excision of Ted Transposons and Internal Eliminated Sequences in Euplotes Crassus." *Nucleic Acids Research* 19 (12): 3229–36. doi:10.1093/nar/19.12.3229.

Turanov, Anton A, Alexey V Lobanov, Dmitri E Fomenko, Hilary G Morrison, Mitchell L Sogin, Lawrence A Klobutcher, Dolph L Hatfield, and Vadim N Gladyshev. 2009. "Genetic Code Supports Targeted Insertion of Two Amino Acids by One Codon." *Science*. doi:10.1126/science.1164748.

Vallabhaneni, Haritha, Hua Fan-Minogue, David M. Bedwell, and Philip J. Farabaugh. 2009. "Connection between Stop Codon Reassignment and Frequent Use of Shifty Stop Frameshifting." *RNA*. doi:10.1261/rna.1508109.

Vogt, Alexander, Aaron David Goldman, Kazufumi Mochizuki, and Laura F. Landweber. 2013. "Transposon Domestication versus Mutualism in Ciliate Genome Rearrangements." *PLoS Genetics* 9 (8): 1–7. doi:10.1371/journal.pgen.1003659.

Wang, Ruan-lin, Wei Miao, Wei Wang, Jie Xiong, and Ai hua Liang. 2018. "EOGD: The Euplotes Octocarinatus Genome Database." *BMC Genomics* 19 (1). doi:10.1186/s12864-018-4445-z.

Wang, Ruan-lin, Jie Xiong, Wei Wang, Wei Miao, and Aihua Liang. 2016. "High Frequency of +1 Programmed Ribosomal Frameshifting in Euplotes Octocarinatus." *Scientific Reports*. doi:10.1038/srep21139.

Wang, Yurui, Yuanyuan Wang, Yalan Sheng, Jie Huang, Xiao Chen, Khaled A.S. AL-Rasheid, and Shan Gao. 2017. "A Comparative Study of Genome Organization and Epigenetic Mechanisms in Model Ciliates, with an Emphasis on Tetrahymena, Paramecium and Oxytricha." *European Journal of Protistology* 61. Elsevier GmbH: 376–87. doi:10.1016/j.ejop.2017.06.006.

Yang, Guang, Concetta De Santi, Donatella De Pascale, Sandra Pucciarelli, Stefania Pucciarelli, and Cristina Miceli. 2013. "Characterization of the First Eukaryotic Cold-Adapted Patatin-like Phospholipase from the Psychrophilic Euplotes Focardii: Identification of Putative Determinants of Thermal-Adaptation by Comparison with the Homologous Protein from the Mesophilic Euplotes." *Biochimie* 95 (9): 1795–1806. doi:10.1016/j.biochi.2013.06.008.

Yang, Guang, Guang Yang, Lino Aprile, Vincenzo Turturo, Sandra Pucciarelli, Stefania Pucciarelli, and Cristina Miceli. 2013. "Characterization and Comparative Analysis of Psychrophilic and Mesophilic Alpha-Amylases from Euplotes Species: A Contribution to the Understanding of Enzyme Thermal Adaptation." *Biochemical and Biophysical Research Communications* 438 (4): 715–20. doi:10.1016/j.bbrc.2013.07.113.

Yang, Guang, Hua Yao, Matteo Mozzicafreddo, Patrizia Ballarini, Sandra Pucciarelli, and Cristina Miceli. 2017. "Rational Engineering of a Cold-Adapted α-Amylase from the Antarctic Ciliate Euplotes Focardii for Simultaneous Improvement of

Thermostability and Catalytic Activity." *Applied and Environmental Microbiology*. doi:10.1128/AEM.00449-17.

Yao, Meng Chao, Ching Ho Yao, and Bob Monks. 1990. "The Controlling Sequence for Site-Specific Chromosome Breakage in Tetrahymena." *Cell*. doi:10.1016/0092-8674(90)90142-2.

Yu, Guo Liang, and Elizabeth H. Blackburn. 1991. "Developmentally Programmed Healing of Chromosomes by Telomerase in Tetrahymena." *Cell*. doi:10.1016/0092-8674(91)90077-C.

Additional Project

A-1. Transfection approaches in *Euplotes*

A-1.1 Introduction and aims

In this section, experimental approaches are listed for the development of transfection techniques that can be applied to genetic manipulation and functional studies in *Euplotes* species.

This work was supported by the Marine Microbiology Initiative (MMI - Gordon and Betty Moore Foundation), which previously supported The Marine Microbial Eukaryote Transcriptome Sequencing Project (MMETSP) (Keeling et al. 2014). MMI aims to accelerate development of genetic tools to enable development of experimental model systems in marine microbial ecology (Waller et al. 2018). It seeks to gain a comprehensive understanding of marine microbial communities, including ecological roles in the oceans, their diversity, functions and behaviors, and their origins and evolution.

Developing robust model systems is complex and risky; success is not guaranteed. It was a challenging project with a high potential pay-off. This is the context in which my PhD project is co-founded.

Marine ciliates, particularly of the genus *Euplotes*, have been studied for over a hundred years and have provided significant insights into microbial ecology, endosymbiont biology, and long-term cold adaptation (Nanney and Caughey 1953; Hammerschmidt et al. 1996; Pucciarelli et al. 2009; Luporini et al. 2016).

These organisms have an unusual genetic organization with two genomes: a micronuclear genome (mic) representing the germ line, and a macronuclear genome (MAC) containing single gene nanochromosomes amplified to thousands of copies for their somatic life. This unique organization has been beneficial in elucidating universal principles in the biology of telomeres, transposons, chromatin and small RNAs. However, this same genome structure also poses challenges that have likely made many the typical transfection and reverse genetics transfection techniques unsuccessful to date.

Compared to other model ciliates, molecular genetic tools in the *Euplotes* system are far less powerful and a transformation system is necessary to enable more systematic studies and to understand the complex programmed DNA rearrangements and transposition mechanisms that occur in the formation of the new MAC after each sexual cycle and also how these organisms, function in marine ecosystems.

A few examples of successful transfection in *Euplotes* species have been reported in the literature, (Bender, Kämpfer, and Klein 1999; Erbeznik, Yao, and Jahn 1999) but subsequent replications have not been possible. Starting from this knowledge we tried to adjust different physical and liposomal methods for *E. crassus* transfection.

The physical transfection methods use various tools to deliver nucleic acids in the cells, *(e.g.* microinjection, biolistic particle delivery, electroporation) (Mehier-Humbert and Guy 2005). Their application can cause cell damage and it is not always easy to apply to a discrete number of cells, indeed it is possible to microinject only one cell at a time. This means that takes time to obtain concrete results on a certain number of cells. Despite these limits, microinjection was successfully used to transfect ciliates like *Tetrahymena thermophila* and *Paramecium caudatum* (Takenaka et al. 2002).

The biolistic method uses gold particles that make complexes with nucleic acids and then these complexes are shot into the recipient cell with very high velocity and pressure.

Electroporation implies the application of short electrical pulses to the cells that disturbs the stability of the cellular membrane, creating small holes in the membrane itself through which nucleic acids can pass. It has been successfully used to transfect conjugating *T. thermophila* cells (Gaertig and Gorovsky 1992).

Once optimal transfection conditions are meet, biolistic and electroporation permit the transfection of a large number of cells, at a time.

Chemical transfection methods include the use of cationic lipids. The general principle guiding these methods relies on the use of cationic carrier molecules that complex with the negatively charged nucleic acids and, thus, are able to neutralize the strong negative charges given by the phosphate groups of the DNA and RNA molecules.

The efficiency of these methods is largely affected by factors like the cell type, the nucleic acid/ chemicals ratio, the pH of the solution and the cell membrane conditions (Kim and Eberwine 2010).

Transfection in order to be successful requires both an effective DNA-delivery system and a reliable way to select successfully-transfected cells. A proper selectable marker inserted in the vector and a correspondent selective applied on the harvested cells is crucial.

We tried to consider all the possible variables in each step of transfection protocols and we tested the following methods:

- Bio-Rad Biolistic PDS-1000/He Particle Delivery System with 0.6 μm and 1.6 μm golden nanoparticles (AuNPs);
- microinjection with Eppendorf InjectMan NI 2 using Eppendorf Femtotips Microinjection Capillary Tips on exconjugant cells;
- electroporation using Bio-Rad Gene Pulser with 0.2 cm cuvettes;
- Lipofectamine 2000 Transfection Reagent (Invitrogen) and Lipofectamine 3000 Transfection Reagent (Invitrogen);
- Effectene Transfection Reagent (QIAGEN);
- FuGENE HD Transfection Reagent (Promega).

I performed all the experiments in strict collaboration with Rachele Cesaroni or by myself, at the University of Bern and at University of Camerino.

A-1.2 *Euplotes* as organism of study

Our attention was focused on the hypotrichous marine ciliates *Euplotes crassus* and *Euplotes focardii*. The former is mesophilic and has a cosmopolitan distribution, being collected from most of the Earth's oceans, the latter is a strictly psychrophilic Antarctic species and survives from -2°C to 15°C. They are characterized by dimorphic nuclei: a transcriptionally inert, diploid germline mic, and a transcriptionally active, polyploid somatic MAC.

The E. focardii growth rate is much slower due to the cold adaptation: about 1 division every 3 days. It is difficult to maintain mating types in this species. Conjugation is very peculiar and ends with a single exconjugant (Valbonesi and Luporini 1993). We tested tools on *E. crassus* first, considering the better growing conditions compared to *E. focardii.*

E. crassus (DP1 strain) is 60-80 μm in size, is able to perform both vegetative and conjugation cycles, its growth rate is 1,5 divisions per day, at 24°C in sea water, fed with algae (*Dunaliella salina* or *Dunaliella tertiolecta*) and/or bacteria (*Escherichia coli)* It is strongly autofluorescent when it is fed with bacteria and, especially, algae. We found out that when cultures are fed on *E. coli*, they grow to a higher density than on

algae as food source, reaching a cell density of 3000 cells/ml, making many analyses easier.

A-1.3 Transfection vectors

A-1.3.1 Delivery controls

To test the delivery system's effectiveness, we used Label IT® Plasmid Delivery Control, Cy®3 (Mirus) and a Synthetic 25 bp long DNA-RNA-cy3 hybrid. These vectors with a fluorescent red probe facilitated the visual tracking, following cellular uptake without being expressed by the cells.

A-1.3.2 Resistance marker

E. crassus displays naturally high resistance levels to several drugs/antibiotics that are typically used for selection in transfection experiments (*e.g.* resistance to ampicillin 100 µg/ml). Through growth curves and survival test assays we determined that *E. crassus* was sensitive to G418 7.5 mg/ml and even more sensitive to it when grown in a culture medium of 10% artificial seawater + 90% 0.3 M glucose. This facilitate the selection of transfected cells in attempts to develop transfection.

We optimized the G418 resistance gene (neomycin gene) according to the *Euplotes crassus* codon usage. A non-codon-optimized neomycin gene was previously used Bender et al. 1999.

A-1.3.3 Artificial nanochromosomes

We synthesized constructs resembling the *Euplotes* MAC nanochromosome structure. They contain either a GFP reporter and/or a drug selection marker, both optimized according to the euplotid codon usage. The flanking non-coding regions belong to constitutive highly expressed *Euplotes* genes. Telomeres on both ends were added by PCR with Phusion DNA Polymerase (Thermo Fisher Scientific) to obtain blunt ends products. Both artificial nanochromosomes were checked by sequencing.

GFP artificial nanochromosomes (940 bp) are composed of: a 62 bp *E. crassus* 5' UTR from a highly expressed gene as promoter, a 717 bp GFP coding sequence, a 105 bp *E. crassus* 3' UTR from a highly expressed gene, and 28 bp telomeres on both ends (Figure 29).

GFP-neo artificial nanochromosomes (3193 bp) are composed of the GFP-tagged β-tubulin gene and G418 resistance gene: 49 bp β-tubulin 5’ UTR, 1338 bp β-tubulin cds, a 24 bp long spacer, 717 bp GFP coding sequence, 64 bp β-tubulin 3' UTR; 64 bp α-tubulin 3' UTR, 794 bp G418 resistance gene (neo), 87 bp α-tubulin 5' UTR, and 28 bp telomeres on both ends (Figure 30).

Figure 29. GFP artificial nanochromosome (940 bp) map and sequence.

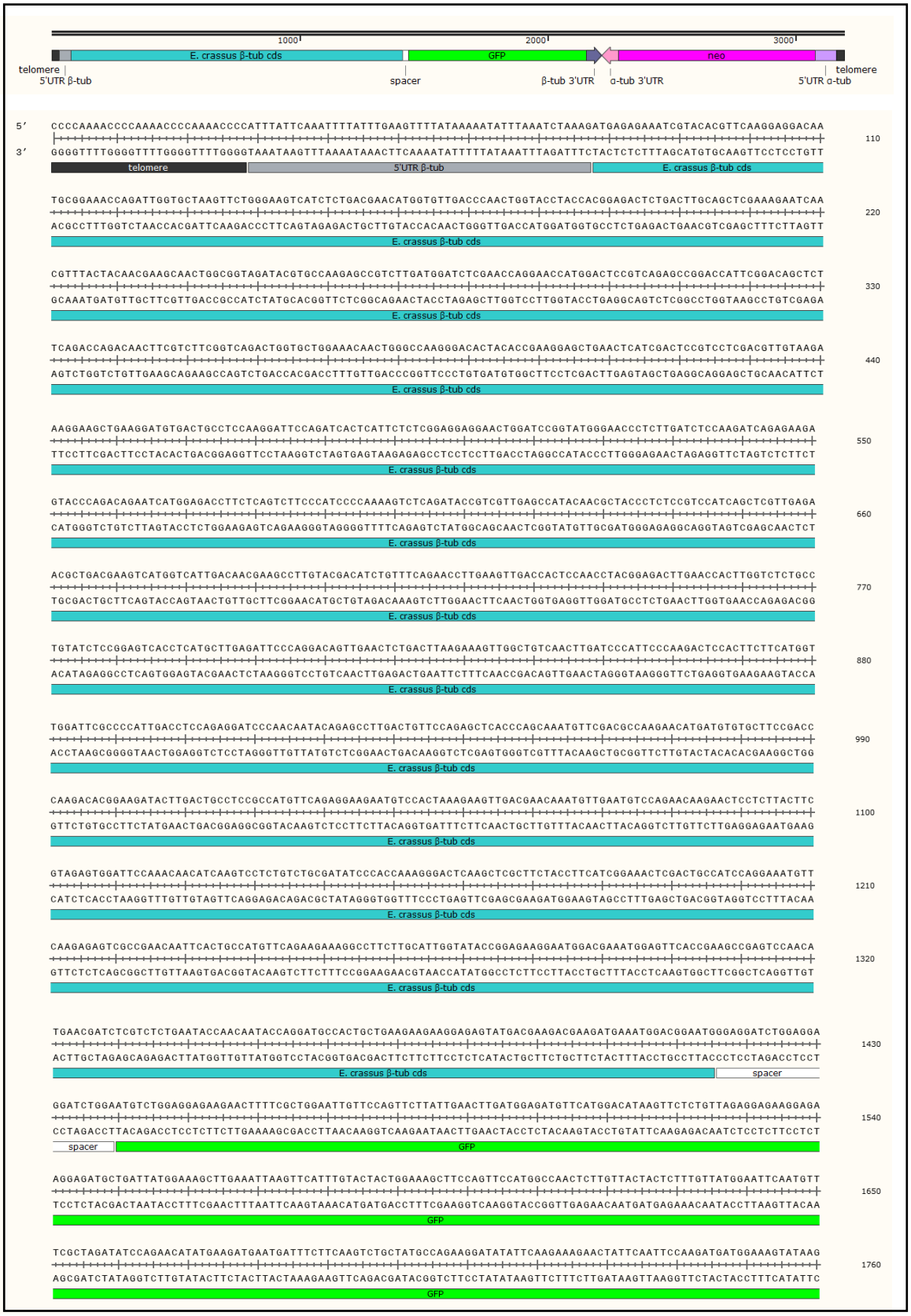
1000
2000
3000
E. crassus β-tub cds
GFP
neo
telomere
5'UTR β-tub
spacer
β-tub 3'UTR
α-tub 3'UTR
telomere
5'UTR α-tub
5′
3′
110
220
330
440
550
660
770
880
990
1100
1210
1320
1430
1540
1650
1760

Figure 30. GFP-neo artificial nanochromosomes (3193 bp) map and sequence.

A-1.4 Transfection approaches

A-1.4.1 Biolistic

The Bio-Rad Biolistic PDS-1000/He Particle Delivery System with 0.6 μm and 1.6 μm AuNPs was used. We adjusted the conditions for *E. crassus* starting from the protocol used in *Tetrahymena termophila* (Bruns and Cassidy-Hanley 1999).

I used 10 mM HEPES pH 7.4 as transfection buffer to test the system. Cells were then transfered to sea water without any construct and survived well.

Later, GFP-neo artificial nanochromosomes were used. 10^5 vegetative *E. crassus* cells or 10^5 mating DP1 and DP3 *E. crassus* strains (50 h after mixing) were placed on a filter paper soaked with 10 mM HEPES pH 7.4. They were shot with 0.6 μm or 1.6 μm AuNPs coated with 1.25 μg of the construct. Shooting conditions were set as follows: rupture disk 1550 psi, helium pressure 1750 psi, vacuum 26 inches Hg, gap distance ⅜ inches, 1st shelf. The filter paper was then fold and placed into 50 ml of sea water. After the transfection cells looked healthy.

The antibiotic selection started after 24 h; increasing concentrations of G418 were added every 4 days, from 1 mg/ml up to 10 mg/ml.

Unfortunately, I did not obtain any viable clones after 30 days of antibiotic selection: all cells died with 6 mg/ml of G418 and I did not get any proof of nucleic acids uptake, GFP espression was not detected by fluorescence microscopy**.**

A-1.4.2 Microinjection

Eppendorf InjectMan NI 2 with Eppendorf Femtotips Microinjection Capillary Tips was used on exconjugant cells. The constructs tested were a synthetic 25 bp long DNA-RNA-cy3 hybrid or the GFP-neo artificial nanochromosomes.

Two strains of different mating types (DP1 and DP3) of *E. crassus* were mixed (pairs formed in 5-6 h). Exconjugant cells with Anlagen (Figure 31) and pairs were isolated in sea water with 2% or 4% BSA and drops were prepared for the injection. Around 2-4 μg/μl of constructs were used. After transfection cells were resuspended in 700 μl of sea water.Usually 70% of exconjugants reorganize and turn into vegetative cells. The rescue ratio after microinjection was far less (even without any construct injected). Few cells managed to divide and could be evaluated for transfection efficacy.

After a few cell divisions, increasing concentration of G418 were added every 4 days, from 1 mg/ml up to 10 mg/ml (Erbeznik, Yao, and Jahn 1999).

We did not obtain any positive clones for the GFP-neo artificial nanochromosomes. All cells died with 4 mg/ml of G418 and we did not get any proof of nucleic acids uptake; also, GFP espression was not detected by fluorescence microscopy**.**

However, we had evidence of successful DNA injection into the Anlagen using the DNA-RNA-cy3 hybrid as a control and monitoring by fluorescent microscopy (Figure 32).

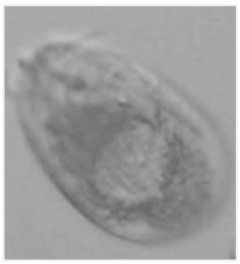

Figure 31. *E. crassus* exconjugant cell with visible Anlagen.

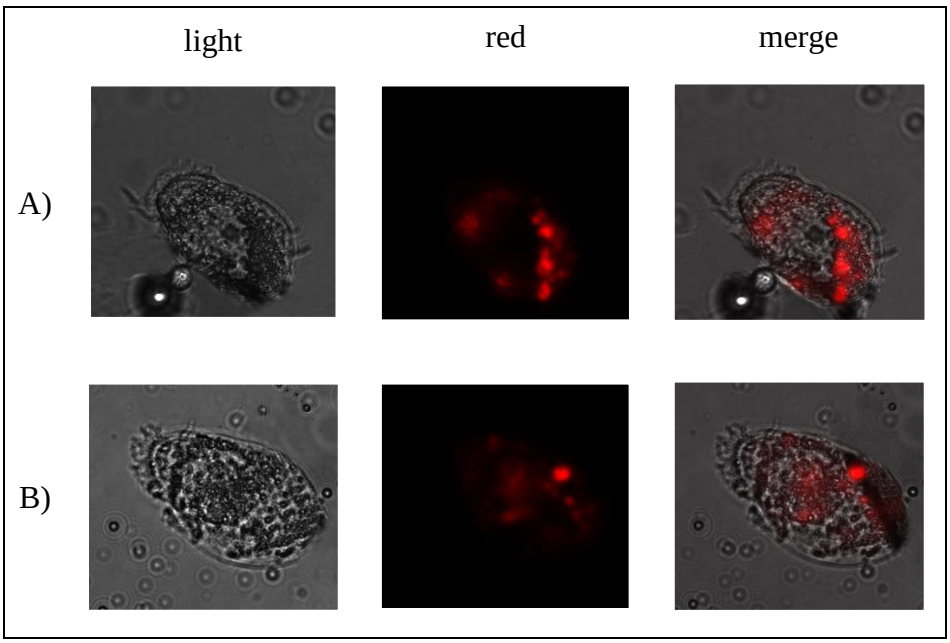

Figure 32. E. crassus exconjugant cells injected with a synthetic 25 bp long DNA-RNA-cy3. One was injected in the cytoplasm (A), the other was injected in the Anlagen (B).

A-1.4.3 Electroporation

A Bio-Rad Gene Pulser with 0.2 cm cuvettes was used for electroporation, together with Lipofectamine® 2000 Transfection Reagent (Invitrogen).

$2x10^4$ *E. crassus* cells were collected and resuspended in 0.3 M glucose solution (7% sea water and 93% of 0.3 M glucose solution). For each round of transfection, 250 µl of cells were used. 0.25 µg of Label IT® Plasmid Delivery Control Cy®3 (Mirus) were added alone or mixed with 2.5 µl of Lipofectamine® 2000 Transfection Reagent (Invitrogen). The sample was transferred to the cuvette. Conditions were set as follows: 0.2 kV, 25 µFD, 100 Ω. Time constant around 1.2.

More than 50% of cells were viable after electroporation (a few cells fused together), then cells were resuspended in 3 ml of sea water.

The plasmid was visible in the cytoplasm immediately after the electroporation by fluorescent microscopy.

A-1.4.4 Lipofectamine® Transfection Reagent (Invitrogen)

Lipofectamine® 2000 Transfection Reagent (Invitrogen) and Lipofectamine® 3000 Transfection Reagent (Invitrogen) were used with Label IT® Plasmid Delivery Control Cy®3 (Mirus) or GFP artificial nanochromosomes. The protocol of the supplier was followed for the preparation of the DNA–lipofectamine complex.

$4x10^3$ *E. crassus* cells were collected and resuspended in 1 ml of Opti-MEM® medium on a 24-well plate. 2.5 µl of Lipofectamine® 2000 or 3000 Transfection Reagent (Invitrogen) mixed with 0.5 µg of the transfection vector were added to the cells. The plate was incubated for 30 min at 37°C 30 and then 3 h and half at 28°C. After 4 h the cells were washed and resuspended in sea water. After the transfection *Euplotes* looked healthy and viable.

As a proof of nucleic acid uptake, PCR verification on very well washed cells using specific primers for the GFP sequence was performed and gave positive results, but GFP espression was not detected by fluorescence microscopy**.**

The plasmid with the fluorescent red probe was visible inside the cells immediately after Lipofection (4 h). Then, after 24 h it was mostly visible in the samples with Lipofectamine® 2000 Transfection Reagent (Invitrogen) that helped the DNA to enter the cells and protected it from the lysosomal pathway (Figure 33).

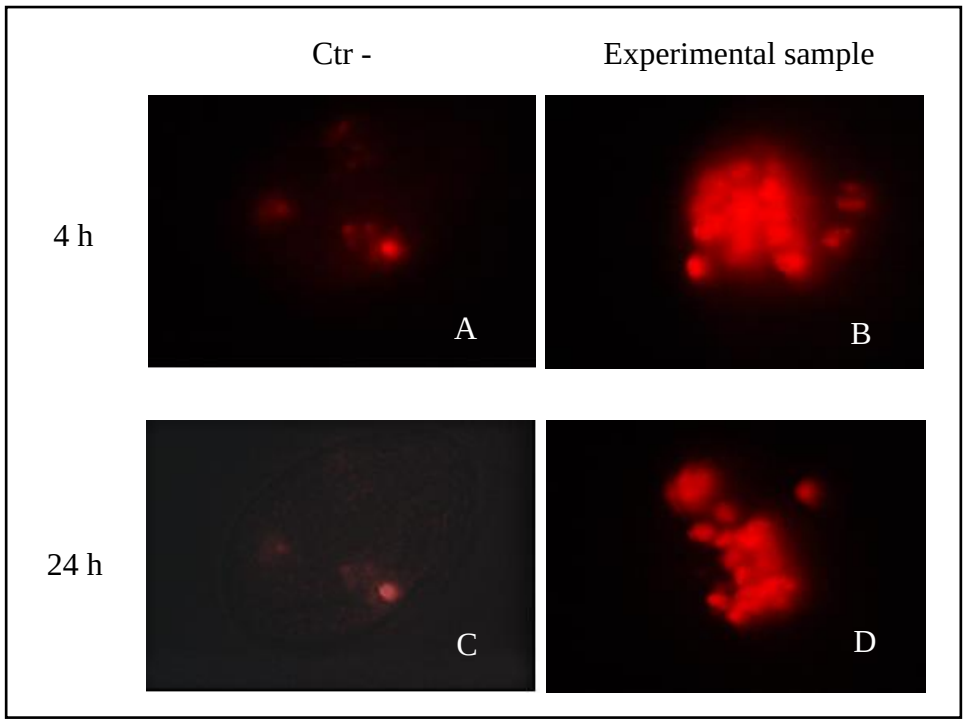

Figure 33. *E. crassus* cells 4 h after the transfection with Label IT® Plasmid alone (A) and Label IT® Plasmid + Lipofectamine® 2000 (B). *E. crassus* cells 24 h after the transfection with Label IT® Plasmid alone (C) and Label IT® Plasmid + Lipofectamine® 2000 (D).

A-1.4.5 Effectene Transfection Reagent (QIAGEN)

Effectene Transfection Reagent (QIAGEN) were complexed with GFP-neo artificial nanochromosomes following the supplier's protocol except for doubling the amount of DNA from 0.4 to 0.8 µg (Bender, Kämpfer, and Klein 1999).

$2x10^3$ *E. crassus* cells were collected and resuspended in 1 ml of 500 mM sorbitol, 0.5 mM Tris-HCl pH 7.0. The DNA-Effectene complex was added and the cells were incubated 3 h at 24°C. 1 ml of sea water was added after 1 h, bacteria as food source (1:1000) were added after 2 h, and cells were washed after 3 h and resuspended in sea water. Immediately after the DNA-Effectene complex addition, cells stopped moving. They recovered later on, but their number decreased after the washing step.

After a few cells divisions (more than 24 h) the selection drug G418 was added, either at the maximum concentration of 10 mg/ml (no resistance was shown) or at increasing concentrations from 1 mg/ml up to 10 mg/ml (added every 4 days).

As a proof of nucleic acid uptake, PCR verification on very well washed cells using specific primers for the GFP sequence was performed and gave positive results, but GFP espression was not detected by fluorescence microscopy.

A-1.4.6 FuGENE HD Transfection Reagent (Promega)

$2x10^3$ *E. crassus* cells were collected and resuspended in 1 ml of 500 mM sorbitol, 0.5 mM Tris-HCl pH 7.0. The DNA-FuGENE HD Transfection Reagent (Promega) complex was added (amount of DNA 0.8 μg) and cells were incubated 1 h and 30 min at 24°C., 1 ml of sea water was added after 1 h and after 2 h. Then cells were washed and resuspended in 400 μl of sea water. After the transfection the cells looked healthy and viable, but their number decreased after the washing step.

After a few cells divisions (more than 24 h) G418 at 10 mg/ml was added as selection drug, but no resistance was shown. There was no proof of nucleic acid uptake.

A-1.5 Conclusions

The following outcomes were reached:

- We defined conditions for growing *Euplotes* cultures to a higher cell density than on algae as the food source, making many analyses easier.
- We generated artificial nanochromosomes resembling the structure of those of the *Euplotes* MAC. They contain either a GFP reporter and/or a drug selection marker optimized according to the *Euplotes* codon usage. These can be used in the future to try other existing and newly developed transformation approaches.
- We found that *E. crassus* was much more sensitive to selective agents (*e.g.*, G418, Paromomycin, and Puromycin) when grown in a culture medium of 10% artificial seawater + 90% 0.3 M glucose. The same sensitivity was found in *E. focardii*, that has a much slower growth rate due to the cold temperature. This should facilitate the selection of transformed cells in future attempts to develop transfection.
- We investigated and developed appropriate conditions for maintaining *Euplotes* cell viability during various transfection approaches: the biolistics, Effectene Transfection Reagent (QIAGEN), FuGENE HD Transfection Reagent (Promega) and Lipofectamine 3000 Transfection Reagent (Invitrogen),
- We were able to see the *E. crassus* cells transfected with Cy3 labelled plasmid delivery control by: electroporation, electroporation with plasmid incubated in Lipofectamine 2000 Transfection Reagent, direct treatment of plasmid with

Lipofectamine 2000 Transfection Reagent, and microinjection of plasmid in the developing MAC of exconjugant cells (with RNA-DNA-cy3 hybrid).

However, when we tried to use artificial nanochromosomes with the G418 resistance gene and GFP tagged β-tubulin, cells died under an increasing concentration of antibiotic and we could not detect any localized signal, as it was for the labelled plasmid used as control nor any proof of gene integration, checking by PCR.

In conclusion, we succeeded in preparing vectors and setting conditions for delivering DNA into the cells by several methods, but we did not obtain evidence for incorporation of the vectors into the nucleus/genome or for the expression of the introduced genes. The reasons for the lack of success to date are not understood, and it remains possible that further alteration of experimental parameters or a more appropriate use of promoters for expression may provide successful transfection using these approaches.

A-1.6 References

Bender, Jörg, Matthias Kämpfer, and Albrecht Klein. 1999. "Faithful Expression of a Heterologous Gene Carried on an Artificial Macronuclear Chromosome in Euplotes Crassus." *Nucleic Acids Research* 27 (15): 3168–72. doi:10.1093/nar/27.15.3168.

Bruns, Peter J., and Donna Cassidy-Hanley. 1999. "Chapter 27 Biolistic Transformation of Macro- and Micronuclei." *Methods in Cell Biology*. doi:10.1016/S0091-679X(08)61553-8.

Erbeznik, Milutin, Meng Chao Yao, and Carolyn L. Jahn. 1999. "Characterization of the Euplotes Crassus Macronuclear RDNA and Its Potential as a DNA Transformation Vehicle." *Journal of Eukaryotic Microbiology* 46 (2): 206–16. doi:10.1111/j.1550-7408.1999.tb04605.x.

Gaertig, Jacek, and Martin A Gorovsky. 1992. "Efficient Mass Transformation of Tetrahymena Thermophila by Electroporation of Conjugants." *Proceedings of the National Academy of Sciences*. doi:10.1073/pnas.89.19.9196.

Hammerschmidt, Brigitte, Martin Schlegel, Denis H. Lynn, Detlef D. Leipe, Mitchell L. Sogin, and Igor B. Raikov. 1996. "Insights into the Evolution of Nuclear Dualism in the Ciliates Revealed by Phylogenetic Analysis of RRNA Sequences." *Journal*

of Eukaryotic Microbiology. doi:10.1111/j.1550-7408.1996.tb01396.x.

Keeling, Patrick J., Fabien Burki, Heather M. Wilcox, Bassem Allam, Eric E. Allen, Linda A. Amaral-Zettler, E. Virginia Armbrust, et al. 2014. "The Marine Microbial Eukaryote Transcriptome Sequencing Project (MMETSP): Illuminating the Functional Diversity of Eukaryotic Life in the Oceans through Transcriptome Sequencing." *PLoS Biology* 12 (6). doi:10.1371/journal.pbio.1001889.

Kim, Tae Kyung, and James H. Eberwine. 2010. "Mammalian Cell Transfection: The Present and the Future." *Analytical and Bioanalytical Chemistry*. doi:10.1007/s00216-010-3821-6.

Luporini, Pierangelo, Bill Pedrini, Claudio Alimenti, and Adriana Vallesi. 2016. "Revisiting Fifty Years of Research on Pheromone Signaling in Ciliates." *European Journal of Protistology* 55. Elsevier GmbH: 26–38. doi:10.1016/j.ejop.2016.04.006.

Mehier-Humbert, Sophie, and Richard H. Guy. 2005. "Physical Methods for Gene Transfer: Improving the Kinetics of Gene Delivery into Cells." *Advanced Drug Delivery Reviews*. doi:10.1016/j.addr.2004.12.007.

Nanney, David L, and Patricia A Caughey. 1953. "Mating Type Determination in Tetrahymena Pyriformis." *Proceedings of the National Academy of Sciences of the United States of America*.

Pucciarelli, Sandra, Antonietta La Terza, Patrizia Ballarini, Sabrina Barchetta, Ting Yu, Francesca Marziale, Valerio Passini, Barbara Methé, H. William Detrich, and Cristina Miceli. 2009. "Molecular Cold-Adaptation of Protein Function and Gene Regulation: The Case for Comparative Genomic Analyses in Marine Ciliated Protozoa." *Marine Genomics*. doi:10.1016/j.margen.2009.03.008.

Takenaka, Yasuhiro, Nobuyuki Haga, Terue Harumoto, Tadashi Matsuura, and Youji Mitsui. 2002. "Transformation of Paramecium Caudatum with a Novel Expression Vector Harboring Codon-Optimized GFP Gene." *Gene*. doi:10.1016/S0378-1119(01)00886-1.

Valbonesi, Alessandro, and Pierangelo Luporini. 1993. "Biology of Euplotes Focardii, an Antarctic Ciliate." *Polar Biology*. doi:10.1007/BF00233140.

Waller, Ross F., Phillip A. Cleves, Maria Rubio-Brotons, April Woods, Sara J. Bender, Virginia Edgcomb, Eric R. Gann, et al. 2018. "Strength in Numbers: Collaborative Science for New Experimental Model Systems." *PLoS Biology* 16 (7): 1–10. doi:10.1371/journal.pbio.2006333.